

O-alkylated/acylated coumarin analogues: Synthesis, anti-diabetic evaluation and docking studies



**UNIVERSITY OFTM
KWAZULU-NATAL**

**INYUVESI
YAKWAZULU-NATALI**

Nomandla Innocentia Ngcoya

BSc. Hons(UKZN)

Supervisor: Dr. P. Singh

2016

Westville Campus

O-alkylated/acylated coumarin analogues: Synthesis, anti-diabetic evaluation and docking studies

A Thesis

Submitted in partial fulfilment for the degree of

MASTER OF SCIENCE

In the

School of Chemistry and Physics

College of Agriculture, Engineering and Science

University of Kwazulu Natal, Westville Campus

By

Nomandla Innocentia Ngcoya

2016

Supervisor: Dr. P. Singh

Declaration

I, Nomandla Innocentia Ngcoya, certify that the experimental work in this thesis and the discussion is a result of my own research which was carried out in the school of chemistry and physics at the University of Kwazulu Natal (Westville), under the supervision of Dr. P. Singh.

The work carried out for this thesis is the authors original work except where otherwise indicated and has not been submitted by any candidate for any degree.

Signed.....

N.I. Ngcoya

I hereby certify that this statement is correct.

Signed.....

Dr. P. Singh (Supervisor)

“For no matter how many promises God has made, they are “Yes” in Christ.

And so through him the “Amen” is spoken by us to the glory of God”

2 Corinthians 1:20

Abstract

Diabetes mellitus (DM) represents a group of chronic disorders with diverse multiple etiology. It is characterized by high blood glucose (hyperglycemia) resulting from the malfunctioning in insulin secretion and/or insulin action, leading to impaired metabolism of carbohydrates, lipids and proteins in the body. According to 2013 WHO report, approximately 4.9 million people have died thus far and around 415 million are currently suffering from DM worldwide. Different approaches such as anti-diabetic drugs, insulin injection, and lifestyle modification are currently being used to control/treat diabetes. However, these techniques are not so effective and suffer a number of limitations which is why the development of novel potent anti-diabetic drugs is highly anticipated.

Recent literature review revealed that the coumarins have potential to act as anti-diabetic agents with excellent pharmacological profile. Hence, the aim of this project was to synthesize variedly substituted coumarin analogues and to test their anti-diabetic potential under *in vitro* conditions. Accordingly, three 4-methylcoumarins bearing hydroxyl moiety were synthesized using substituted phenols and a β -ketoester using the Pechmann reaction. The hydroxyl group of synthesized coumarins was then engaged in further transformations by its alkylation and acylation using a variety of alkyl/acyl halides under basic conditions. The synthesized compounds were structurally characterized using different spectroscopic techniques *viz.* proton nuclear magnetic resonance spectroscopy (^1H NMR, FT-IR and HR-MS). 2D NMR such as heteronuclear multiple bond correlation (HMBC), heteronuclear single quantum coherence spectroscopy (HSQC) and correlation spectroscopy (COSY) were also conducted to assign each proton and carbon resonances of the compounds synthesized.

All the synthesized compounds were tested *in vitro* for their anti-diabetic activity using the standard drug (acarbose) as a control. Some of the coumarin derivatives exhibited excellent anti-diabetic activity, even better than the standard drug, based on the IC_{50} data. The effect of alkyl chain length and electronic nature (electron-donating/withdrawing) of substituents attached to coumarin ring on the anti-diabetic activity was monitored, and a detailed structure activity relationship (SAR) was established. The *in vitro* anti-oxidant activity of compounds further revealed the importance of hydroxyl (-OH) groups in coumarins for their antioxidant activity. The alkylation or acylation of coumarins significantly reduced their antioxidant activity. On the other hand, the attachment of nitro (-NO₂) group to the aromatic ring of coumarin, impressively increased the antioxidant activity. Molecular docking simulations were finally conducted to predict the binding propensities of the compounds in the binding site of α -glucosidase, an enzyme that regulates the sugar level in the body. Since, the X-ray data for this protein is not available in protein data bank, its 3D model was generated using homology modelling technique. The predicted free binding energies predicted these compounds to be good inhibitors for the protein. Docking data suggested the importance of both the hydrogen bonding and hydrophobic forces in their host-guest relationship.

Acknowledgements

I would like to thank the Good Lord who gave me the strength to come this far, He carried me through hard times and gave me the strength to carry on when I felt like giving up.

My supervisor, Doctor Parvesh Singh, who continually and convincingly conveyed a spirit of adventure in regards to research.

I would like to thank my parents, my mother, Nomthandazo Vincentia Dlamini and my father, Mfaninkosi Phillip Ngcoya for their unconditional love and support throughout the past two years.

My grandmother, Zenzile Philomena Dlamini, for her encouragement.

I would like to thank Mr Suhas Shintre who welcomed me to the natural products lab and showed me around. He was always there to offer me assistance when needed.

To the natural products research group, I am extremely grateful and indebted to you guys for your expert, sincere and valuable guidance and encouragement extended to me.

To Dr. Nagaraj Kerru who proof read my thesis, Dr. Ramgopal Mopuri who did my biological evaluation studies, Ms. Caryl Janse van Rensburg who did my HRMS and Dillip who assisted me with NMR, words fail to express how grateful I am for your assistance.

My brother, Sbongiseni Micheal Ngcoya, your presence kept me going because I knew that you look up to me as your older sibling.

Immeasurable appreciation to Fezile Potwana for making this study possible. The person who welcomed me to UKZN Westville with a warm heart, showed me around and made every moment in the lab enjoyable with your jokes.

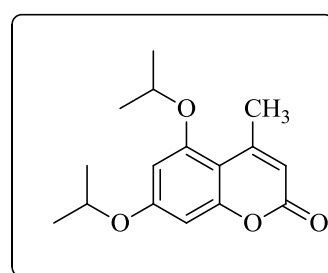
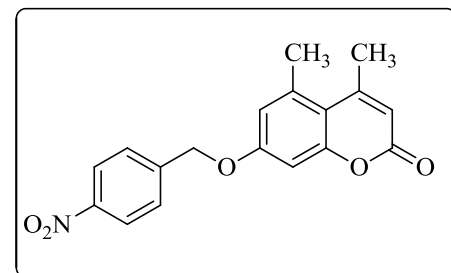
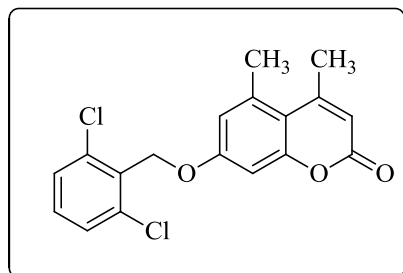
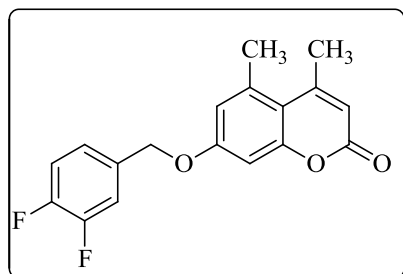
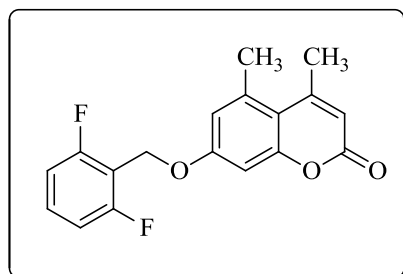
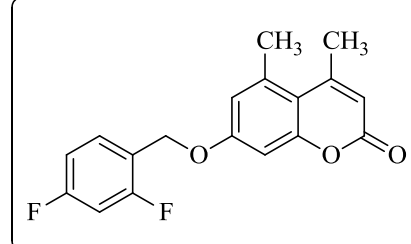
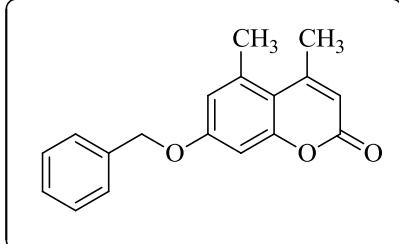
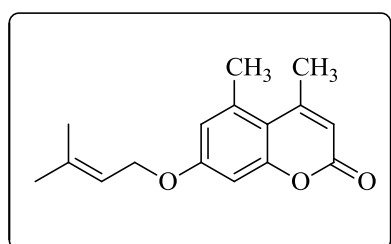
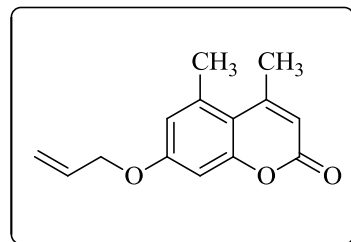
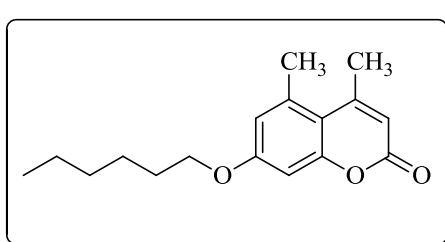
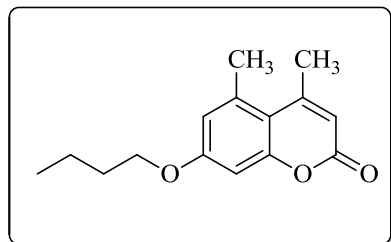
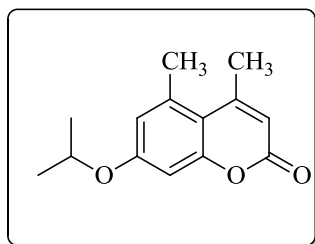
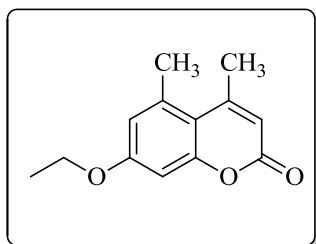
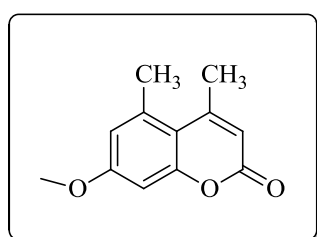
I would like to express my deepest gratitude to Langaletu Daniel Mthembu, who has the attitude and the substance of a genius, for motivating me and for his unceasing encouragement and support.

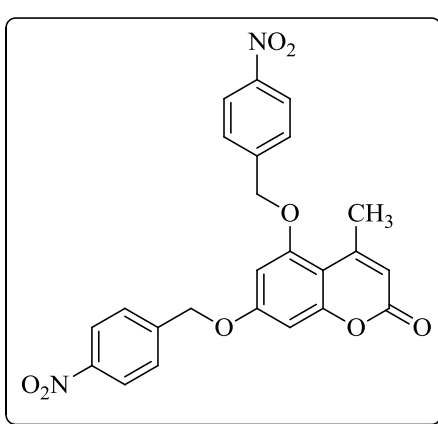
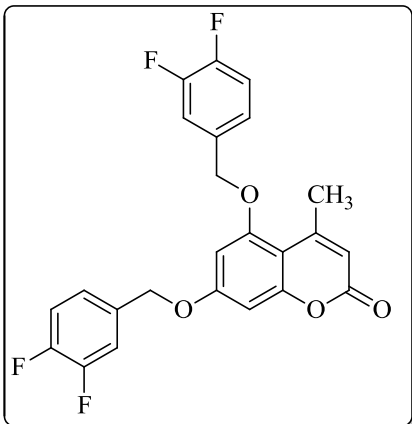
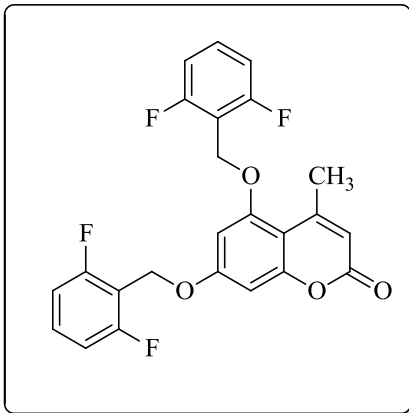
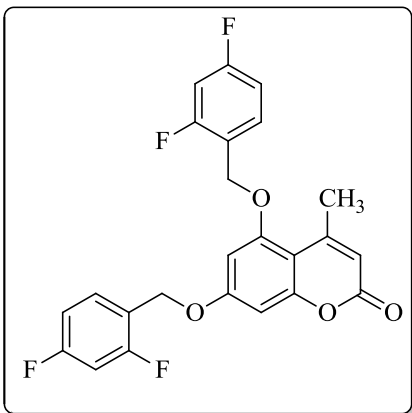
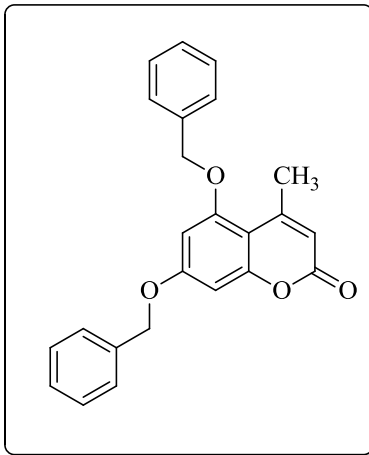
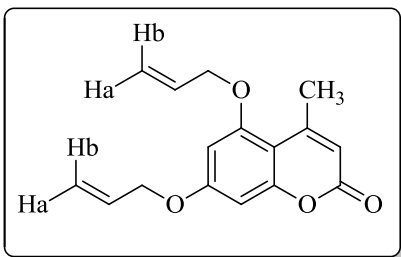
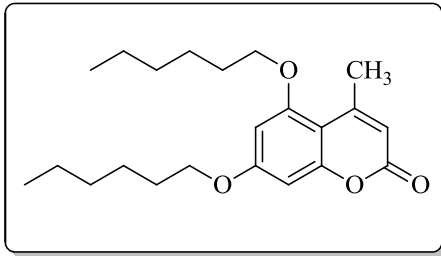
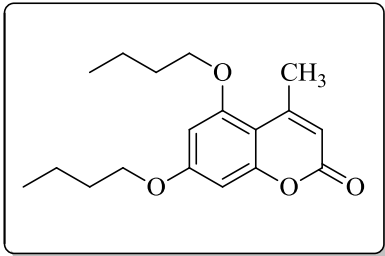
I would also like to thank my friends, Nontokoza Duma, Ayanda Shabalala, Simelwe Mpfana, Zintle Base, Nokulunga Nxele, Phakamile Mthlane, Nomfundo Kheswa, Samkelisiwe Ngubane and Neha Manhas, who kept me going with their prayers, love, support and motivated me to push harder everyday.

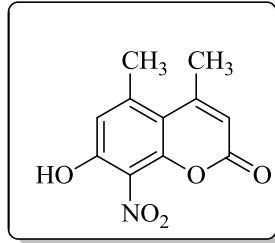
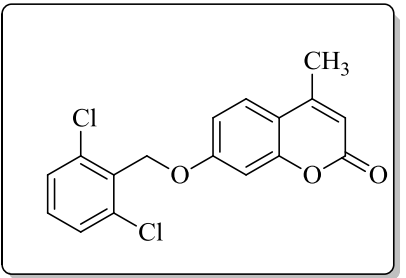
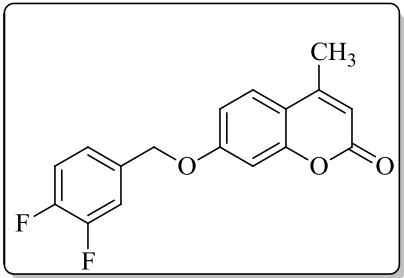
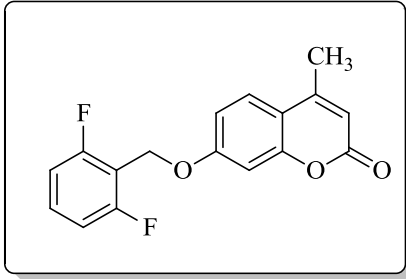
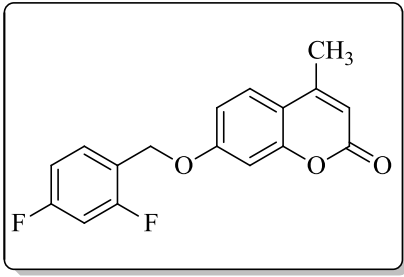
I am also grateful to everyone who, directly and indirectly, lent me their helping hand in this venture.

“Merci beaucoup”

Novel compounds synthesized







Previously synthesized coumarins

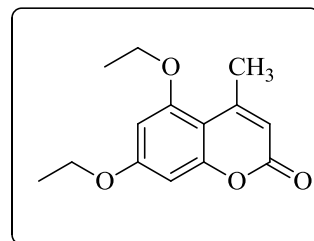
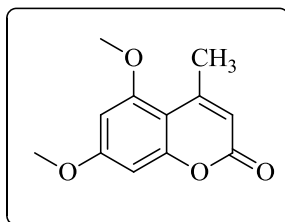
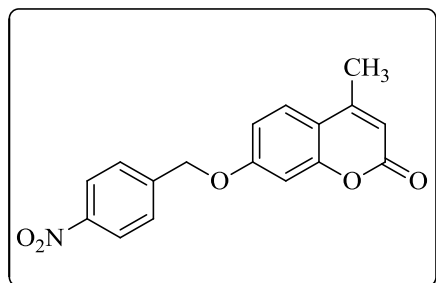
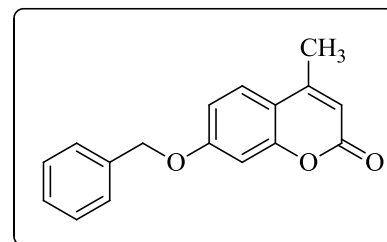
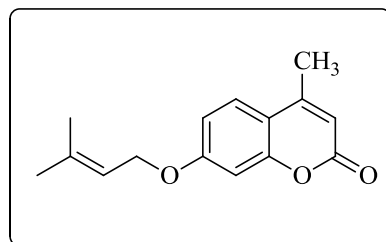
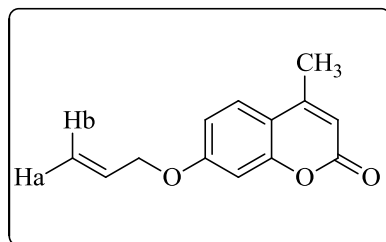
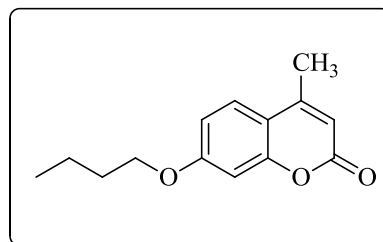
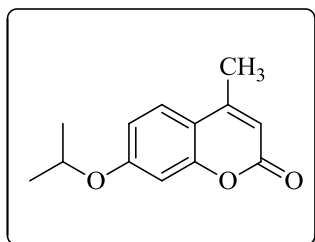
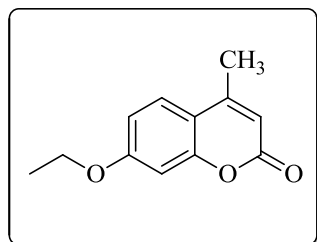
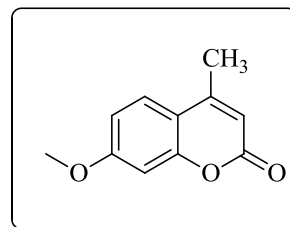
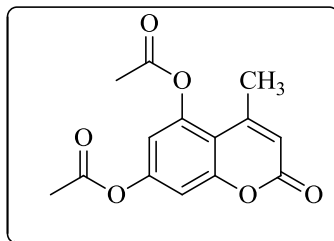
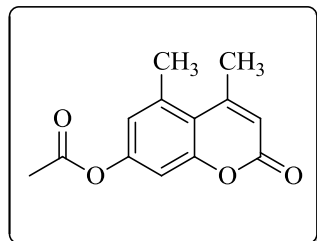
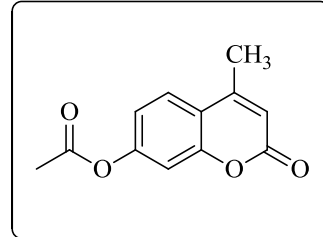
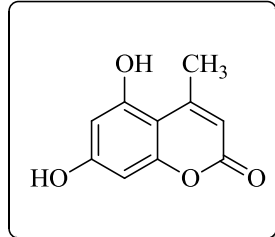
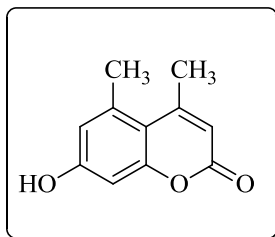
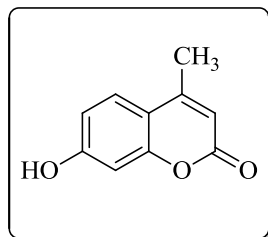


Table of contents	Page no.
Chapter 1. Introduction	1
1.1. Diabetes mellitus.....	1
1.2. Introduction to coumarins	2
1.3. What makes coumarins effective?.....	4
1.4. Biological activities of coumarins	4
1.5. How to enhance the activity of the coumarin?	6
1.6. Fluorine as a substituent.....	6
1.7. Synthetic methods of coumarins.....	7
1.7.1. The Pechmann Reaction	8
1.7.2. Knoevenagel condensation	8
1.7.3. Wittig Reaction	9
1.7.4. Perkin condensation reaction	9
1.7.5. Kostanecki-Robinson reaction	9
1.7.6. Reformatsky reaction	10
1.7.7. Ponndorf reaction	10
1.7.8. Houben-Hoesch reaction	10
1.8. Applications of coumarins	11
1.9. Antidiabetic activity testing	12
1.10. Antioxidant activity assay	13
1.10.1. DPPH scavenging activity	14
1.10.2. Hydroxyl radical scavenging activity	14
1.10.3. Superoxide radical scavenging activity	14
1.10.4. Hydrogen peroxide scavenging assay	14
1.10.5. Thiobarbituric acid method	14
1.10.6. In vivo methods	15
1.11. Introduction to molecular modelling	15
1.12. Aim and objectives	17

Chapter 2. Literature survey

2.1.	Past work on the coumarin and 4-methyl coumarin derivatives.....	18
2.2.	4-Methylcoumarins with antioxidant activity.....	18
2.3.	4-Methylcoumarins with antimicrobial activity.....	19
2.4.	Coumarins with photochromic properties.....	24
2.5.	Coumarin derivatives with catalytic activity.....	25
2.6.	4-Methylcoumarins with antibacterial activity.....	26
2.7.	4-Methylcoumarins where no activity was tested.....	27
2.8.	Coumarins with phytotoxic activity.....	30
2.9.	Coumarins with cytotoxic activity.....	31
2.10.	Coumarins with antifouling properties.....	33

Chapter 3. Experimental Section

3.1.	General experimental procedure.....	34
3.2.1.	Synthesis of 4-methylcoumarins (A-C).....	35
3.2.2.	Acetylation of 4-methylcoumarins (A-C).....	36
3.2.3.	Alkylation of 4-methylcoumarins (A-C).....	38
3.2.4.	Nitration of 4-methylcoumarins.....	54
3.3.	Antidiabetic and antioxidant activity testing methods.....	55
3.3.1.	DPPH radical scavenging activity.....	55
3.3.2.	Determination of α -glucosidase inhibitory activity of coumarins.....	55
3.3.3.	Determination of α -amylase inhibitory activity of coumarins.....	55
3.3.4.	Statistical analysis.....	56
3.3.5.	Homology modelling.....	56
3.3.6.	Molecular docking method.....	56

Chapter 4. Results and discussion

4.1.	Synthesis of 7-hydroxycoumarins (A-C).....	58
4.2.1.	Synthesis of single O-acetylated coumarins (A1-B1).....	59

4.2.2.	Synthesis of single O-alkylated coumarins (A2-A13, B2-B13).....	62
4.3.	Synthesis of double O-acetylated/alkylated coumarins (C1-C12).....	68
4.4.	Nitration of coumarins (A-C).....	71
4.5.	Anti-diabetic and Anti-oxidant evaluation of coumarin analogues.....	74
4.6.	Docking results.....	86
	Chapter 5. Conclusion and Recommendations	95
	References	97

List of Figures	Page no.
Figure 1.1. Structure of coumarin.....	2
Figure 1.2. Structures of the α -benzopyrone and the β -benzopyrone.....	3
Figure 1.3. Chemical structure of novobiocin.....	3
Figure 1.4. Chemical structure of Geiparvarin, a coumarin with cytotoxic activity....	4
Figure 1.5. Chemical structure of Dicoumarol, a coumarin with antibacterial activity.....	5
Figure 1.6. Chemical structure of warfarin, a coumarin that has anticoagulant activity.....	5
Figure 4.1. ^1H (a) and ^{13}C (b) NMR spectrum of 4-methyl-2-oxo-2H-chromen-7-yl acetate (A1).....	61
Figure 4.2. ^1H (a) and ^{13}C (b) NMR spectrum of 4, 5-dimethyl-7-(propan-2-yloxy)-2H- chromen-2-one (B4).....	65
Figure 4.3. ^1H (a) and ^{13}C (b) NMR spectrum (expansion) of [(2,6-difluorobenzyl)oxy]-4,5-dimethyl-2H-chromen-2-one (B11).....	67
Figure 4.4. ^1H (a) and ^{13}C (b) NMR spectrum of 4, 5-dimethyl-7-(propan-2-yloxy)-2H-chromen-2-one (C4).....	70
Figure 4.5. ^1H NMR spectrum of B15 (a) and B(b).....	73
Figure 4.6. HMBC spectrum of B15 showing important correlations.....	74
Figure 4.7. In vitro α -Glucosidase activity of coumarin derivatives (B1-B9, B15, and C2-C8) along with the standard inhibitor (acarbose).....	75
Figure 4.8. In vitro α -amylase inhibition activity of coumarin derivatives (B1-B9, B15, and C2-C8) along with the standard inhibitor (acarbose).....	79
Figure 4.9. DPPH radical scavenging activity of coumarin derivatives (B1-B9, B15, and C2-C8) along with the standard drug (ascorbic acid).....	80
Figure 4.10. Sequence alignment of α -glucosidase from <i>S. cerevisiae</i> (uniprot access code: P53341)) with the <i>S. cerevisiae</i> from isomaltase (pdb code: 3AJ7). Sequence overlaps are highlighted in blue whereas the conservative substitutions are highlighted in green.....	89
Figure 4.11. Overlay of the predicted homology model of α -glucosidase (shown in red flat ribbons format) with the <i>Sacchromyces cerevisiae</i> isomaltase (shown in green flat ribbon format), with the computed RMSD <math><1.5\text{\AA}</math>...	90
Figure 4.12. Docked complex of B2 (blue sticks) with the α -glucosidase. Only interacting amino acids (red lines) of enzyme are shown for clarity purpose. Conventional hydrogen bonds as green dotted lines, non-	90

	conventional hydrogen bonds as grey dotted lines and hydrophobic interactions are depicted as magenta dotted lines.....	
Figure 4.13.	Docked complex of B3 with the α -glucosidase. Only interacting amino acids (red lines) of enzyme are shown for clarity purpose. Conventional hydrogen bonds as green dotted lines, non-conventional hydrogen bonds as grey dotted lines and hydrophobic interactions are depicted as magenta dotted lines.....	91
Figure 4.14.	Docked complex of B6 with the α -glucosidase. Only interacting amino acids (red lines) of enzyme are shown for clarity purpose. Conventional hydrogen bonds as green dotted lines, non-conventional hydrogen bonds as grey dotted lines, electrostatic as yellow dotted line and hydrophobic interactions are depicted as magenta dotted lines.....	91
Figure 4.15.	Docked complex of B5 with the α -glucosidase. Only interacting amino acids (red lines) of enzyme are shown for clarity purpose. Conventional hydrogen bonds as green dotted lines, non-conventional hydrogen bonds as grey dotted lines and hydrophobic interactions are depicted as magenta dotted lines.	92
Figure 4.16.	Docked complex of B9 with the α -glucosidase. Only interacting amino acids (red lines) of enzyme are shown for clarity purpose. Conventional hydrogen bonds as green dotted lines, non-conventional hydrogen bonds as grey dotted lines, electrostatic as yellow dotted lines and hydrophobic interactions are depicted as magenta dotted lines.....	92
Figure 4.17.	Docked complex of B11 with the α -glucosidase. Only interacting amino acids (red lines) of enzyme are shown for clarity purpose. Conventional hydrogen bonds as green dotted lines, non-conventional hydrogen bonds as grey dotted lines and hydrophobic interactions are depicted as magenta dotted lines.....	93
Figure 4.18.	Docked complex of C5 with the α -glucosidase. Only interacting amino acids (red lines) of enzyme are shown for clarity purpose. Conventional hydrogen bonds as green dotted lines, non-conventional hydrogen bonds as grey dotted lines and hydrophobic interactions are depicted as magenta dotted lines.....	93
Figure 4.19.	Docked complex of C7 with the α -glucosidase. Only interacting amino acids (red lines) of enzyme are shown for clarity purpose. Conventional hydrogen bonds as green dotted lines, non-conventional hydrogen bonds as grey dotted lines and hydrophobic interactions are depicted as magenta dotted lines.....	94
Figure 4.20.	Docked pose of acarbose in the binding pocket of α -glucosidase. Only interacting amino acids (red lines) of enzyme are shown for clarity purpose. Conventional hydrogen bonds as green dotted lines, non-conventional hydrogen bonds as grey dotted lines and hydrophobic interactions are depicted as magenta dotted lines.	94

List of schemes	Page no.
Scheme1.1. Synthesis of 4,7-substituted coumarin <i>via</i> the Pechmann reaction.....	8
Scheme1.2. Synthesis of coumarin using the Knoevenagel condensation reaction.....	8
Scheme1.3. Synthesis of 4,7-substituted coumarin using the Wittig reaction.....	9
Scheme1.4. Synthesis of substituted coumarins <i>via</i> the Perkin reaction.....	9
Scheme1.5. Synthesis of 3,4-substituted coumarin <i>via</i> the Kostanecki-Robinson reaction...	10
Scheme1.6. Synthesis of 4-substituted coumarin <i>via</i> the Reformatsky reaction.....	10
Scheme1.7. Synthesis of substituted coumarins using the Ponnendorf reaction.....	10
Scheme1.8. Synthesis of 4,7-substituted coumarin <i>via</i> the Houben-Hoesch reaction..	11
Scheme2.1. Synthetic route for 4-methylcoumarin derivatives.....	19
Scheme2.2. Synthesis of 4-methylcoumarins with aryl groups.....	20
Scheme2.3.1. Synthesis of esterified coumarins.....	20
Scheme2.3.2. Synthesis of imines.....	21
Scheme2.3.3. Synthesis of a triazolethione and a thiadiazole.....	22
Scheme2.3.4. Synthesis of pyrazole and pyrrole derivatives.....	22
Scheme2.4.1. Esterification reaction of 7-O-substituted coumarin.....	23
Scheme2.4.2. Synthesis of imines with aryl groups.....	24
Scheme2.5. Synthesis of Bis-spiropyrans.....	24
Scheme2.6. Synthesis of metal containing 4-methylcoumarins.....	25
Scheme2.7. Synthesis of 4-methylcoumarins with long chain fatty acids.....	26
Scheme2.8. Synthesis of nitrogen containing 4-methylcoumarins.....	27
Scheme2.9.1. Synthesis of 8-hydroxy-4-methylcoumarin.....	27
Scheme 2.9.2. Synthesis of 4-methylcoumarin via a Co/SBA-15 catalysed reaction.....	28
Scheme2.10. Synthesis of 4-methylcoumarin via a sawdust-SO ₃ H catalysed reaction..	29
Scheme2.11. Preparation of o-substituted coumarin derivatives.....	29
Scheme2.12. Synthesis of sulfonamide-containing coumarins.....	30
Scheme2.13. Synthesizing 4-methylcoumarins from β -substituted acrylates.....	30
Scheme2.14. Synthesis of simple 4-methylcoumarins.....	31
Scheme2.15. Synthesis of 7-hydroxy-4-methylcoumarin derivatives.....	32
Scheme2.16.1. Synthesis of 3-(4-methyl-2-oxo-2H-chromen-7-yloxy) propanoic acid...	33
Scheme2.16.2. Synthesis of coumarins containing aminophosphonates.....	33

Scheme 2.17.	Synthesis of 7-hydroxy-4-methylcoumarin via the Pechmann reaction...	33
Scheme 4.1.	Synthesis of coumarins (A-C) from ethyl acetoacetate and substituted phenols.....	58
Scheme 4.2.	Proposed mechanism of the Pechmann reaction.....	59
Scheme 4.3.	O-acylation reaction of coumarins (A and B) bearing single hydroxy group.....	60
Scheme 4.4.	O-alkylation reaction of coumarins (A and B) bearing single hydroxy group.....	62
Scheme 4.5.	O-acetylation/alkylation reactions of coumarin C bearing double hydroxyl groups.....	68
Scheme 4.6.	Nitration of 4-methylcoumarins (A-C).....	71

List of tables	Page no.
Table 4.1. Experimental properties of three different 4-methylcoumarins (A-C) synthesized from ethyl acetoacetate and substituted phenols in Scheme 4.1.....	59
Table 4.2. Shows experimental properties of compounds (A2-A13, B2-B13) synthesized via the acetylation and alkylation reactions of coumarins (A-B).....	63
Table 4.3. Shows the experimental properties of compounds synthesized via the acetylation and alkylation reactions of coumarin C.....	69
Table 4.4. In vitro IC ₅₀ values of antioxidant and α -glucosidase inhibition activities of the acetylated (B1), alkylated (B2-B9 and C2-C7) and nitrated (B15) coumarin analogues along with the reference drugs (Ascorbic acid and Acarbose).....	76
Table 4.5. In vitro IC ₅₀ values of antioxidant and α -glucosidase inhibition activities of the coumarin analogues (A1-A13, B10-B14, C1 and C9-C12), their precursors (A-C) and the reference drugs (Ascorbic acid and Acarbose).....	82

List of abbreviations

1D-	One dimensional
2D-	Two dimensional
3D-	Three dimensional
Abs-	absorbance
aq.-	aqueous
Ar-	aryl
bs-	broad singlet
CDCl ₃ -	deuterated chloroform
CH ₃ -	methyl
CF ₃ -	Trifluoromethyl
COSY-	Correlation Spectroscopy
CS ₂ -	Carbon disulfide
d-	doublet
dd-	doublet of doublets
dddd-	doublet of doublet of doublet of doublets
DM-	Diabetes Mellitus
DMF-	Dimethylformamide
DMSO-d ₆ -	deuterated dimethyl sulfoxide
DNA-	Deoxyribonucleic acid
DPPH-	1-diphenyl-2-picrylhydrazyl
EDTA-	Ethylenediaminetetraacetic acid
EtOH-	Ethanol
F-	Fluorine
FeCl ₃ -	Iron trichloride
FT-IR-	Fourier Transform-Infrared Spectroscopy
H-	Hydrogen
HCl-	Hydrochloric acid
H ₂ O ₂ -	Hydrogen peroxide
HIV-	Human Immunodeficiency Virus

HMBC-	Heteronuclear Multiple Bond Coherence
HNO ₃ -	Nitric acid
Hr-	hour
HRMS-	High Resolution Mass Spectroscopy
HSQC-	Heteronuclear Single Quantum Coherence
Hz-	Hertz
I ₂ -	Diiodine
IC ₅₀ -	half maximal inhibitory concentration
IZ-	Inhibition zone
H ₂ O-	Water
H ₂ SO ₄ -	Sulfuric acid
K ₂ CO ₃ -	Potassium carbonate
KH ₂ PO ₄ -	Potassium Dihydrogen Phosphate
KOH-	Potassium hydroxide
KSCN-	Potassium thiocyanate
L-	Litre
M-	molarity
mg-	milligram
MHz-	Mega Hertz
MIC-	minimum inhibitory concentration
Min-	minute
ml-	milliliter
mmol-	millimole
mmol/L-	millimole/litre
mM-	micro molar
mol-	mole
μL-	microliter
μg/ml-	micrograms per milliliter
NaOH-	Sodium hydroxide
nm-	nanometer

NMR-	Nuclear Magnetic Resonance
NOESY-	Nuclear Overhauser Effect Spectroscopy
OH-	hydroxyl
Pd-	Palladium
Pd/C-	Palladium on carbon
pH-	Potential of hydrogen
ppm-	parts per million
R _f -	Retention value
rpm-	revolutions per minute
s-	singlet
SeO ₂ -	Selenium dioxide
t-	triplet
TLC-	Thin Layer Chromatography
Tris-HCl-	Trizma-hydrochloric acid buffer
tt-	triplet of triplets
T1D-	Type 1 diabetes
T2D-	Type 2 diabetes
v/v-	volume/volume
X-Ray-	X-radiation

List of Symbols

- α - alpha
- π - pi
- σ - sigma
- β - beta
- %- percentage
- μ - micro
- δ - chemical shift
- J - coupling constant
- $^{\circ}\text{C}$ - degrees Celsius
- \AA - Angstrom

CHAPTER 1

Introduction

1.1. Diabetes mellitus

Diabetes mellitus (DM) is a group of metabolic diseases illustrated by abnormally high levels of plasma glucose or hyperglycemia. Approximately, 382 million people are living with diabetes mellitus worldwide {International Diabetes Federation (IDF), 2014} with greater number of cases in developing countries particularly in the Middle East and North Africa. Since 1936, the two main distinctive clinical forms of diabetes (type 1 and type 2) have been identified. Type 1 (T1D) or insulin-dependent diabetes, usually diagnosed in children and young adults, is caused by the destruction of the insulin-producing beta cells of the Islets of Langerhans in the pancreas, leading to a deficiency of insulin. Insulin is a peptide hormone that is produced in the Islets of Langerhans in the pancreas and causes glucose uptake into liver, fat, muscle and storage as glycogen in the muscle and liver. In T1D condition, the body does not produce enough insulin that is required to perform these metabolic functions. Type 2 diabetes (T2D) or non-insulin-dependent diabetes mellitus (NIDDM) is the common form of diabetes that is characterized by insulin resistance or reduced insulin sensitivity, combined with reduced insulin secretion and hyperglycemia. T2D is usually accompanied by cardiovascular and neurological complications (Zhao *et al.*, 2015). The important contributing factors for T2D include (i) body cell resistance to insulin (ii) increased hepatic glucose production (iii) decreased insulin-mediated glucose transport into adipose tissue and muscle and (iv) impaired beta-cell function leading to loss of early phase of insulin release in response to hyperglycaemic stimuli.

Currently, a number of antidiabetic drugs targeting different receptors such as α -glucosidase, aldose reductase (ALR), dipeptidyl peptidase-4 (DPP-4), protein tyrosine phosphatase 1B (PTP1B), peroxisome proliferator activated receptor-g (PPAR-g) and free fatty acid receptor1 (FFA1) are available in the market. Commonly used to treat diabetes but they produce various complications (most notably high risk of hypoglycaemia, bodyweight gain and gastric symptoms). Amongst these receptors, the α -glucosidase has gained significant attention of medicinal chemists and various potent anti-diabetic agents have been designed and synthesised by inhibition of this enzyme.

The α -glucosidase enzyme is present in the epithelium cells of intestine (Taha *et al.*, 2015) which catalyse the digestion/ break down of carbohydrates (Taha *et al.*, 2015) into absorbable monosaccharides leading to increased glucose level in blood. Hence, the inhibition of α -

glucosidase reduces blood glucose level by delaying digestion of carbohydrates, and in turn suppresses postprandial hyperglycaemia (Wang *et al.*, 2016). However, the effectiveness of existing α -glucosidase inhibitors has significantly been hampered by various unwanted side effects including flatulence, diarrhea, and abdominal discomfort and anaemia. Hence, the search for new α -glucosidase inhibitors with better pharmacological profiles is still underway (Kazeem *et al.*, 2016).

The α -amylase is another enzyme that catalyses the cleavage of glucose (Zhao *et al.*, 2015), and is also very effective in the treatment of DM. It is involved in the conversion of starch and glycogen into glucose, the α -amylase enzyme hydrolyzes the alpha bonds of the alpha-linked polysaccharides. To reduce the post-prandial increase of blood glucose, the activity of the enzymes alpha-glucosidase and alpha-amylase must be inhibited.

1.2. Introduction to coumarins

Research on coumarins has increased significantly over the years due to their versatile pharmacological and biochemical properties (Avó *et al.*, 2013). The major factor being the biological activities that they possess (Borges *et al.*, 2005) and their low toxicity (Garazd, Garazd *et al.*, 2005). Their potential contribution in the prevention and treatment of diseases is an attractive highlight in the pharmaceutical industry (Peng *et al.*, 2013). Much attention has been invested in coumarin derivatives ever since the coumarin which was classified as a toxic substance by the Food and Drug Administration (FDA) in 1954 was declared safe. It was classified as toxic because it caused liver tumours in rats. It has been proven that rats are a poor model to compare with humans for this metabolism because rats excrete coumarin metabolites in bile, hence causing liver tumours while humans and hamsters excrete them in urine (Lacy *et al.*, 2004).

Coumarins also known as 2-H-1-chromene-2-ones (Gao *et al.*, 2013) belong to the lactone family that has a benzopyrone framework (**Figure 1.1**), where a benzene ring is fused with a pyrone ring.

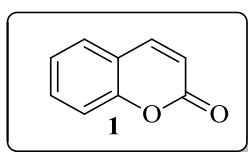


Figure 1.1: Structure of coumarin

The benzopyrone ring can be further subdivided into two groups, the α -benzopyrone and the β -benzopyrone. The difference between the two is that the α -benzopyrone has a carbonyl group at position number 2 and the β -benzopyrone has a carbonyl group at position number 4 (**Figure 1.2**).

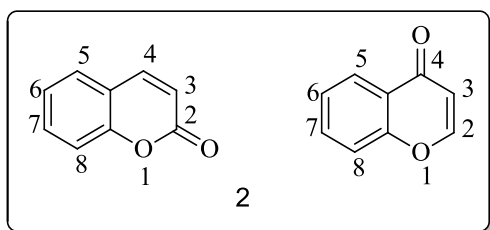


Figure 1.2: Structures of the α -benzopyrone and the β -benzopyrone

The coumarins not only occur naturally but have been synthesized using different synthetic methods (Lacy *et al.*, 2004). Natural coumarins can be extracted from different plants using different methods such as maceration under sonification, supercritical fluid extraction and infusion. Since these methods are time consuming and require sophisticated instruments, the synthesis of coumarins has increased over the years (Tyagi *et al.*, 2007). Different coumarins have also been isolated from microorganisms and animals (Borges *et al.*, 2005).

The first coumarin was extracted in 1820 from a tonka bean called *Coumarouna odorata* Aube (Vogel, 1820.; Borges *et al.*, 2005) or *Dipteryx odorata* Wild, Fabaceae which is commonly known as Coumarou, hence the name coumarin (Lacy *et al.*, 2004). Subsequently, the coumarin core has been discovered in naturally occurring antibiotics such as chlorobiocin, novobiocin and coumermycin A₁ (Matos *et al.*, 2012). Novobiocin (**Figure 1.3**) which is extracted from *Streptomyces niveus* (Lanoot *et al.*, 2002) is used in the treatment of methicillin-resistant *Staphylococcus aureus* which causes most of the deadliest infections that are hard to treat (Walsh *et al.*, 1993). In addition, coumarins have also been isolated from other plant families (Avo *et al.*, 2013), where they have been localized in their roots, stems, leaves, flowers, fruits, peels and seeds (Wang *et al.*, 2013).

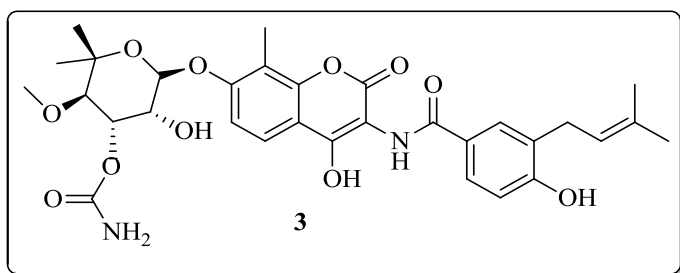


Figure 1.3: Chemical structure of novobiocin

1.3. What makes coumarins effective?

Coumarins are common motifs found in drugs, spices, agricultural chemicals and dyes (Gao *et al.*, 2013). The benzopyrone framework of coumarins interact efficiently with the enzymes and receptors by establishing strong bonding network. For instance, the π - π conjugated system that is found in the fused structure of the benzene ring and the α -pyrone is electron rich and has good charge-transport properties. Moreover, the coumarins have good bioavailability, and thus are rapidly absorbed and distributed in the body. They have high partition coefficients which increases their absorption rate once in the aqueous solution (Lacy *et al.*, 2004).

1.4. Biological activities of coumarins

The major reason for the massive increase in the synthesis of coumarins and their derivatives is because of the wide spectrum of biological activities that they possess. These include anti-cancer (Hitotsuyanagi *et al.*, 1996) and anti-HIV activities (Bedoya *et al.*, 2005). They are also known as antioxidants (Khoobi *et al.*; 2011), enzymatic inhibitors or vasorelaxants (Quezada *et al.*, 2010) including antidiabetic (Lee *et al.*, 2004) activities which are commonly found in natural coumarins. The 3,4-unsubstituted coumarins, being the most common naturally occurring coumarins, show the potential of having activities like antimicrobial (Imran *et al.*, 2015), antimalarial (Cubukcu *et al.*, 1990) and antitumor activity (Murakami *et al.*, 1997).

The synthetic coumarin analogues are also equally important and exhibit a variety of biological activities. For instance, Geiparvarin, a synthetic monoamine oxidase inhibitor is known to have potent cytotoxic activity (**Figure 1.4**) (Miglietta *et al.*, 2001).

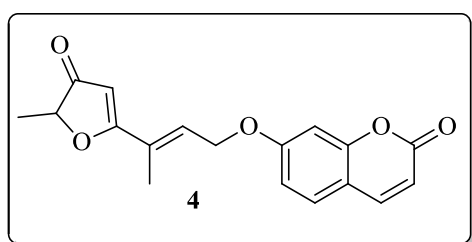


Figure 1.4: Geiparvarin as cytotoxic agent.

Similarly, the coumarins with anti-bacterial (Emami *et al.*, 2008), anti-inflammatory (Kontogiorgis *et al.*, 2005), anti-carcinogenic (Nair *et al.*, 1991) and analgesic activity (Gupta *et al.*, 2011) are documented in the literature. Coumarins have anticoagulant (Golfakhrabadi *et al.*, 2014) and antithrombotic properties (Jain *et al.*, 2013). They also have antiviral (Hwu *et al.*, 2008), anti-osteoporosis (Sashidhara *et al.*, 2013), antisepsis (Zhang *et al.*, 2005),

hepatoprotective (Atmaca *et al.*, 2011), anti-neurodegenerative (Jameel *et al.*, 2015), antifungal (Sardari *et al.*, 1999), anti-parasitic (de Alcantara *et al.*, 2015), antimycobacterial (Virsdioia *et al.*, 2010), anti-depressive (Sashidhara *et al.*, 2011), appetite-suppressor (Link, 1959), anti-allergic (Buckle *et al.*, 1975), herbicidal (Nazemi *et al.*, 2015), anthelmintic (Patil *et al.*, 2015), inhibition of platelet aggregation (Lee *et al.*, 2003), immunomodulatory (Prousis *et al.*, 2014) activities. Activities like estrogenic (Jiménez-Orozco *et al.*, 2011), molluscicidal (Schönberg *et al.*, 1954), anticonvulsant (Amin *et al.*, 2008), tyrosinase inhibitor (Fais *et al.*, 2009), antihyperlipidemic (Yuce *et al.*, 2009), anti-parkinsonism (Asif, 2015), antipyretics (Eissa *et al.*, 2009), bronchodilator (Leal *et al.*, 2000), antimoebic (Iqbal *et al.*, 2009) and antiulcer (Goel *et al.*, 1997) have also been reported. Coumarins are also active in the central nervous system (CNS) (Borges *et al.*, 2005), antinociceptive (de Almeida Barros *et al.*, 2010; Alipour *et al.*, 2014) and anticholinesterase (Razavi *et al.*, 2013; Emami *et al.*, 2015). Dicoumarol (5) is an example of coumarin with antibacterial activity (Goth, 1945) while warfarin (7) possesses anticoagulant activity (Golfakhrabadi *et al.*, 2014).

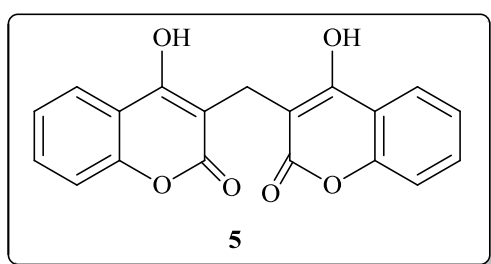


Figure 1.5: Chemical structure of Dicoumarol

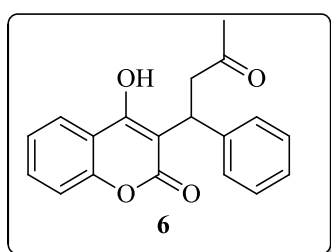


Figure 1.6: Chemical structure of warfarin.

1.5. How to enhance the activity of the coumarin?

The search for new drugs is crucially important as the old drugs have tendency to lose their effectiveness after a certain period of time due to several sociological and physiological factors. The structural manipulation of existing drugs or preparation of completely new chemical entities with better pharmacological profiles are the main areas of current drug development. Keeping this in view, several developments have been made to improve the activity profiles of coumarin based drugs. For example, an increase in anti-inflammatory activity of coumarins has been observed when a halogen is introduced at the 6th position and any functional group (other than hydrogen) and an Ar group is substituted at the 8th position (Pu *et al.*, 2014). Another way of increasing the biological activity of coumarins is by substituting fluoro and sulfonamide moieties into the coumarin ring (Kalkhambkar, 2008). The presence of sulfonamide moiety has been reported to increase the antibacterial and antitumor activities in several other pharmacophores (Zani *et al.*, 1998). Similarly, the incorporation of Schiff bases or the positioning of hydrophobic groups at position 2, 3 and 4 into the coumarin have been observed to increase its cytotoxic activity (Naik *et al.*, 2006). Analgesic activity has also been amplified by substituting 2, 4-dichloro or 2, 6-dihydro phenyl groups into the coumarin core (Asif, 2015). Similarly, the same authors reported that having an acyl phenyl group at position 4 increases the bacterial activity against *H. pylori* metronidazole resistant strains. Coumarins with substitution at position 4 are also reported to exhibit good antimicrobial activity (Matos *et al.*, 2012).

1.6. Fluorine as a substituent

The introduction of fluorine into a heterocycle significantly influences the biological activity of the compound in a positive way. More than 20% of existing pharmaceuticals (Sahoo *et al.*, 2012) contain fluorine in their structure e.g. Prozac (Wong *et al.*, 1995) and ciprofloxacin (Oxford Handbook of Infectious Diseases and Microbiology, 2009).

Due to the fact that fluorinated compounds are the least abundant naturally, the synthesis of fluorine containing compounds has increased over the years (Müller *et al.*, 2007). Fluorine enhances the metabolic stability by lowering the susceptibility of nearby moieties to cytochrome P₄₅₀ enzymatic oxidation (Park *et al.*, 2001). Having a CF₃ group or any F substituent in a compound increases the potency of the compound (Roth *et al.*, 1990). It is well known that fluorine is the most electronegative element and the C-F bond is the strongest. C-C bonds adjacent to this bond are also strengthened while C=C bonds are weakened (Smart,

1994). Intermolecular interactions are also influenced by the very low polarizability of organofluorine substituents (Smart, 2001). An increase in potency is also experienced in cases where C-F replaces a C=O bond (Black *et al.*, 2005).

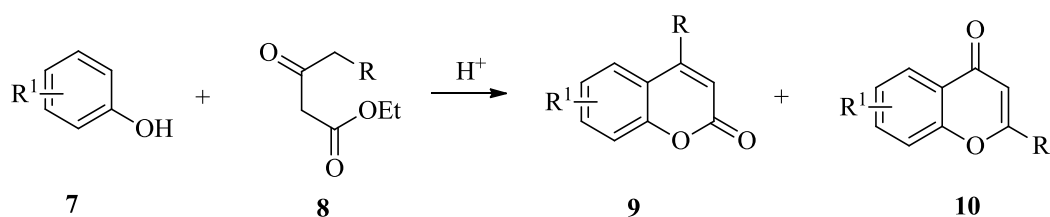
When methoxy groups are replaced by trifluoromethoxy groups, stereoelectronic effects are maximized because of the large size of fluorine (Müller *et al.*, 2007). Introducing fluorine into a piperidine ring is advantageous because it decreases the basicity of the nitrogen center while increasing the oral bioavailability of the compound because of the σ -inductive effect of fluorine (Morgenthaler *et al.*, 2007). When the amine basicity is increased by introducing fluorine, the membrane permeability is also increased (Avdeef, 2001). Fluorine atoms can deprotonate an amine at physiological pH, which increases the bioavailability of the compound (van Neil *et al.*, 1999). Organic fluorine has a very low proton affinity and is weakly polarizable (Paulini *et al.*, 2005). When substituted in the para position of benzyl ring, it enhances the binding affinity by a factor of 6 (Olsen *et al.*, 2003).

1.7. Synthetic methods of coumarins

Although, the coumarins occur naturally, their low abundance in plants, tedious isolation procedures and considerably low yields necessitate their synthesis in the organic laboratories. Traditionally, a number of methods such as Perkin reaction (Perkin, 1868), Pechmann (Pechmann, 1884), Wittig (Wittig *et al.*, 1954), Reformatsky (Reformatsky, 1887) and Knoevenagel (Knoevenagel, 1898) reaction, have been used for the synthesis of coumarin derivatives. The Perkin, Pechmann and Knoevenagel reactions are usually more favourable when preparing coumarins that have substituents at the third and fourth positions. Different acidic and basic catalysts have been used to catalyse these reactions. In addition, a range of established synthetic methods *viz.* the Claisen rearrangement (Claisen, 1925), the Vilsmeier-Haack (Vilsmeier *et al.*, 1927) and Suzuki cross-coupling reactions (Suzuki, 1991), Nickel-catalyzed cycloaddition (Nakai *et al.*, 2015) and Pd-catalyzed site-selective cross-coupling reactions (Zhang *et al.*, 2007), Kostanecki-Robinson (Kostanecki *et al.*, 1901), Ponndorf (Ponndorf, 1925) and Houben-Hoesch reactions (Hoesch, 1915) have also been employed in coumarin synthesis. The one-pot Wittig reaction/cyclization usually favours the formation of 3,4-unsubstituted coumarins (Wittig *et al.*, 1954). Substitution of different functional groups on the coumarin core, at different positions results in expansion of the properties of coumarin chromophores. Some of the traditional reactions used in coumarin synthesis are briefly described in the following section.

1.7.1. The Pechmann reaction

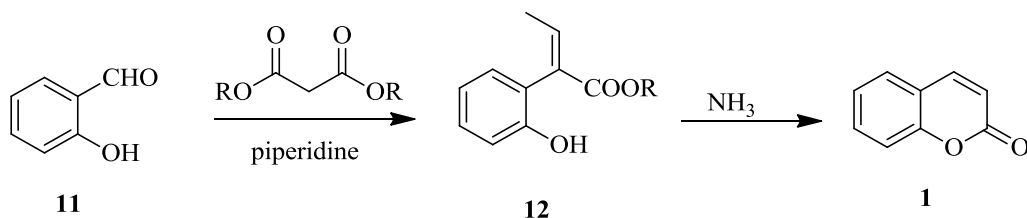
The Pechmann reaction (**Scheme 1.1**) involves the condensation of substituted phenols (**7**) with β -ketoesters (**8**) (Pechmann, 1884) in the presence of an acid in catalytic amount. The coumarins (**9**) synthesized using this approach are usually obtained in high yields. The chromone (**10**) is the commonly observed side product in the Pechmann reaction. The usage of corrosive acids, long reaction duration (>20 hr) and formation of side-products, are few limitations of the reaction.



Scheme 1.1. Pechmann reaction for synthesis of substituted coumarins.

1.7.2. Knoevenagel condensation

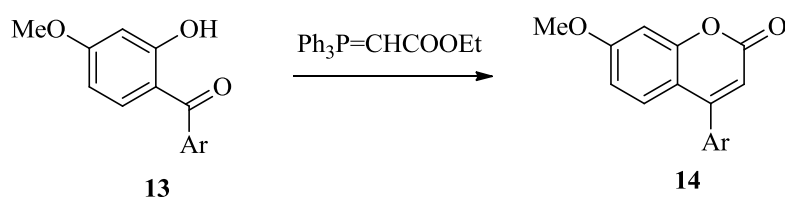
The Knoevenagel condensation is also one of the simplest and most common methods that has been used for the synthesis of coumarins (Knoevenagel, 1898). This reaction involves the condensation of aldehydes (**11**) with methylene compounds that are activated in the presence of ammonia or any other amine, yielding coumarin (**1**) (**Scheme 1.2**). This reaction is usually conducted in organic solvents in the presence of catalytic amount of organic bases like pyridine and piperidine. The disadvantages associated with the Knoevenagel condensation include expensive catalysts, laborious multi-step procedures, and long reaction time. The modification of Knoevenagel reaction where malonic acid and pyridine are used in the presence or absence of piperidine, is known as the Doebner reaction (Doebner, 1902).



Scheme 1.2. Synthesis of coumarin using the Knoevenagel condensation reaction.

1.7.3. Wittig reaction

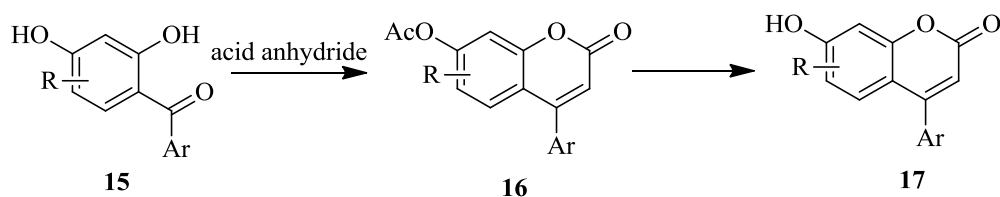
The Wittig reaction (**Scheme 1.3**) involves the formation of an alkene after the condensation of ethoxycarbonylmethylenetriphenylphosphorane and 2-hydroxybenzophenones, which after cyclization results into a coumarin system. The reaction proceeds through betaine and/or oxaphosphetane intermediates. The Horner-Emmons-Wadsworth reaction is a modification of the Wittig reaction where the ylide is replaced with a phosphine oxide carbanion or a phosphonate carbanion (Wittig *et al.*, 1954).



Scheme 1.3. Synthesis of 4,7-substituted coumarin using the Wittig reaction.

1.7.4. Perkin condensation reaction

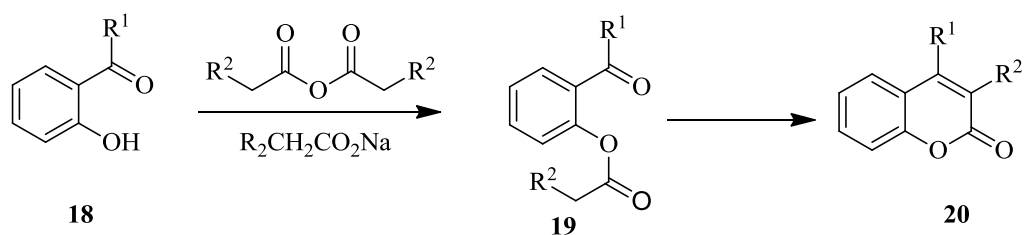
The Perkin condensation (**Scheme 1.4**) is another old method that is used for the synthesis of coumarins. In this reaction *ortho*-hydroxyarylketones (**15**) are reacted with acid anhydride in the presence of base which after cyclization yields coumarin scaffold (Perkin, 1868). This method is commonly used to synthesize neoflavones that have complicated structures (Garazd *et al.*, 2005). The requirement of very strong acids, multi-step reactions and limited substrate scope are few limitations of this reaction.



Scheme 1.4. Synthesis of substituted coumarins via the Perkin reaction.

1.7.5. Kostanecki-Robinson reaction

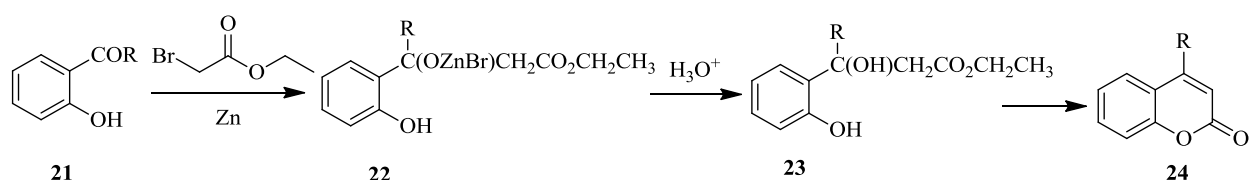
This method is commonly used to synthesize 3- and 4-substituted coumarins, and involves the acylation of *ortho*-hydroxyaryl ketones with aliphatic acid anhydrides and salts of the corresponding acids. The acylation step is followed by cyclisation (Kostanecki *et al.*, 1901).



Scheme 1.5. Synthesis of 3,4-substituted coumarins *via* the Kostanecki-Robinson reaction

1.7.6. Reformatsky reaction

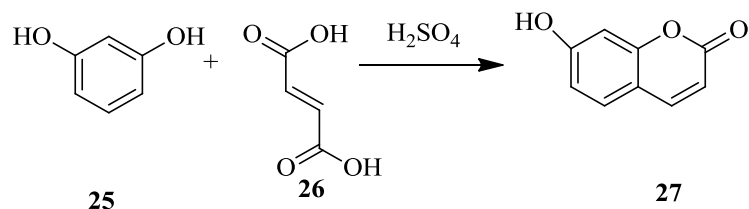
In this reaction, β -hydroxy esters are prepared by condensing ketones or aldehydes (**21**) with organozinc derivatives of α -halo esters. When the reaction conditions are favourable, lactonisation takes place yielding coumarins in good yields (**Scheme 1.6**) (Reformatsky, 1887). The requirement of highly sensitive reaction conditions is one of the major limitations of this reaction.



Scheme 1.6. Synthesis of 4-substituted coumarin *via* the Reformatsky reaction.

1.7.7. Ponndorf reaction

This reaction is very useful to synthesize 3,4-dihydrocoumarins by reacting substituted phenols with maleic or fumaric acids in the presence of sulfuric acid at elevated temperatures (Ponndorf, 1925).

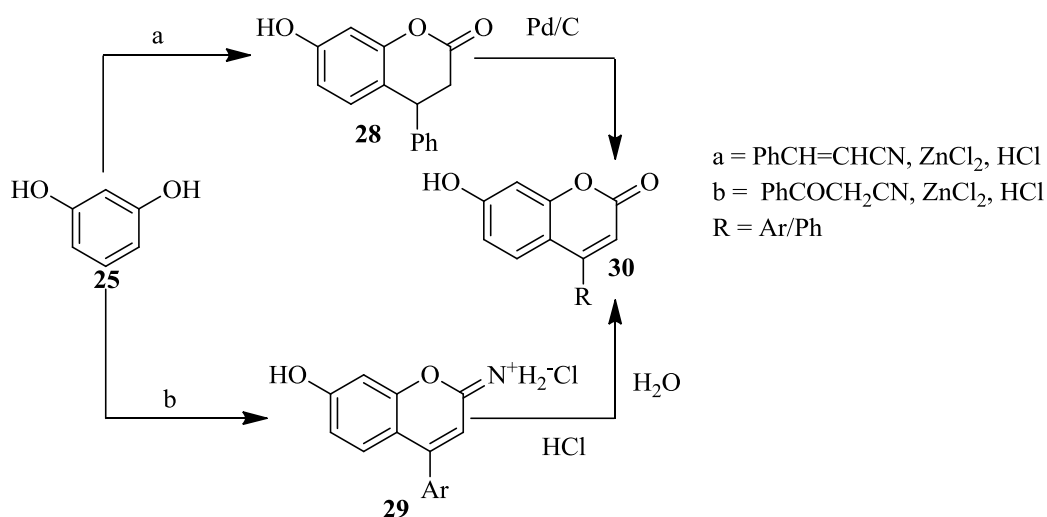


Scheme 1.7. Synthesis of 3,4-dihydrocoumarins coumarins using the Ponndorf reaction.

1.7.8. Houben-Hoesch reaction

In this reaction, the hydrochloride salt of imino coumarins (**29**) is first prepared using phenols and 3-oxo-3-phenylpropanenitrile as starting materials (**Scheme 1.8**, path b), which upon acid

hydrolysis yielded the 4-arylcoumarins (**30**) in high yields. On the other hand, the coupling of same phenols with (2*E*)-3-phenylprop-2-enenitrile (**Scheme 1.8**, path a) affords a hydrogenated coumarin compound (**28**) that undergoes dehydrogenation in the presence of Pd/C to yield the 4-arylcoumarin (**30**) (Hoesch, 1915).



Scheme 1.8. Synthesis of 4,7-substituted coumarin via the Houben-Hoesch reaction.

1.8. Applications of coumarins

Coumarins are not only used in medicinal chemistry but they are also used as additives in food and cosmetics, to make insecticides, optical brighteners, dispersed fluorescent (Xu *et al.*, 2015) and laser dyes (Kalita *et al.*, 2012), triplet sensitizers (Kallikat *et al.*, 2012). “Their derivatives have shown to be novel lipid lowering agents that have moderate triglyceride lowering activity. Most of the coumarin derivatives can remove reactive oxygen species like hydroxyl free radicals, super oxide radicals, or hypochlorous acid to prevent free radical injury (Chunduru *et al.*, 2013).” There are a number of coumarin derivatives that function as human immunodeficiency virus (HIV) integrase inhibitors. Their inhibitory activity against serine proteases and matrix metalloproteases (MMPs) has led to their evaluation as anti-invasive compounds (Chunduru *et al.*, 2013).

They have a very strong fluorescence in the visible-light range which allows them to be used as organic light-emitting diodes (LEDs) (Avó *et al.*, 2013). Artificial ion receptors, biological stains and fluorescent probes that have been derived from coumarins can be used to monitor timely enzyme activity, complex biological events and to obtain accurate pharmacological and pharmacokinetic properties. Coumarin-based derivatives also have applications in the fields of bromatology, material and supramolecular chemistry (Peng *et al.*, 2013). Also used in solar

cells and optical data storage devices. Their stability and solubility in different organic solvents combined with their photochemical characteristics has increased their potential to be used in electronic and photonic applications and in beverage manufacture (Phadtare *et al.*, 2013). Their pleasant odour allows them to be used for such purposes (Bai *et al.*, 2015).

Since salinity limits plant growth and seed germination as well as yield production, coumarins which are known for their plant growth regulatory and cytotoxic properties, are used to improve plant tolerance to salinity. Coumarin pre-treatment alleviates the adverse effect of salinity on the growth of wheat seedlings by increasing the osmoregulation process and antioxidant defence system (Saleh *et al.*, 2015). They are used in the preparation of coumarino-pyrones, chromenes, furocoumarins and 2-acylresorcinols, which are then used to synthesize pharmaceuticals and agrochemicals (Calvino-Casilda *et al.*, 2010).

1.9. Antidiabetic activity testing

Antidiabetic activity studies can either be done *in vivo* by making use of animal models or *in vitro* by using isolated tissues, cell culture systems or tissue slice preparations. *In vitro* studies are commonly used because they help determine the mechanism of action of a drug while *in vivo* studies demonstrate how these mechanisms behave under clinical conditions (Thorat *et al.*, 2012). Antidiabetic activity can be tested by studying the inhibition of carbohydrate digesting enzymes, inhibition of intestinal glucose uptake (Adolfsson *et al.*, 1967), insulin secretion from β cells of the pancreas (Santerre *et al.*, 1981; Masuda *et al.*, 1995; Asfari *et al.*, 1992) and models where the insulin target tissue is the muscle or adipocytes (Colca, 1995; Kuehnle, 1996).

The three carbohydrate digesting enzymes that can be inhibited are α -amylase, α -glucosidase and sucrase. For testing the α -amylase activity, an enzyme-starch system is used to study the effect of a compound, which is made up of the mixture of sample and α -amylase (100mg) in 25mL of 4% potato starch solution. The mixture is then incubated at 37°C for 60 minutes. When the incubation time has elapsed, 0.1M NaOH is added to stop the activity of the enzyme. Centrifugation is carried out for 15 minutes, then the amount of glucose is determined in the supernatant (Ou *et al.*, 2001).

For both α -glucosidase and sucrase inhibitory activity assay, a crude enzyme solution of rat intestinal α -glucosidase and sucrase is prepared by following Dahlqvist's method (Dahlqvist, 1964). Ten microliters of enzyme solution is mixed with different concentrations of sample

and incubated at 37°C for 10 minutes. Thereafter, the volume is made up to 210 µL with maleate buffer at a pH of 6.0. Then to start the enzyme reaction when doing the assay for the α-glucosidase inhibitory activity, 200µL of a 2mM solution of *p*-nitrophenyl-α-D-glucopyranoside is added and the mixture is incubated for an additional 30 minutes at the same temperature. The reaction is stopped by putting the mixture in boiling water for 5 minutes. The absorption of free *p*-nitrophenol is read at 400 nm, after adding 1.0 mL of 0.1M disodium hydrogenphosphate solution (Honda *et al.*, 1993).

In the case of testing the sucrase inhibitory activity, the enzyme reaction is started by adding 100µL of 60mM sucrose solution and the mixture is incubated for 30 minutes before it is terminated with 200µL of 3,5-dinitrosalysilic acid reagent and leaving the mixture in boiling water for 5 minutes. For this particular activity, the absorbance is read at 540nm. All experiments are carried out in triplicates and the percentage of the inhibition is calculated with the aid of the formula:

$$\% \text{inhibition} = \frac{\text{Abs control} - \text{Abs sample}}{\text{Abs control}} \times 100$$

Abs control = absorbance of the control (without test sample)

Abs sample = absorbance of the test sample (Honda *et al.*, 1993).

When using a method where the muscle is the target tissue for insulin, either the total uptake of glucose (Chaudry *et al.*, 1975), or the transport of 2-deoxy-glucose are measured (Gliemann, 1972; Foley *et al.*, 1981; Müller *et al.*, 1993).

1.10. Antioxidant activity assay

Diseases like cancer, neural disorders, cardiovascular and Alzheimer's are caused by free radicals (Kinnula *et al.*, 2004). Aging is also caused by free radicals. Antioxidants are used to prevent diseases caused by free radicals. There is a variety of biological tests that can be done to investigate the antioxidant activity of a compound under *in vivo* and *in vitro* assays (Alam *et al.*, 2013). *In vitro* methods include radical scavenging methods like the 1-diphenyl-2-picrylhydrazyl (α, α -diphenyl- β -picrylhydrazyl) (DPPH) (Manzocco *et al.*, 1998), peroxyntirile (Kooy *et al.*, 1994), superoxide (Robak *et al.*, 1988) and hydroxyl radical scavenging activities (Kunchandy *et al.*, 1990). The percentage inhibition of all the methods are calculated using an equation similar to the equation used when testing for sucrase inhibitory activity. Some of the methods are discussed below:

1.10.1. DPPH scavenging activity

When testing for this activity, 0.2 mL of the sample or compound is diluted in methanol then 2 mL of 0.5 mM of DPPH solution is added to this mixture. The absorbance is measured at 517 nm after 30 minutes. The antioxidant potential is evaluated by monitoring the change in optical density of the DPPH radicals (Manzocco *et al.*, 1998).

1.10.2. Hydroxyl radical scavenging activity

The reaction mixture containing 100 μ L of 28mM 2-deoxy-Dribose in 20mM $\text{KH}_2\text{PO}_4\text{-KOH}$ buffer at pH 7.4, 500 μ L of sample, 200 μ L mixture of 1.04mM EDTA and 200 μ M FeCl_3 (v/v) in equivalent ratio, 100 μ L of 1.0mM H_2O_2 and 100 μ L of 1.0mM ascorbic acid, is incubated for 1 hour at a temperature of 37°C. After the incubation period, 1ml of 1% thiobarbituric acid and 1.0ml of 2.8% trichloroacetic acid is added to the mixture and incubated for another 20 minutes at 100°C. The mixture is allowed to cool then the absorbance is measured at 532nm (Kunchandy *et al.*, 1990).

1.10.3. Superoxide radical scavenging activity

The superoxide anion radical is first generated and when the reaction has been initiated, the absorbance is measured at 560nm against a blank. A reaction vessel is charged with 3.5ml of 16mM Tris-HCl buffer which has a pH of 8.0, 0.5ml of 0.3mM nitroblue tetrazolium, 0.5ml of 0.936mM NaOH solution and 1.0ml sample. To start the reaction, 0.5ml of 0.12mM phenazine methosulfate solution is added to the reaction vessel and the mixture is incubated at 25°C for 5 minutes then the absorbance is measured (Robak *et al.*, 1988).

1.10.4. Hydrogen peroxide scavenging assay

For testing this activity a 40mM solution of hydrogen peroxide is first prepared in a 50mM phosphate buffer at pH 7.4 then the concentration of hydrogen peroxide is determined by measuring the absorption at 230nm. Then the extract, which is usually between 20-60 μ g/ml, in distilled water is added to the hydrogen peroxide and the concentration is determined again after 10 minutes (Ruch *et al.*, 1989).

1.10.5. Thiobarbituric acid method

To 1ml of the sample solution, 2ml of 20% trichloroacetic acid and 2ml of 0.67% of thiobarbituric acid is added. The mixture is put into boiling water for a period of 10 minutes

then it is cooled at 3000rpm for 20 minutes. The mixture is centrifuged and the absorbance activity of the supernatant is measured at 552nm when it has reached its maximum (Ottolenghi, 1959).

Other *in vitro* methods include, nitric oxide scavenging activity (Maccocci *et al.*, 1994), trolox equivalent antioxidant capacity method (Seeram *et al.*, 2006), metal chelating activity (Dinis *et al.*, 1994), *N,N*-dimethyl-*p*-phenylene diamine dihydrochloride (DMPD) method (Fogliano *et al.*, 1999), Ferric reducing-antioxidant power (FRAP) assay (Benzie *et al.*, 1999), cupric ion reducing antioxidant capacity method (CUPRAC) (Apak *et al.*, 2008), hydroxyl radical averting capacity (HORAC) method (Ou *et al.*, 2002), total radical-trapping antioxidant parameter (TRAP) method (Ghiselli *et al.*, 1995), ferric thiocyanate (FTC) method (Kikuzaki *et al.*, 1991), oxygen radical absorbance capacity (ORAC) method (Prior *et al.*, 2003) and phosphomolybdenum method (Prieto *et al.*, 1999). The β -carotene linoleic acid method (Kabouche *et al.*, 2007) and the xanthine oxidase method (Noro *et al.*, 1983) uses a slightly different formula to calculate the percentage inhibition.

$$\% \text{ inhibition} = \left[1 - \left(\frac{As}{Ac} \right) \right] \times 100$$

1.10.6. *In vivo* methods

In vivo methods include, the ferric reducing ability of plasma (Benzie *et al.*, 1996), reduced glutathione (GSH) estimation (Ellman, 1959), glutathione peroxidase (GSHP_x) estimation (Wood, 1970), Superoxide dismutase (SOD) method (McCord *et al.*, 1969), catalase (CAT) (Aebi, 1984), γ -glutamyl transpeptidase activity (GGT) assay (Singal *et al.*, 1982), lipid peroxidation (LPO) assay (Ohkawa, 1979) and the LDL assay (El-Saadani *et al.*, 1989).

1.11. Introduction to molecular modelling

The interest in computational chemistry to integrate structural data of the target or receptor sites to determine the structure that has the best chance of showing a particular activity at its optimum has increased over the years (Laurie *et al.*, 2005; Geppert *et al.*, 2012; Valkov *et al.*, 2012). Molecular docking is a computational approach used to design a virtual grid of fragments and screens them for the best fragments which are then grown or linked together to optimize the fragments to obtain a lead compound (Kumar *et al.*, 2012). The virtual grid that is created is a library of different receptors and it is created using receptor 3D structures. The grid is usually large enough to cover the entire region of interest on the receptor. After generating the grid, the docking of ligand is performed by generating its different conformations using

different sampling methods. During the docking process, the ligand conformations are randomly oriented and minimized (Miller III *et al.*, 1975; Laurie *et al.*, 2005; Singh *et al.*, 2011; Neuvirth *et al.*, 2004), and the best orientation that form a stable complex with the protein of interest is determined (Lengauer *et al.*, 1996; Huang *et al.*, 2010). Different scoring functions available in different docking programs are employed to select the best conformation. The scoring functions calculate a binding score using either a force-field based, knowledge based or empirical scoring function, depending on the docking program used (Kitchen *et al.*, 2004). Force-field based scoring functions which are usually more expensive than the other scoring functions are designed on first principles according to the non-bonded interactions like van der Waals and electrostatic interactions (Jones, 1924; Miller III *et al.*, 1975). Docking programs that use force-field based scoring functions include DOCK (Ewing *et al.*, 2001), AutoDock (Morris *et al.*, 1998) and GOLD (Verdonk *et al.*, 2003).

Scoring functions like SMOG (DeWitte *et al.*, 1996), PMF score (Muegge *et al.*, 1999) and DrugScore (Gohlke *et al.*, 2000) use the knowledge based scoring functions in which the frequency and distance between experimental protein-ligand are determined from their interactions. In this case, if interactions occur frequently, then that interaction is more likely to be considered. The interactions are then converted into a scoring function. Priority is given to attractive interactions over repulsive interactions. Unlike force-field based scoring functions, knowledge based scoring functions are computationally cheap, fast and simple (Miller III *et al.*, 1975).

Like knowledge based scoring functions, empirical scoring functions are inexpensive and easy to use. Empirical scoring functions are based on fitting together the data from receptor-ligand complexes with known binding affinities (Miller III *et al.*, 1975). Liu *et al.* used an algorithm to determine the protein-DNA binding sites that can be used in chromatin-immunoprecipitation microarray experiments (Liu *et al.*, 2002). The best way to describe the binding in docking studies is to look at the protein or target as a lock and the ligand or any other receptor as a key. When you are docking you are trying to find the best orientation of the key that will unlock the lock (Jorgensen, 1991; Levinthal *et al.*, 1975; Wodak *et al.*, 1978; Kuntz *et al.*, 1982; Salemme, 1976).

It is worth noting that docking, when used alone, is not 100% accurate because scoring functions are accurate within a certain time frame that allows the screening of a certain amount of receptors. It is highly recommended that after docking methods like molecular dynamics

and molecular mechanical/ generalized born surface area should be used to confirm the results since these are more accurate (Plewczynski *et al.*, 2011).

1.12. Aim and objectives

The coumarins have great potential to act as anti-diabetic agents in addition to their diverse wide spectrum of biological activities. For example, the coumarins isolated from many medicinal plants such as *Aegle marmelos* (Mamun-or-Rashid *et al.*, 2014), *Zanthoxylum schinifolium* (Nguyen *et al.*, 2016) and *Persea americana* (Lima *et al.*, 2012), have shown promising activity against diabetes. Similarly, the synthetic biscoumarins (Zawawi *et al.*, 2015) or those thiazole pharmacophoric unit (Wang *et al.*, 2015) have shown impressive anti-diabetic activity.

Hence, the aim in this work was to synthesize a variety of functionalized coumarins and to test their anti-oxidant and anti-diabetic activities. Another motivation for this work originated from a report where the presence of hydroxyl substituent at position 4 was observed to display moderate inhibitory activity for α -glucosidase enzyme (Shen, 2010). It was envisaged that the replacement of –OH group/s in the coumarin ring with the hydrophobic moieties such as the alkyl group might increase its activity by promoting their interactions with the hydrophobic cavity of α -glucosidase.

Objectives:

1. To synthesize –OH substituted coumarins.
2. To perform single and double O-alkylation of coumarins.
3. To synthesize few fluorine-containing 4-methylcoumarins.
4. To evaluate the synthesized coumarins for their antidiabetic and antioxidant activities under *in vitro* conditions.
5. To perform *in silico* docking simulations to determine the binding modes of compounds in the catalytic site of α -glucosidase.

Different recently published articles on the synthesis and biological activities of coumarins are discussed in chapter 2. The details of experimental procedures and computational methods are provided in chapter 3, whereas the detailed discussion of both synthetic and experimental results is shown in chapter 4. Finally, the key findings of this study are summarized in chapter 5 along with relevant recommendations for future work.

CHAPTER 2

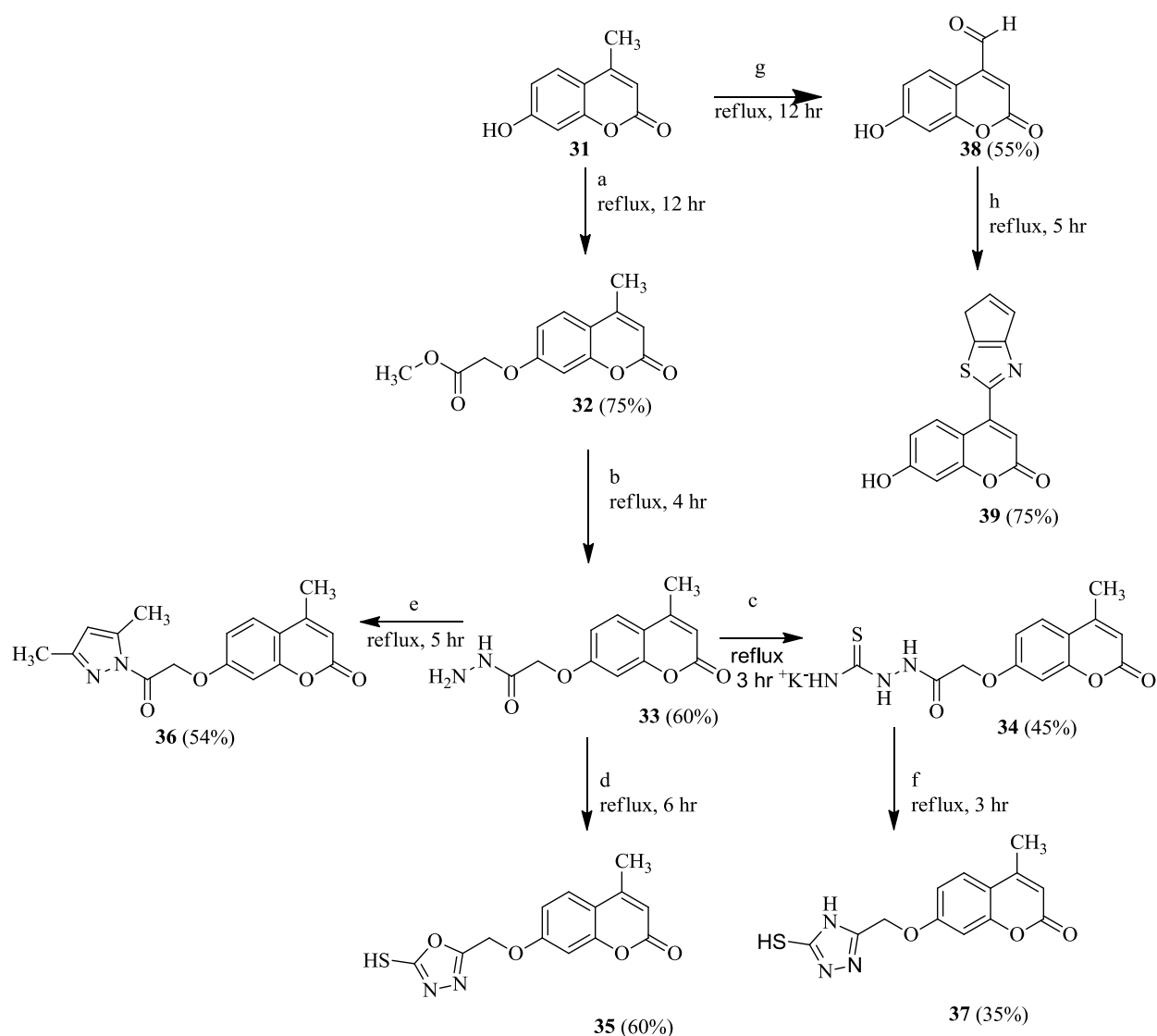
Literature review

2.1. Past work on the coumarin and 4-methyl coumarin derivatives.

A careful review of the recent synthetic approaches employed by researchers worldwide to prepare new coumarin analogues was conducted and discussed along with their biological activity profiles (wherever applicable) and relevant structure activity relationship (SAR) in the following sections.

2.2. 4-Methylcoumarins with antioxidant activity

A variety of functionalized coumarins were synthesized using 7-hydroxy-4-methylcoumarin (**31**) as a precursor (**Scheme 2.1**), and tested for their antioxidant activities. The treatment of **31** with methylbromoacetate yielded methyl-((4-methyl-2-oxo-2*H*-chromen-7-yl) oxy) acetate (**32**) which upon reaction with hydrazine hydrate resulted in 2-((4-methyl-2-oxo-2*H*-chromen-7-yl) oxy) acetohydrazide (**33**). The reaction of **33** with KSCN resulted in **34** which after cyclization in the presence of a base formed triazole substituted coumarin (**37**). Similarly, the treatment of **33** with CS₂ and acetylacetone resulted in the oxadiazole (**35**) and pyrazole (**36**) tagged coumarin analogues, respectively. An aldehyde moiety in **38** was introduced at 4-position by the oxidation of **31** with SeO₂, and utilized in condensation with *o*-aminothiophenol to yield **39** in good yields. 7-hydroxy-2-oxo-2*H*-chromene-4-carbaldehyde (**38**) and 4-(benzo [d] thiazol-2-yl)-7-hydroxy-2*H*-chromen-2-one (**39**) exhibited potent scavenging activity compared to the standard drug (Vitamin C) (Al-Amiery *et al.*, 2015).

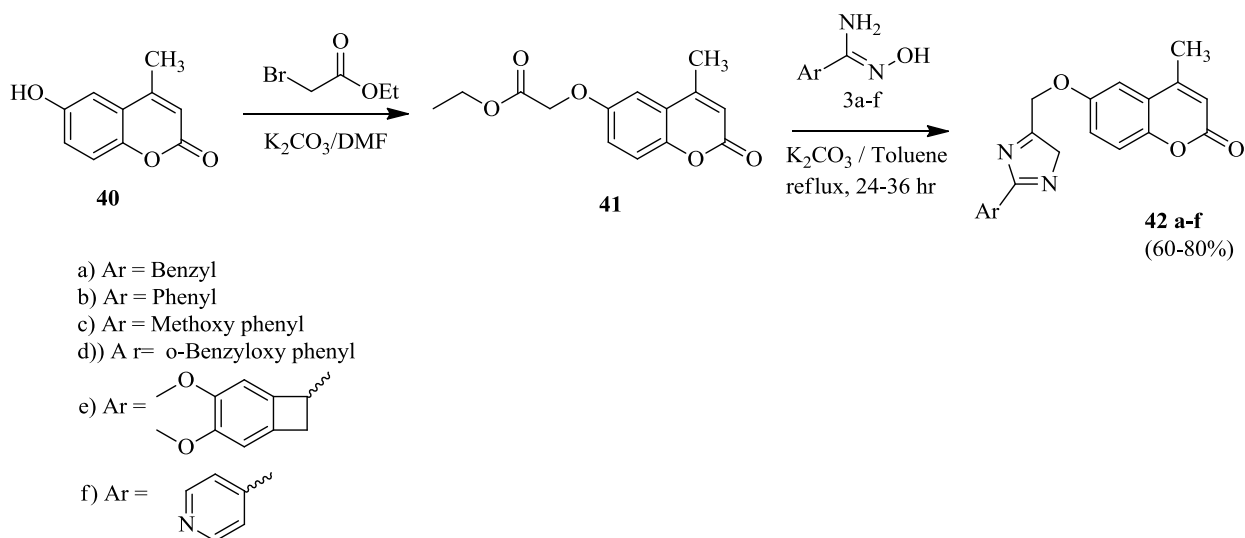


a) Methyl bromoacetate; b) Hydrazine; c) KSCN; d) CS₂; e) Acetylacetone; f) KOH; g) SeO₂; h) o-aminophenol

Scheme 2.1. Synthetic route for 4-methylcoumarin derivatives.

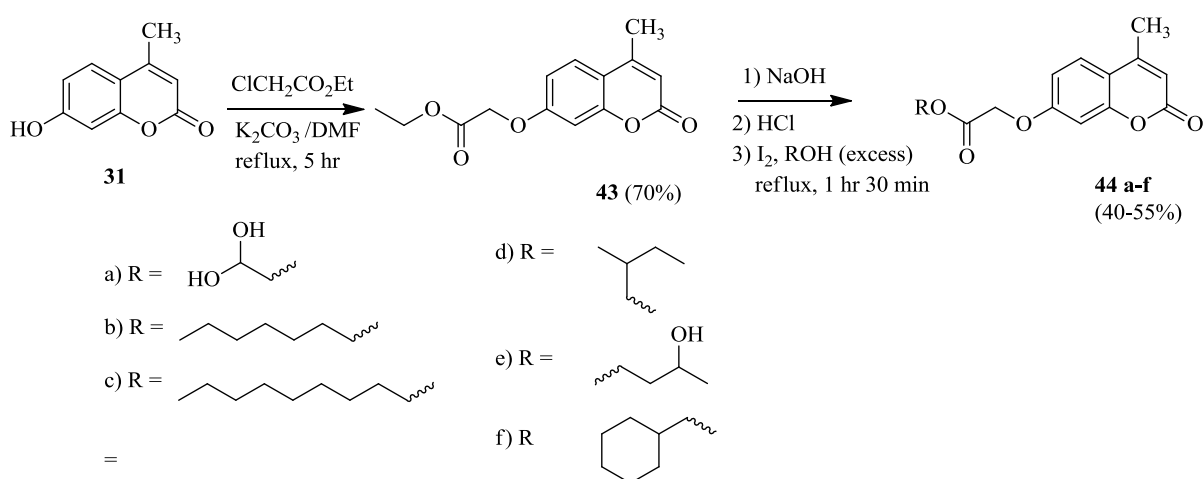
2.3. 4-Methylcoumarins with antimicrobial activities.

In another similar study, the 6-hydroxy-4-methylcoumarin (**40**) was prepared from hydroquinone and ethyl acetoacetate, and alkylated with ethyl bromoacetate to give the corresponding ester (**41**) (**Scheme 2.2**). The coupling of **41** with different amidoximes yielded its hybrids with imidazoles (**42**) in high yields. Amongst the synthesized compounds, **42a**, **42e** and **42f** displayed good bacterial activity against the *S.aureus* and *E.coli* strains, even better than ampicillin. Both **42e** and **42f** also showed good antifungal activity for *A.terreus* and *R.solani* compared to the standard drug clotrimazole (Krishna *et al.*, 2015).



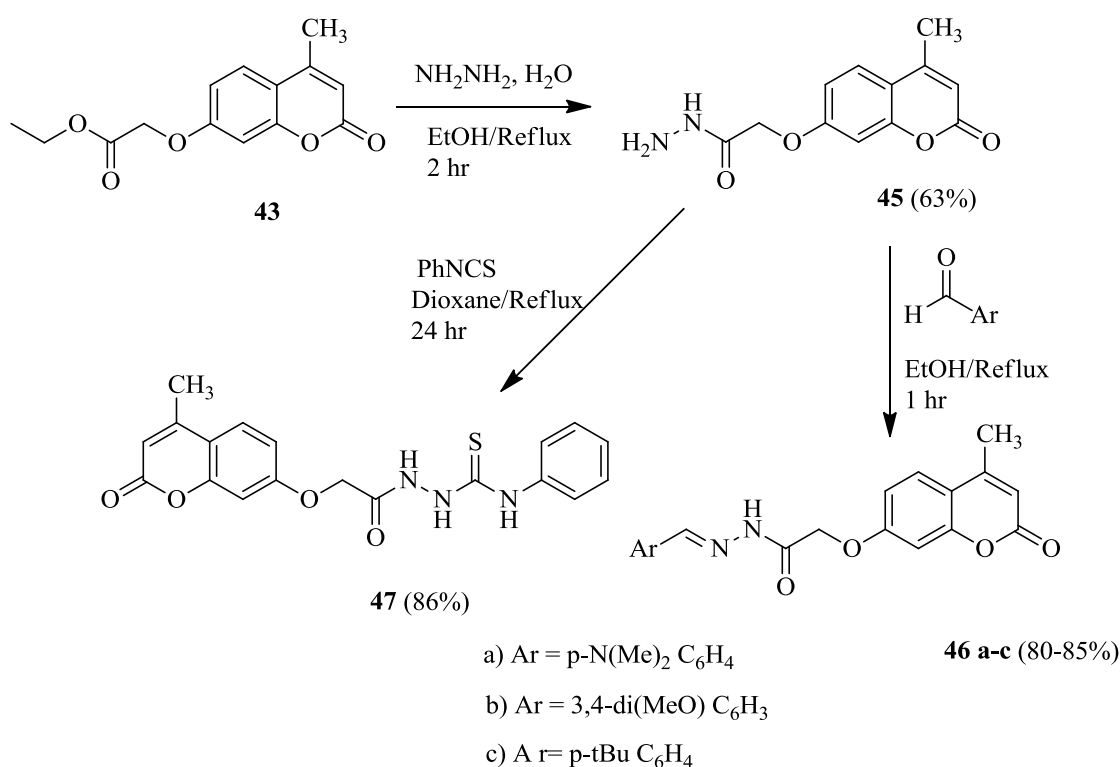
Scheme 2.2. Synthesis of 4-methylcoumarins with aryl groups.

The ethyl 2-(4-methyl-2-oxo-2H-chromen-7-yloxy) acetate (**43**) was prepared by refluxing a mixture of 7-hydroxy-4-methylcoumarin (**31**) with ethyl chloroacetate in the presence of anhydrous potassium carbonate, and transesterified to **44** using different alcohols (**Scheme 2.3.1**) (Zayane *et al.*, 2015). The *in vitro* antibacterial testing further revealed the compounds **44b** and **44e** to be the most active against *P.savatoni* with inhibition zones (IZ) of 11mm and 13mm, respectively, although weaker relative to ampicillin (IZ = 22mm). Similarly, the two compounds **44a** (IZ = 10mm) and **44d** (13mm) which were found to be potent anti-fungal activity against *A.niger* exhibited weaker activity in comparison to the standard compound carbendazime (IZ = 32.5mm).



Scheme 2.3.1. Synthesis of esterified coumarins.

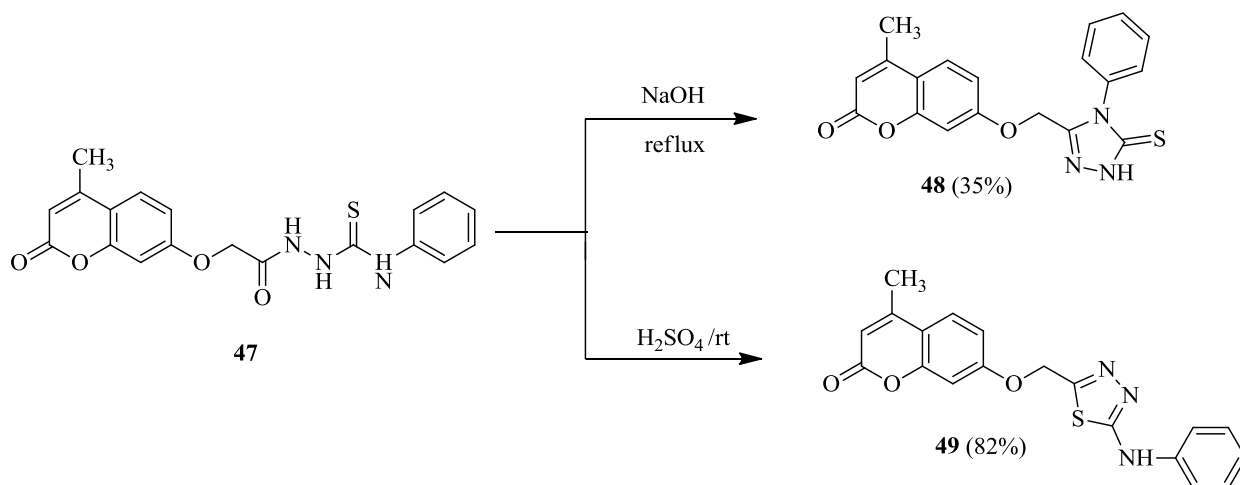
In another investigation (**Scheme 2.3.2**), ethyl 2-(4-methyl-2-oxo-2*H*-chromen-7-yloxy) acetate (**43**) was reacted with hydrazine hydrate to yield 2-(4-methyl-2-oxo-2*H*-chromen-7-yloxy) acetohydrazide (**45**), which was coupled with few aromatic aldehydes to form imines **46** (Zayane *et al.*, 2015). A thiourea analogue (**47**) was also prepared by refluxing **45** with phenyl isothiocyanate in dry dioxane. All the compounds (**46-47**) showed weaker activity (IZ = 8.5 to 11mm) against *Pseudomonas huttensis* relative to the ampicillin (IZ = 18mm). In their antifungal activity evaluation, only compounds **46** were found to be active. The antifungal activity of the compounds **46a-c** showed activity against *Aspergillus niger* with inhibition zones of 9, 10.5 and 11mm, respectively.



Scheme 2.3.2. Synthesis of imines.

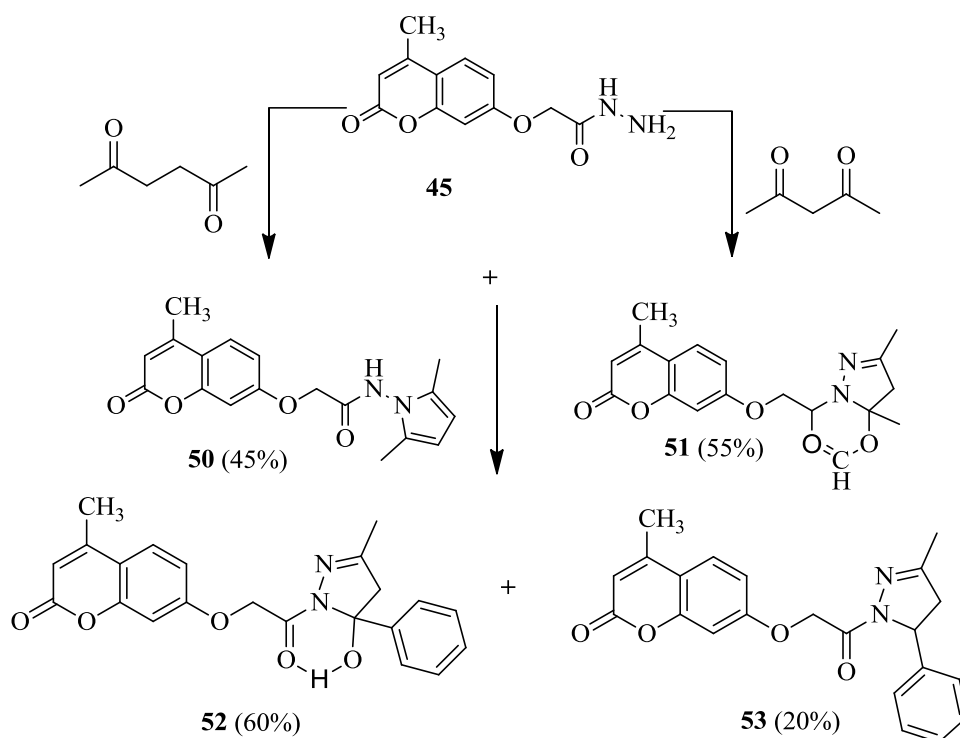
The refluxing of 2(2-((4-methyl-2-oxo-2*H*-chromen-7-yl)oxy) acetyl)-*N*-phenylhydrazinecarbothioamide (**47**) under basic conditions led to the formation of triazolethione (**48**) in low yields (**Scheme 2.3.3.**) (Zayane *et al.*, 2015). On the other hand, a thiadiazole (**49**) was obtained in 82% yield when the same starting material (**47**) was reacted with H₂SO₄ at room temperature. The *in vitro* antibacterial evaluation studies further revealed that the conversion of **47** into a triazolethione and thiadiazole led to the decrease in its activity against *Pseudomonas huttensis* with inhibition zone (IZ) from 11mm to 9 and 9.5mm,

respectively. Similarly, no significant change in the antifungal activity of **47** against *A.flavus* and *A. niger* was observed after its transformation.



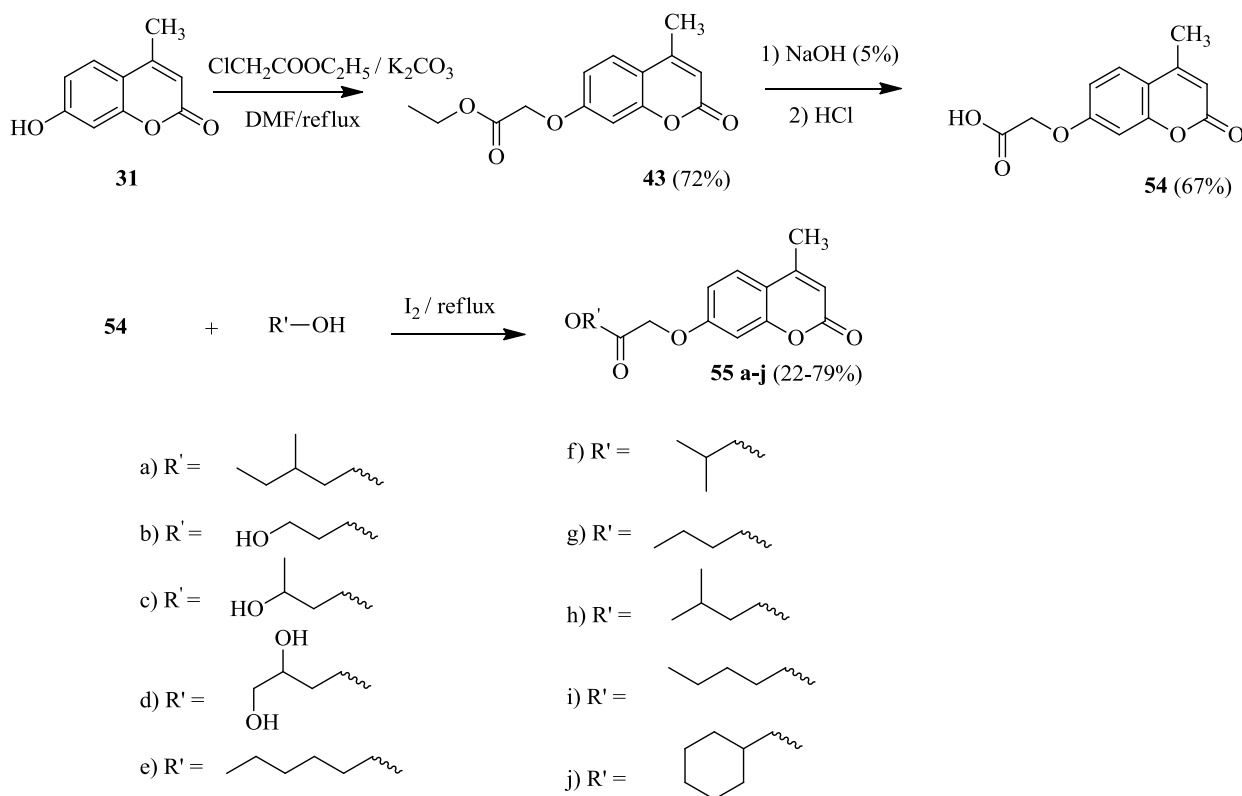
Scheme 2.3.3. Synthesis of a triazolethione and a thiadiazole.

Two sets of hybrids (**Scheme 2.3.4**) of coumarin with pyrazoles and pyrroles were synthesized by refluxing **45** with different diketones in ethanol (Zayane *et al.*, 2015). The three compounds (**50**, **52** and **53**) displayed potent activity against *A. tumefasciens* with IZ values of 9, 10.5 and 11mm. Compounds **52** and **53**, on the other hand, were active against *P. savatonoi*. Additionally, compounds (**50**, **51**, **52** and **53**) showed good antifungal activity against *A. niger* with inhibition zone value of 10, 9.5, 11 and 11mm, respectively.

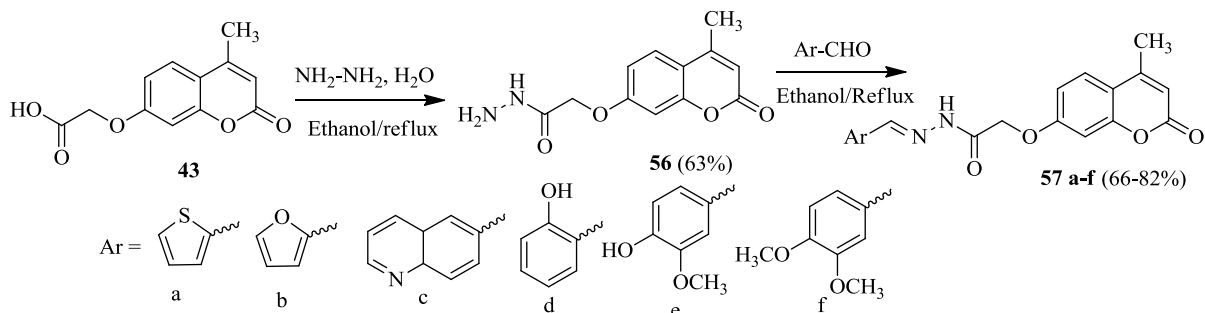


Scheme 2.3.4. Synthesis of pyrazole and pyrrole derivatives.

Different esterified coumarins (**55**) were synthesized by the I₂-assisted esterification of **54** with different alcohols (**Scheme 2.4.1**) (Medimagh-Saidana *et al.*, 2015). In parallel, the coumarin Schiff-bases (**57a-f**) were also synthesized by the condensation reaction of **56** with different aromatic aldehydes (**Scheme 2.4.2**). The antibacterial activity of the synthesized compounds tested against *Pseudomonas sp.* (Pa 499) and *Bacillus sp.* (Bp 420) suggested the **55f**, **55h** and **57e** to be good against *Pseudomonas sp.* (Pa 499) with the respective inhibition zones 5,5 and 8mm, although lower than ampicillin (IZ = 10mm). Only compound **55i** was found to be active against *Bacillus sp.* with IZ value of 6mm when the compounds were tested for their antifungal activity against *Aspergillus niger*, *Botrytis cinerea* and *Fusarium oxysporum f. sp. lycopersici*. Except **55a**, **55e**, **57a** and **57f**, all the remaining compounds showed good activity against *Fusarium oxysporum f. sp. lycopersici* with inhibition zones between 11 and 16mm, better than the standard drug carbendazim (IZ = 10mm).



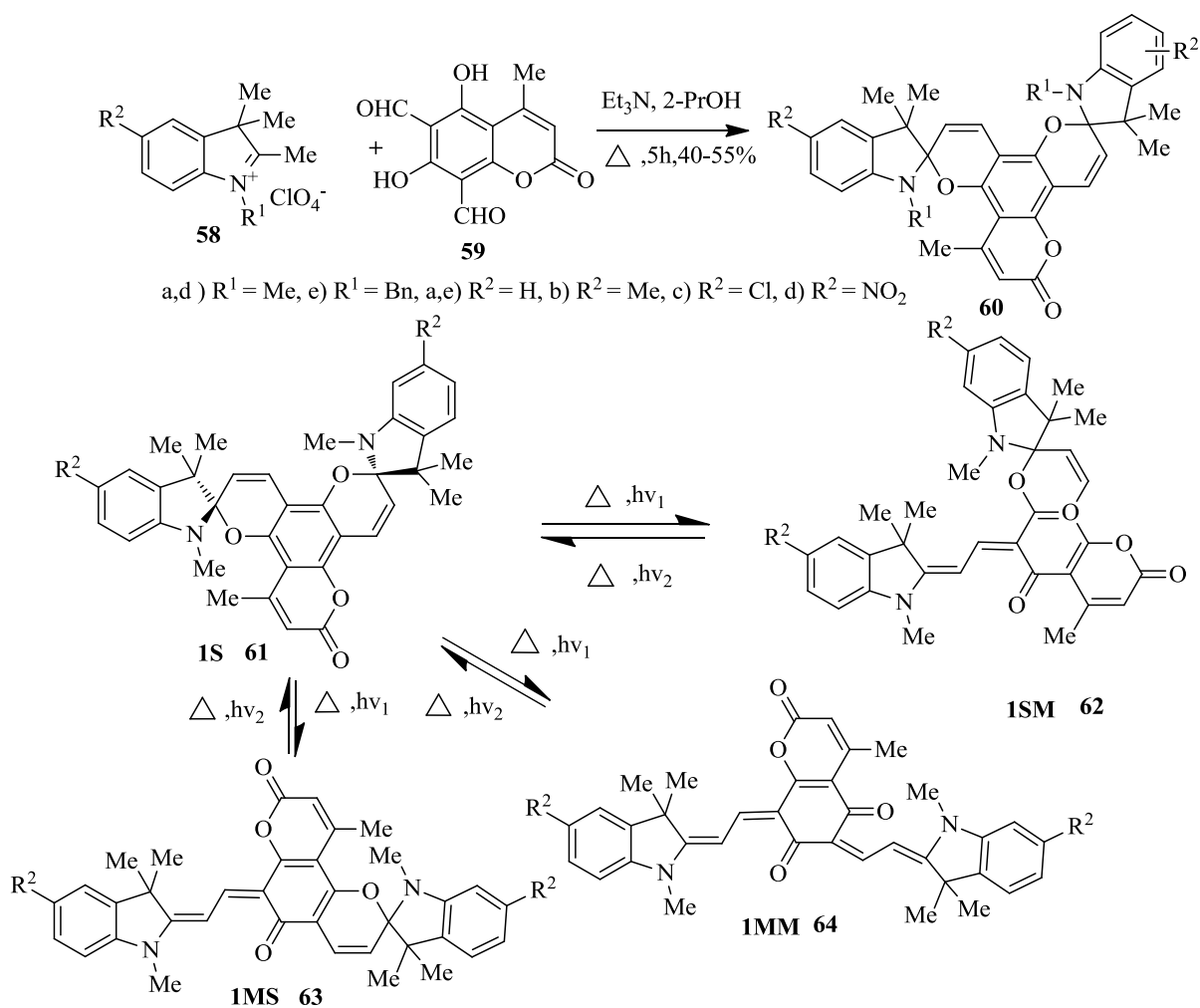
Scheme 2.4.1. Esterification reaction of 7-O-substituted coumarin.



Scheme 2.4.2. Synthesis of imines with aryl groups.

2.4. Coumarins with photochromic properties

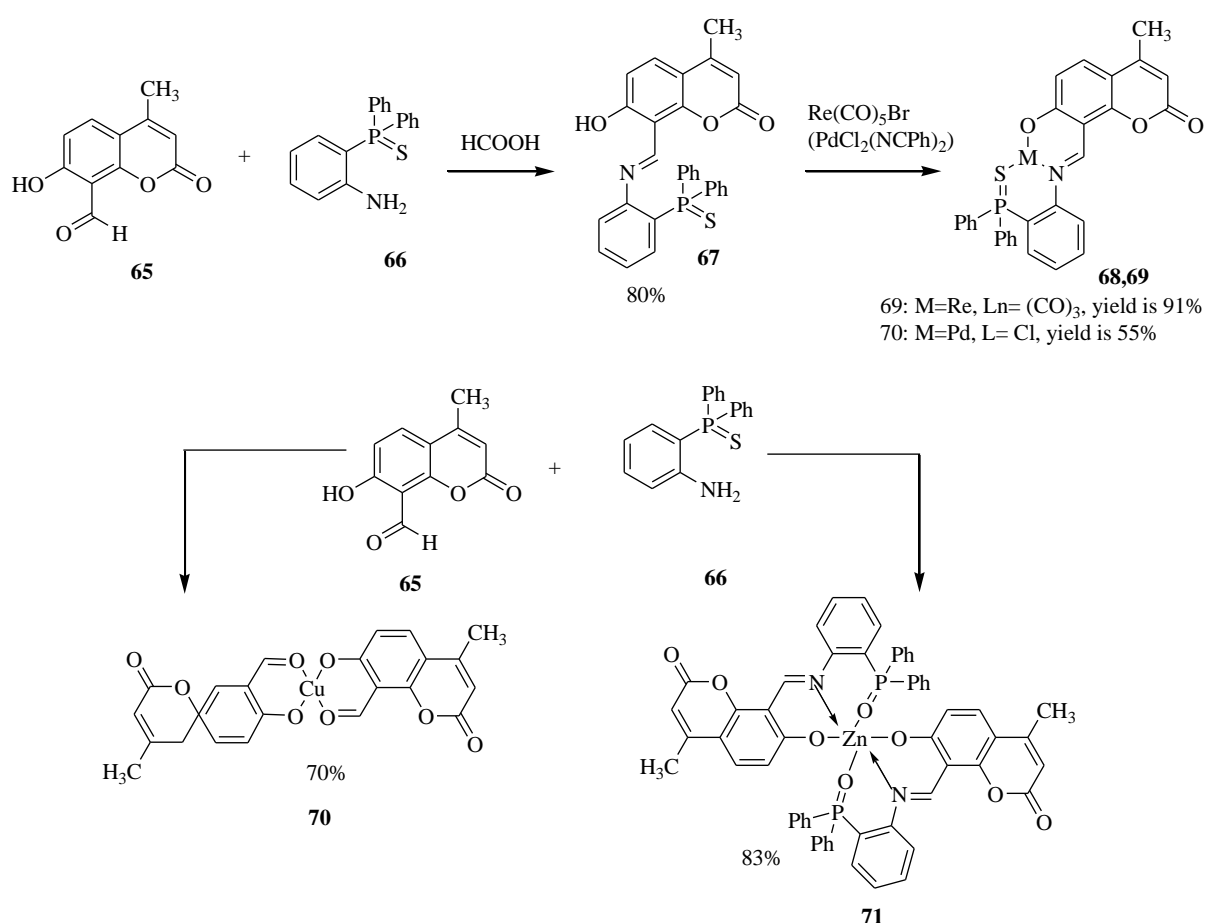
A series of bis-spiroyrans (**60**) were synthesized by condensing 3H-indolium perchlorates **58** with 6,8-diformyl-5,7-dihydroxy-4-methylcoumarin (**59**) in the presence of trimethylamine in moderate yields (**Scheme 2.5**) (Nikolaeva *et al.*, 2015). When the bis-spirocyran in spirocyclic form 1S (ground state) were irradiated, different merocyanine forms (1SM, 1MM) were formed. These compounds in the merocyanine form either had one or two cyclic rings opened.



Scheme 2.5. Synthesis of bis-spiroyrans.

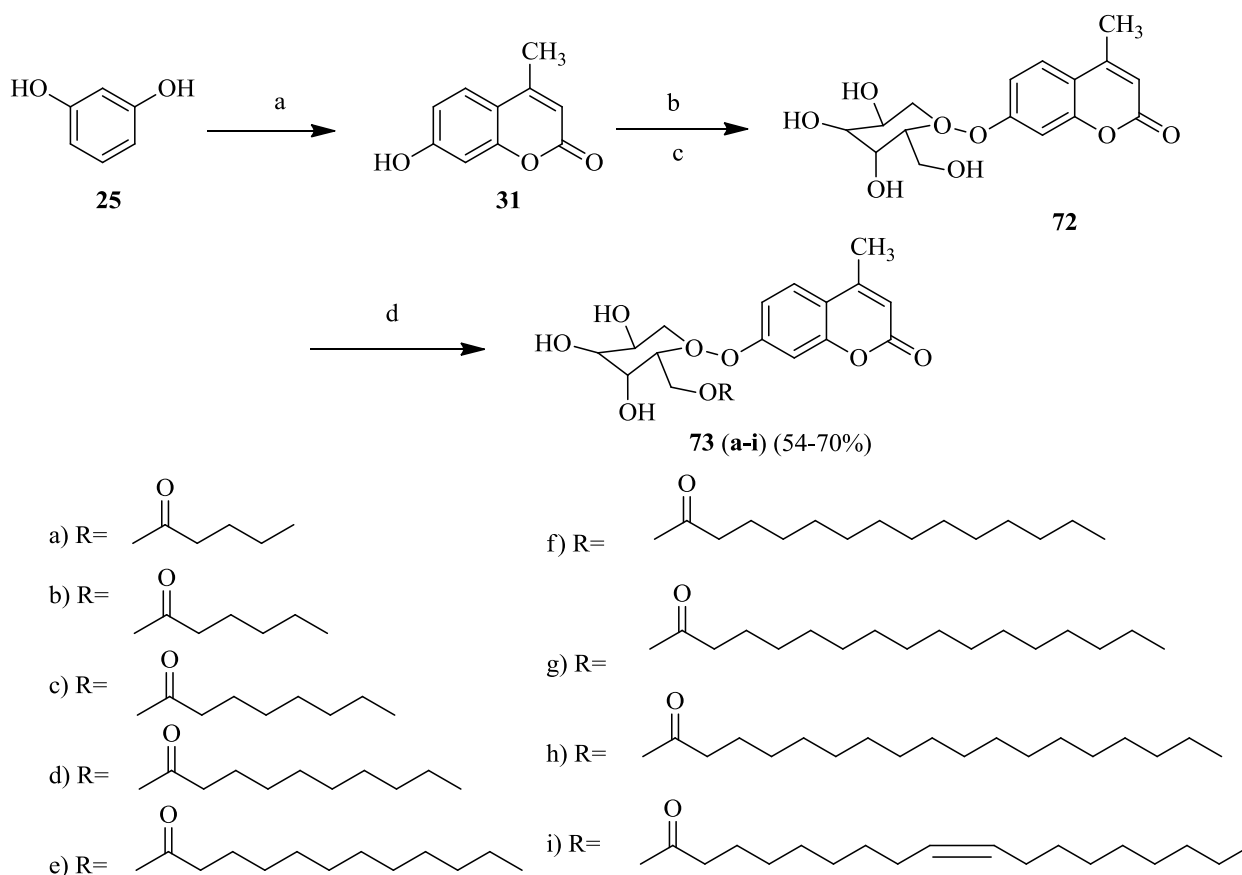
2.5. Coumarin derivatives with catalytic activity

In another report (Aleksanyan *et al.*, 2014), a thiophosphorylated imine **67**, initially prepared from the condensation between **65** and o-(diphenyl-thiophosphoryl) aniline, was utilized in chelation reactions to form metal-complexes (**68 and 69**) with Re and Pd (**Scheme 2.6**). The ligand in these complexes acted as a tridentate utilizing its heteroatoms (O, N, and S) in the metal chelation process. When the o-(diphenyl-thiophosphoryl) aniline and compound **65** were reacted with copper (II) acetate, copper (II) bis(hydroxylate) complex (**70**) was obtained as a product. However, the similar reaction with zinc acetate led to the formation of κ^3 -O,N,O-complex (**71**) which had two anions of the ligand coordinated to the zinc atom.



Scheme 2.6. Synthesis of metal containing 4-methylcoumarins.

The synthesis of 4-methylcoumarin-7-O- β -D-glucoside (**72**) was reported (Duo *et al.*, 2015) from the reaction between 7-hydroxy-4-methylcoumarin (**31**) and tetra-O-acetyl- α -D-glucosyl bromide (**Scheme 2.7**). The coupling of **72** with long-chain fatty acids via enzymatic esterification using immobilized lipase (Novozym 435) afforded **73** in good yields (54-70%).



Reagents and conditions:

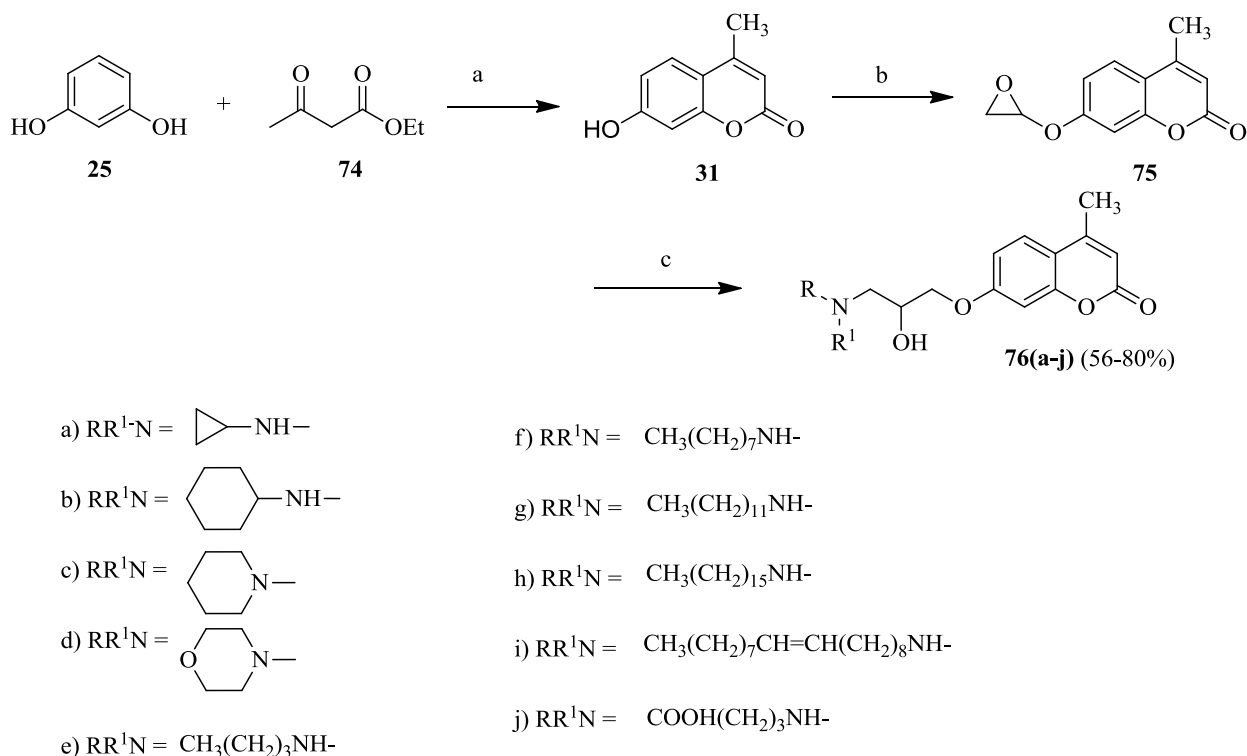
- Ethyl acetoacetate concentrated H₂SO₄, r.t.
- Tetra-O-acetyl- α -D-glucosyl bromide, CHCl₃, K₂CO₃, tetrabutylammonium bromide (TBAB), 50-60°C.
- CH₃OH, Na, r.t.
- Long chain fatty acids, Novozym 435, acetone/pyridine, 3A molecular sieves, 40-50°C.

Scheme 2.7. Synthesis of 4-methylcoumarins with long chain fatty acids.

2.6. 4-Methylcoumarins with antibacterial activity.

The oxirane ring (**75**), formed as an intermediate in the reaction between 7-hydroxy-4-methylcoumarin (prepared using Pechmann reaction) and epichlorohydrin in the presence of a base, was nucleophilically opened with different amines to synthesize a range of coumarinyl amino alcohols (**76**) (**Scheme 16**) (Singh *et al.*, 2015). All the compounds synthesized were then tested for their antibacterial activity against *B. subtilis*, *P. aeruginosa*, *E. coli*, *K. pneumoniae*, *P. vulgaris* and *S. aureus* strains, using novobiocin and erythromycin as standards. Compound **76e** exhibited potent activity against *E. coli* (MIC = 16 μ g/mL) two-fold higher than erythromycin (MIC = 32 μ g/mL) and novobiocin (MIC = 30 μ g/mL). Additionally, **76e** exhibited potential activity against *K. pneumoniae* (MIC= 6.25 μ g/ml) where erythromycin was resistant and novobiocin showed lower activity (MIC = 25 μ g/ml). The testing of all compounds for their antifungal activity against *C. albicans*, *C. terreus* and *S. cerevisiae* revealed the compound **76e** to be most active against *S. cerevisiae* (MIC=3.125 μ g/ml) better

than the standard drug amphotericin B (MIC=12.5 $\mu\text{g/ml}$). Compound **76i** also showed a good activity against *C. albicans* (MIC= 6.25 $\mu\text{g/ml}$) and *S. cerevisiae* (6.25 $\mu\text{g/ml}$).

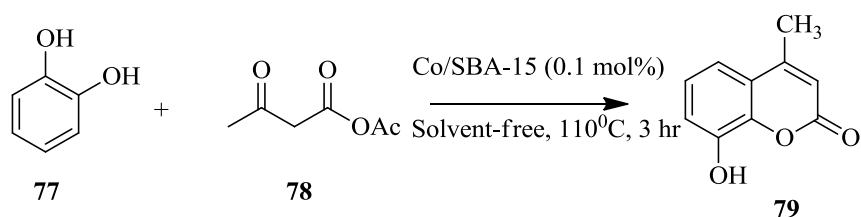


Reagents and conditions: a) conc. H_2SO_4 , 0°C , 24h b) epichlorohydrin, K_2CO_3 , reflux c) RR^1NH , ethanol, r.t., 4-6h.

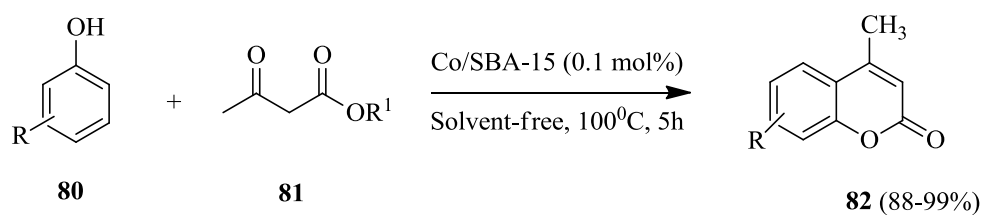
Scheme 2.8. Synthesis of nitrogen containing 4-methylcoumarins.

2.7. 4-Methylcoumarins where no activity was tested.

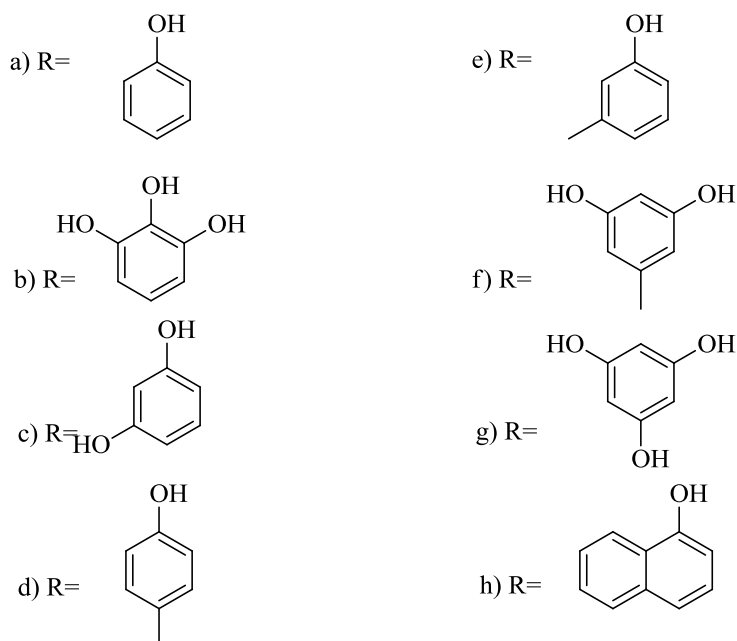
A comparative study (Rajabi *et al.*, 2015) was recently conducted to synthesize 4-methylcoumarins (**79**) from a phenol with a β -ketoester in the presence of a catalyst Co/SBA-15, under solvent and solvent-free conditions (**Scheme 2.9.1**). It was discovered that the coumarins can be obtained in higher yields (>90%) under solvent-free conditions, and was employed to synthesize a variety of similar coumarin derivatives (**82**) using different phenols (**80**) (**Scheme 2.9.2**).



Scheme 2.9.1 Synthesis of 8-hydroxy-4-methylcoumarin.

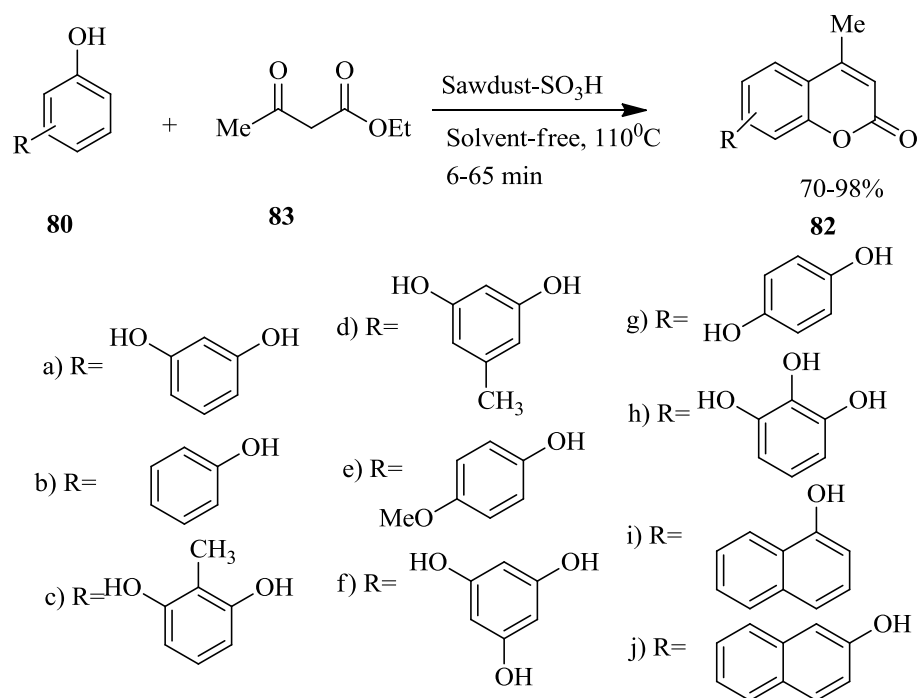


$R^1 = \text{CH}_3, \text{C}_2\text{H}_5$



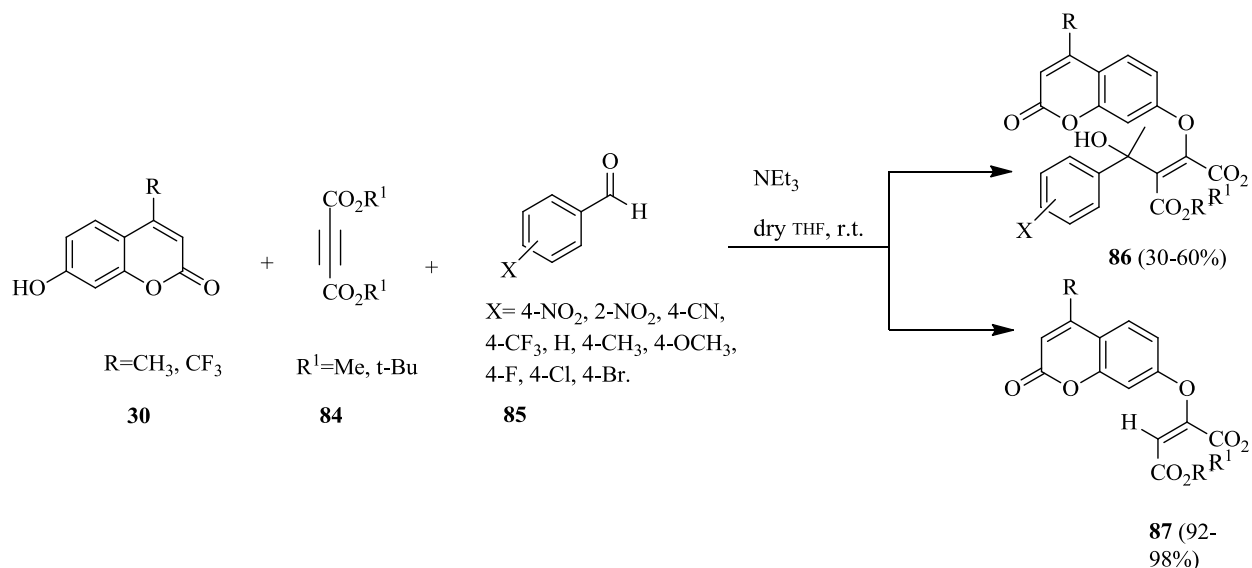
Scheme 2.9.2 Synthesis of 4-methylcoumarin via a Co/SBA-15 catalysed reaction.

Similar green approach was used in another study (Tahanpesar *et al.*, 2015) to prepare different 4-methylcoumarins from phenols with a β -ketoester in the presence of a catalyst using Sawdust-SO₃H as a catalyst (**Scheme 2.10**). The catalyst was found to be inexpensive, efficient, and recyclable for such reactions.



Scheme 2.10. Synthesis of 4-methylcoumarin via a sawdust-SO₃H catalysed reaction.

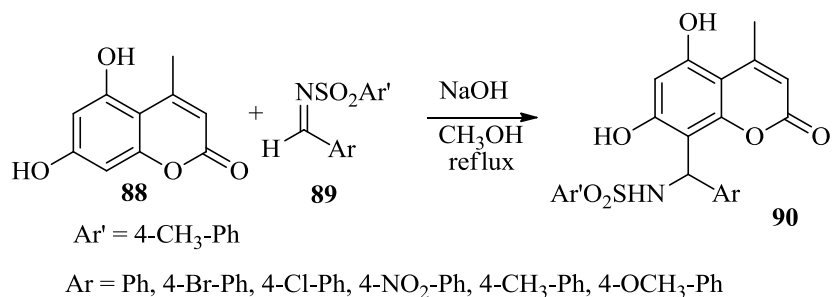
Two different series of *o*-substituted coumarin derivatives (**86**, **87**) were synthesized by employing a three-component reaction between 7-hydroxycoumarins, acetylenic diesters and aryl aldehydes in the presence of trimethylamine in tetrahydrofuran (**Scheme 2.11**) (Asghari *et al.*, 2015).



Scheme 2.11. Preparation of *o*-substituted coumarin derivatives.

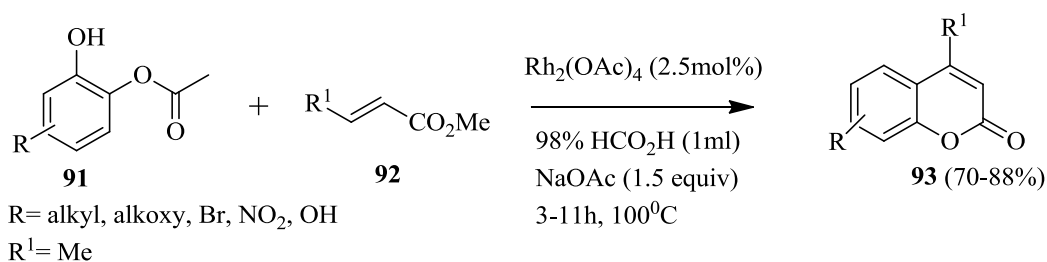
In a recent communication (Farahi *et al.*, 2015), a series of sulfonamide-tagged coumarins (**90**) was reported from the reaction of *N*-sulfonyl imines (**89**) with 5,7-dihydroxy-4-

methylcoumarin (**88**) using aq. NaOH (40%) as a base. The *N*-sulfonyl imines in turn were prepared by the condensation reaction between *p*-toluensulfonamide and different aromatic aldehydes.



Scheme 2.12. Synthesis of sulfonamide-containing coumarins.

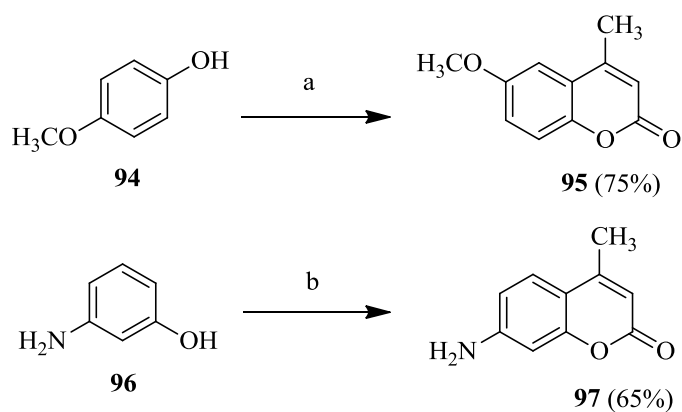
Gadakh *et al.* synthesized substituted methylcoumarins by reacting β -substituted acrylates with substrates containing electron-donating and electron-withdrawing groups via C-H bond activation using $\text{Rh}_2(\text{OAc})_4$ as a catalyst (**Scheme 2.13**).



Scheme 2.13. Synthesizing 4-methylcoumarins from β -substituted acrylates.

2.8. Coumarins with phytotoxic activity

The 6-methoxy-4-methylcoumarin **95** was obtained by refluxing a mixture of ethyl acetoacetate and 4-methoxyphenol in the presence of H_2SO_4 (80%) (**Scheme 2.14**) (Pan *et al.*, 2015). The 7-amino-4-methylcoumarin analogue (**97**), on the other hand, was synthesized in the presence of a Lewis acid (zinc chloride) using *m*-aminophenol and ethyl acetoacetate as starting materials.

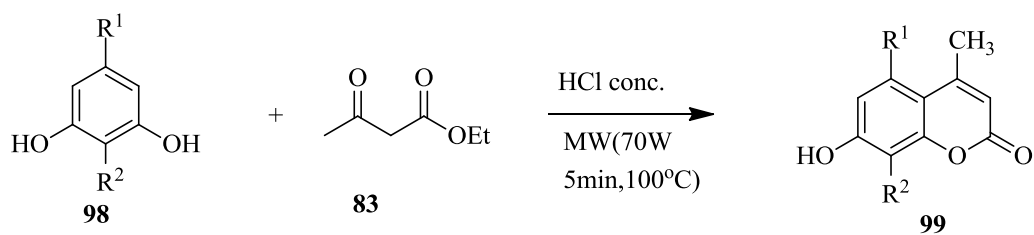


Reagents and conditions: (a) ethyl acetoacetate, 80% H₂SO₄, 100^oC.
 (b) ethyl acetoacetate, ZnCl₂, 80^oC

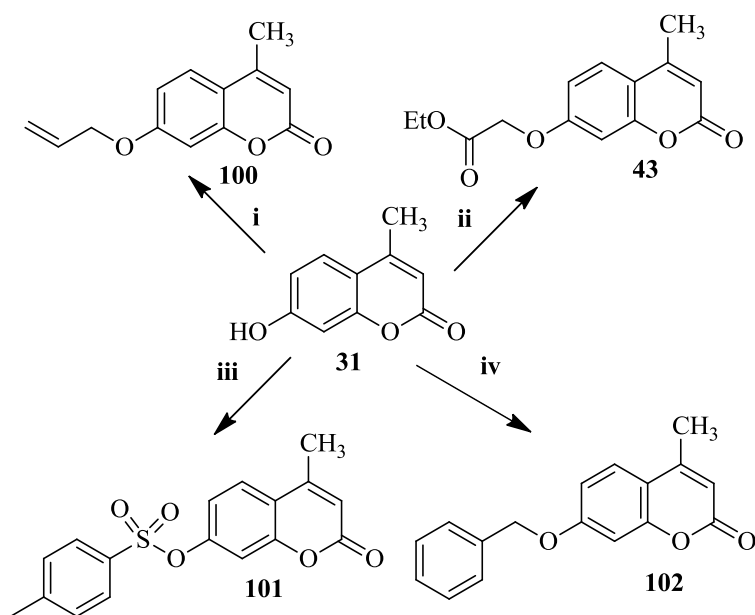
Scheme 2.14. Synthesis of simple 4-methylcoumarins.

2.9. Coumarins with cytotoxic activity

The microwave-assisted synthesis of three coumarins (**99a-c**) was achieved by reacting substituted phenols (**98**) with ethyl acetoacetate. Subsequently, the synthetic potential of **114** was explored with a range of electrophiles to afford the 7-O-substituted coumarins in high yields (**Scheme 2.15**). Compound **31** reduced cell viability by 24.14% and the cell count by 44.52% at a concentration of 50μM (Vianna *et al.*, 2015).



- a) R¹= H, R²= H
 b) R¹= H, R²= OH
 c) R¹= COOH, R²= OH

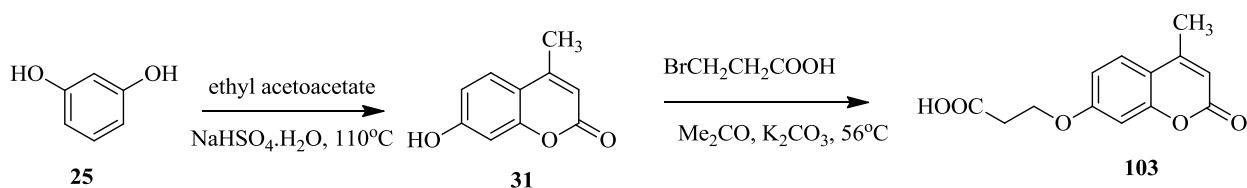


Reaction conditions: i) allyl bromide, K₂CO₃, MeCN, 70W, 70°C, 15min, 81%.
 ii) ethyl 2-bromoacetate, K₂CO₃, MeCN, 70W, 70°C, 15min, 85%.
 iii) tosyl chloride, Et₃N, MeCN, 70W, 70°C, 20min, 99%.
 iv) benzyl bromide, K₂CO₃, MeCN, 70W, 70°C, 20min, 93%.

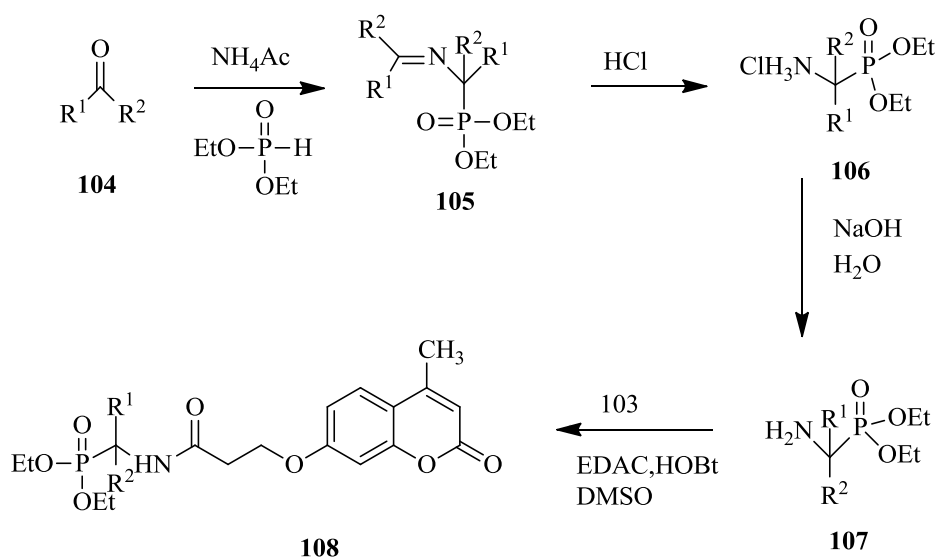
Scheme 2.15. Synthesis of 7-hydroxy-4-methylcoumarin derivatives.

In other similar study (Li *et al.*, 2015), 7-hydroxy-4-methylcoumarin **31**, synthesized from resorcinol **25** and ethyl acetoacetate (Scheme 2.16.1), was coupled with 3-bromopropionic acid in the presence of a base to yield 3-(4-methyl-2-oxo-2H-chromen-7-yloxy) propanoic acid **103**. In parallel, the substituted benzaldehydes **104** were reacted with O, O'-dialkylphosphite to form O, O'-dialkyl ((N-(phenylmethylene)- α -amino)- α -(substituted phenyl) methyl) phosphonates **105** which upon acid hydrolysis yielded the corresponding free bases **107**. The coupling of α -aminophosphonates with 7-hydroxy-4-methylcoumarins was then performed to obtain different phosphonated coumarins **108** (Scheme 2.16.2). The cytotoxicity evaluation of the compounds revealed that the compounds bearing -CH₃ and Phenyl substituents as R₁ and R₂ were the most potent agents with the activity 11 to 12 fold higher than the lead compound

4-methylcoumarin. Moreover, the increasing order of cytotoxicity was; methoxy > bromine > chlorine > fluorine, when these substituents were on the phenyl group.



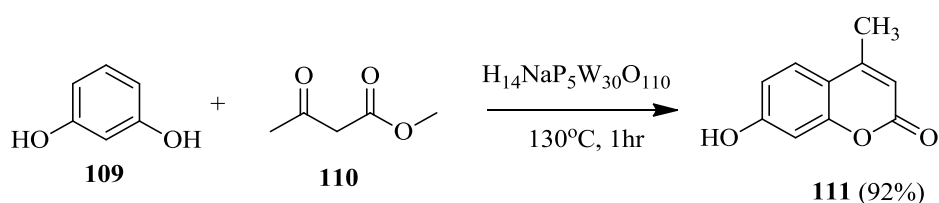
Scheme 2.16.1. Synthesis of 3-(4-methyl-2-oxo-2H-chromen-7-yl)oxy) propanoic acid.



Scheme 2.16.2. Synthesis of coumarins containing aminophosphonates.

2.10 Coumarins with antifouling properties.

The synthesis of 7-hydroxy-4-methylcoumarin, in another report (Perez *et al.*, 2016) was accomplished from resorcinol and ethyl acetoacetate using the $H_{14}NaP_5W_{30}O_{110}$ Preyssler heteropolyacid in equivalent ratio. The 7-hydroxy-4-methylcoumarin synthesized showed some antifouling properties against micro and macrofoulers.



Scheme 2.17. Synthesis of 7-hydroxy-4-methylcoumarin via the Pechmann reaction.

CHAPTER 3

Experimental Section

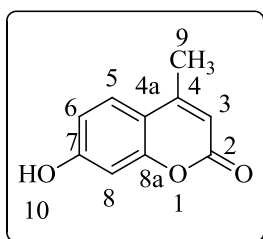
3.1. General experimental procedure

All chemicals (laboratory grade) and solvents used in this study were purchased from Sigma Aldrich and Merck, and used as such without any further purification. The moisture sensitive reactions were carried out under nitrogen atmosphere. Dimethylformamide was dried for 12 hours using molecular sieves 3Å which were preheated at 250°C to regenerate them. The progress of reactions and the purity of the compounds were determined using aluminium backed TLC plates (Kieselgel 60 F254 plates) that were purchased from Merck. The spots were visualized using ultraviolet light with a short wavelength of 254nm. The Nuclear magnetic resonance (NMR) analysis was recorded on a Bruker AVANCE III 400 MHz spectrometer (399.995 MHz for ^1H and 100.4296 MHz for ^{13}C). ^{19}F NMR spectra for fluorine-containing compounds were also recorded at 376.4 MHz. Chemical shifts (δ) were reported in parts per million (ppm). The solvents used for NMR analysis were deuterated chloroform and dimethyl sulfoxide- d_6 . The chemical shifts for ^1H and ^{13}C are referenced to CDCl_3 at 7.24 ppm and CDCl_3 at 77.23 ppm or $\text{DMSO}-d_6$ at 2.50 ppm and $\text{DMSO}-d_6$ at 39.51 ppm. The 2D NMR experiments such as HSQC, HMBC, COSY and NOESY were conducted with $4\text{ K} \times 128$ data points ($t_2 \times t_1$). The spin multiplicities are abbreviated as follows: singlet (s), broad singlet (bs), doublet (d), doublet of doublets (dd), doublet of doublet of doublet of doublets (dddd), triplet (t) and triplet of triplets (tt). The NMR data was analyzed using TopSpin 3.1 software (Bruker). Melting points of compounds were determined in an electrothermal melting point apparatus (Electrothermal IA9100) using sealed capillary tube, and are uncorrected. Infrared spectra were recorded on a Perkin Elmer Spectrum 100 FT-IR spectrometer with universal ATR sampling accessory. High resolution mass data were obtained for novel coumarins using a Bruker microTQF-Q II ESI instrument which is operated at ambient temperatures. The concentration of each sample used in HRMS analysis was approximately 1 ppm.

3.2.1. Synthesis of 4-methylcoumarins (A-C)

Approximately 5.0 grams of a phenol (phloroglucinol/resorcinol/ orcinol) was dissolved in 6ml of ethyl acetoacetate. The solution was then poured slowly into 20ml sulfuric acid at 0°C in such a way that the temperature of the reaction does not rise above 10°C. After the complete addition, the reaction mixture was allowed to stir for 30 minutes at room temperature. The reaction progress was monitored using thin layer chromatography (TLC). After the completion of the reaction, the mixture was poured into crushed ice to precipitate the solid product, and then filtered under suction. The crude product was recrystallized from ethanol. The respective yield of compound A, B and C was 71%, 88% and 60%, respectively.

7-hydroxy-4-methyl-2H-chromen-2-one (A)



Physical description: Cream white crystals

Molecular formula: C₁₀H₈O₃

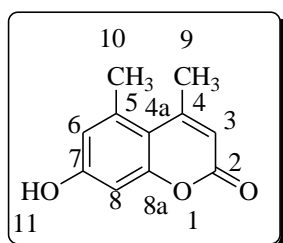
Molecular weight: 176.17 gmol⁻¹

Percentage yield: 71%

R_f value: 0.44

Melting point: 190.0-192.0 °C; **FT-IR data:** $\nu_{\max}(\text{cm}^{-1})$: 1664.42 (C=O stretch), 1595.90 (aromatic ring), 3432.15 (O-H stretch), 3095.33 (C-H stretch); **¹H NMR data (400MHz, DMSO-*d*₆):** δ 10.5 (bs, 1H, OH), 7.57 (dd, 1H, *J* = 8.44, 2.48 Hz, H-6), 6.79 (d, 1H, *J* = 8.64 Hz, H-5), 6.69 (s, 1H, H-8), 6.11 (s, 1H, H-3), 2.50 (d, 3H, *J*=0.92 Hz, H-9); **¹³C NMR data (100MHz, DMSO-*d*₆):** δ 161.1, 160.2, 154.8, 153.5, 126.6, 112.8, 111.9, 110.2, 102.1 and 18.1.

7-hydroxy-4,5-dimethyl-2H-chromen-2-one (B)



Physical description: Light brown crystals

Molecular formula: C₁₁H₁₀O₃

Molecular weight: 190.20 gmol⁻¹

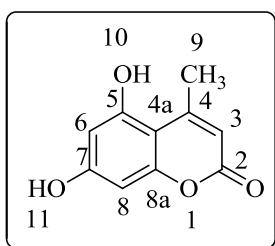
Percentage yield: 88%

R_f value: 0.54

Melting point: 248.0-250.0 °C; **FT-IR data:** $\nu_{\max}(\text{cm}^{-1})$: 3377.12 (O-H stretch), 2986.37 (C-H stretch), 1650.78 (C=O stretch), 1598.61 (aromatic ring), 1249.99 (C-O stretch); **¹H NMR data (400MHz, DMSO-*d*₆):** δ 10.5 (s, 1H, OH), 6.61 (s, 1H, H-6 or H-8), 6.56 (s, 1H, H-6 or

H-8), 6.04 (d, 1H, $J=1.16$ Hz, H-3), 2.53 (s, 3H, H-9 or H-10), 2.27 (s, 3H, H-9 or H-10); ^{13}C NMR data (100MHz, DMSO- d_6): δ 159.8, 156.4, 154.8, 154.5, 142.7, 111.8, 111.7, 107.7, 106.5, 23.4 and 21.1.

5,7-dihydroxy-4-methyl-2H-chromen-2-one (C)



Physical description: Light brown crystals

Molecular formula: $\text{C}_{10}\text{H}_8\text{O}_4$

Molecular weight: 192.17 gmol^{-1}

Percentage yield: 60%

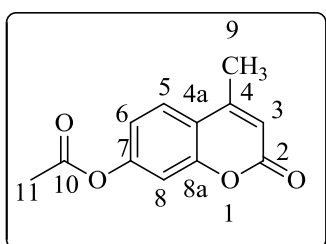
R_f value: 0.25

Melting point: 282-284 °C; **FT-IR data:** $\nu_{\text{max}}(\text{cm}^{-1})$: 3410.09 (O-H stretch), 2934.32 (C-H stretch), 1663.83 (C=O stretch), 1616.02 (aromatic ring), 1237.10 (C-O stretch); **^1H NMR data (400MHz, DMSO- d_6):** δ 10.5 (s, 1H, OH), 10.3 (bs, 1H, OH), 6.25 (d, 1H, $J=2.36$ Hz, H-6 or H-8), 6.16 (d, 1H, $J=2.36$ Hz, H-6 or H-8), 5.83 (d, 1H, $J=0.72$ Hz, H-3), 2.48 (d, 3H, $J=0.68$ Hz, H-9); **^{13}C NMR data (100MHz, DMSO- d_6):** δ 160.9, 160.1, 157.9, 156.4, 154.9, 108.7, 102.0, 99.2, 94.5 and 23.4.

3.2.2. Acetylation of 4-methylcoumarins (A-C)

Approximately 0.5g of the 4-methylcoumarin (A or B) was dissolved in acetic anhydride (3eq) and refluxed in 2ml of acetic acid for 1 hour. For 4-methylcoumarin C, the acetic anhydride was comparatively used in excess (7eq). After completion of the reaction (monitored by TLC), the contents of the flask were poured into crushed ice. The solid product obtained was filtered and washed with hexane. The percentage yield of compounds A1, B1 and C1 were 81, 75 and 97 respectively.

4-methyl-2-oxo-2H-chromen-7-yl acetate (A1)



Physical description: White solid

Molecular formula: $\text{C}_{12}\text{H}_{10}\text{O}_4$

Molecular weight: 218.21 gmol^{-1}

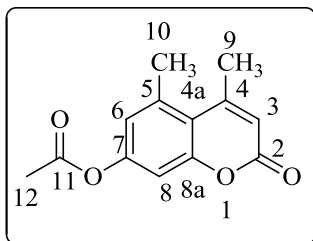
Percentage yield: 81%

R_f value: 0.48

Melting point: 150.0-152.0 °C; **FT-IR data:** $\nu_{\text{max}}(\text{cm}^{-1})$: 3054.06 (C-H stretch), 1756.20 (C=O stretch), 1698.76 (C=O stretch), 1623.90 (aromatic ring), 1154.90 (C-O stretch); **^1H**

NMR data (400MHz, DMSO-*d*₆): δ 7.82 (d, 1H, *J*=8.60 Hz, H-5), 7.26 (d, 1H, *J*=2.12 Hz, H-8), 7.18 (dd, 1H, *J*=2.12, 8.60 Hz, H-6), 6.39 (s, 1H, H-3), 2.44 (d, 3H, *J*=0.56 Hz, H-9), 2.31 (s, 3H, H-11); **¹³C NMR data (100MHz, DMSO- *d*₆):** δ 168.8, 159.6, 153.5, 152.9, 152.8, 126.4, 118.4, 117.5, 113.7, 110.1, 20.8 and 18.1.

4,5-dimethyl-2-oxo-2H-chromen-7-yl acetate (B1)



Physical description: White fluffy solid

Molecular formula: C₁₃H₁₂O₄

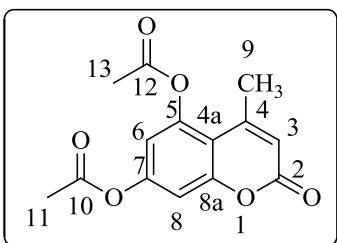
Molecular weight: 232.23 gmol⁻¹

Percentage yield: 75%

R_f value: 0.51

Melting point: 192.0-193.7°C; **FT-IR data:** ν_{\max} (cm⁻¹): 3053.83 (C-H stretch), 1728.26 (C=O stretch), 1623.24 (aromatic ring), 1213.62 (C-O stretch); **¹H NMR data (400MHz, CDCl₃):** δ 7.06 (s, 1H, H-8), 6.79 (d, 1H, *J*=0.84 Hz, H-6), 6.17 (s, 1H, H-3), 2.47 (d, 3H, *J*=1.12 Hz, H-10), 2.42 (s, 3H, H-12), 2.37 (s, 3H, H-9); **¹³C NMR data (100MHz, CDCl₃):** δ 169.3, 159.0, 153.9, 151.2, 147.3, 142.6, 120.7, 115.3, 114.9, 110.9, 21.9, 21.1 and 20.7.

4-methyl-2-oxo-2H-chromene-5,7-diyl diacetate (C1)



Physical description: White solid

Molecular formula: C₁₄H₁₂O₆

Molecular weight: 276.24 gmol⁻¹

Percentage yield: 97%

R_f value: 0.48

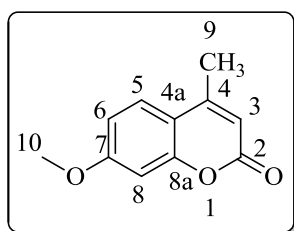
Melting point: 116.3-117.9 °C; **FT-IR data:** ν_{\max} (cm⁻¹): 2939.44 (C-H stretch), 1732.73 (C=O stretch), 1616.11 (aromatic ring), 1198.43 (C-O stretch); **¹H NMR data (400MHz, DMSO-*d*₆):** δ 7.22 (d, 1H, *J*=2.12 Hz, H-6), 7.08 (d, 1H, *J*=2.40 Hz, H-8), 6.38 (d, 1H, *J*=1.08 Hz, H-3), 2.45 (d, 3H, *J*=0.96 Hz, H-9), 2.36 (s, 3H, H-11 or H-13), 2.29 (s, 3H, H-11 or H-13); **¹³C NMR data (100MHz, DMSO-*d*₆):** δ 169.0, 168.5, 158.7, 154.4, 151.9, 151.0, 148.1, 115.7, 114.3, 111.3, 108.4, 21.9, 21.1 and 20.8.

3.2.3. Alkylation of 4-methylcoumarins (A-C)

Approximately 1.0 gram of 4-methylcoumarin (A/B/C) was dissolved in dry DMF. The activated K₂CO₃ (1eq for A and B and 2eq for C) was then added under nitrogen. After stirring

the reaction mixture for 10 minutes, the alkyl halide (1eq for **A** and **B** and 2eq for **C**) was added at 0°C. The reaction mixture was allowed to stir for 18-24 hours at room temperature. The progress of the reaction was monitored using TLC (50% ethylacetate-hexane mixture). After completion, the mixture was poured into crushed ice, and the solid product was obtained through filtration. The O-alkylated coumarins (**A2-A13**, **B2-B14** and **C2-C12**) were obtained in good yields.

7-methoxy-4-methyl-2H-chromen-2-one (A2)



Physical description: Cream white solid

Molecular formula: C₁₁H₁₀O₃

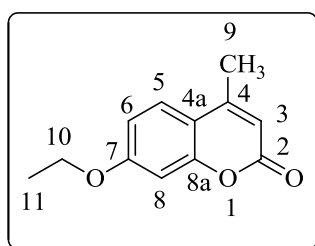
Molecular weight: 190.20 gmol⁻¹

Percentage yield: 81%

R_f value:0.66

Melting point:159-160 °C; **FT-IR data:** $\nu_{\max}(\text{cm}^{-1})$: 3069.40 (C-H stretch), 1727.97 (C=O stretch), 1606.65 (aromatic ring), 1071.57 (C-O stretch); **¹H NMR data (400MHz, DMSO-*d*₆):** δ 7.67 (d, 1H, *J*=8.40Hz, H-5), 6.96-6.94 (m, 2H, H-6/8), 6.20 (s, 1H, H-3), 3.85 (s, 3H, H-10), 2.39 (s, 3H, H-9); **¹³C NMR data (100MHz, DMSO-*d*₆):** δ 162.3, 160.1, 154.7, 153.4, 126.4, 113.1, 112.0, 111.1, 100.7, 55.9 and 18.1.

7-ethoxy-4-methyl-2H-chromen-2-one (A3)



Physical description: White solid

Molecular formula: C₁₂H₁₂O₃

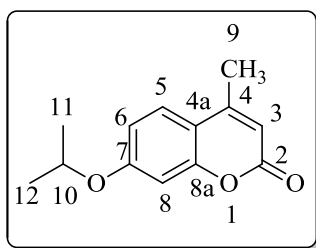
Molecular weight: 204.22 gmol⁻¹

Percentage yield: 81%

R_f value:0.67

Melting point:106-108°C; **FT-IR data:** $\nu_{\max}(\text{cm}^{-1})$: 2986.02 (C-H stretch), 1732.66 (C=O), 1624.07 (aromatic ring), 1143.61 (C-O stretch); **¹H NMR data (400MHz, DMSO-*d*₆):** δ 7.66-7.64 (d, 1H, *J*=9.2 Hz, H-5), 6.94-6.92 (m, 2H, H-6/8), 6.18 (d, 1H, *J*=1.16Hz, H-3), 4.12 (q, 2H, *J*=6.99Hz, H-10), 2.38 (d, 3H, *J*=0.92Hz, H-9), 1.35 (t, 3H, *J*=6.96 Hz, H-11); **¹³C NMR data (100MHz, DMSO-*d*₆):** δ 161.6, 160.1, 154.7, 153.3, 126.4, 112.9, 112.3, 110.1, 101.0, 63.9, 18.1 and 14.3.

4-methyl-7-(propan-2-yloxy)-2H-chromen-2-one (A4)



Physical description: White fluffy solid

Molecular formula: C₁₃H₁₄O₃

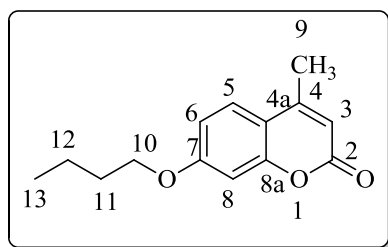
Molecular weight: 302.28 gmol⁻¹

Percentage yield: 77%

R_f value:0.68

Melting point:86.0-87.0 °C; **FT-IR data:** $\nu_{\max}(\text{cm}^{-1})$: 2978.90 (C-H stretch), 1707.79 (C=O stretch), 1605.55 (aromatic ring), 1112.84 (C-O stretch); **¹H NMR data (400MHz, DMSO-*d*₆):** δ 7.64 (d, 1H, *J*=8.60 Hz, H-5), 6.94-6.90 (m, 2H, H-6/8), 6.18 (d, 1H, *J*=1.16 Hz, H-3), 4.79-4.73 (m, 1H, H-10), 2.38 (d, 3H, *J*=1.16 Hz, H-9), 1.29 (d, 6H, *J*=6.04 Hz, H-11/12); **¹³C NMR data (100MHz, DMSO-*d*₆):** δ 160.6, 160.1, 154.8, 153.3, 126.4, 113.0, 112.8, 110.9, 101.9, 70.1, 21.6 and 18.0.

7-butoxy-4-methyl-2H-chromen-2-one (A5)



Physical description: Cream white solid

Molecular formula: C₁₄H₁₆O₃

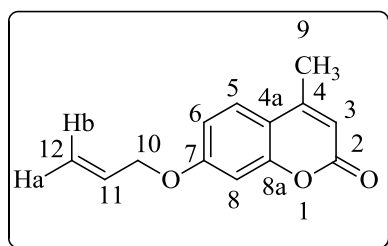
Molecular weight: 232.28 gmol⁻¹

Percentage yield: 79%

R_f value:0.73

Melting point:41-43 °C; **FT-IR data:** $\nu_{\max}(\text{cm}^{-1})$: 2947.83 (C-H stretch), 1708.00 (C=O stretch), 1614.82 (aromatic ring), 1126.33 (C-O stretch); **¹H NMR data (400MHz, DMSO-*d*₆):** δ 7.67 (t, 1H, *J*=1.76Hz, H-5), 6.96-6.94 (m, 2H, *J*=1.44 Hz, H-6/8), 6.19 (d, 1H, *J*=1.12Hz, H-3), 4.07 (t, 2H, *J*=6.52Hz, H-10), 2.39 (d, 3H, *J*=0.88Hz, H-9), 1.75-1.68 (m, 2H, H-11), 1.48-1.39 (m, 2H, H-12), 0.93 (t, 3H, *J*=7.44 Hz, H-13); **¹³C NMR data (100MHz, DMSO-*d*₆):** δ 161.8, 160.1, 154.7, 153.4, 126.4, 112.9, 112.4, 111.0, 101.1, 67.9, 30.4, 18.6, 18.1 and 13.6.

4-methyl-7-(prop-2-en-1-yloxy)-2H-chromen-2-one (A6)



Physical description: White solid

Molecular formula: C₁₃H₁₂O₃

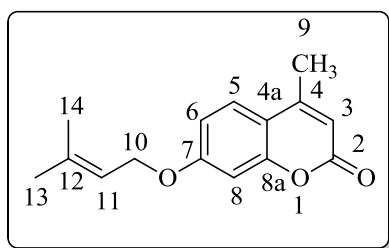
Molecular weight: 216.23 gmol⁻¹

Percentage yield: 90%

R_f value: 0.67

Melting point: 72.0-75.0 °C; **FT-IR data:** $\nu_{\max}(\text{cm}^{-1})$: 2919.25 (C-H stretch), 1717.96 (C=O), 1608.78 (aromatic ring), 1067.88 (C-O stretch); **^1H NMR data (400MHz, DMSO- d_6):** δ 7.68 (d, 1H, $J=9.48\text{Hz}$, H-5), 6.99-6.96 (m, 2H, H-6/8), 6.20 (d, 1H, $J=1.20\text{Hz}$, H-3), 6.10-6.00 (m, 1H, H-11), 5.45-5.40 (m, 1H, H-12a or H-12b), 5.31-5.27 (m, 1H, H-12a or H-12b), 4.69-4.67 (m, 2H, H-10), 2.39 (d, 3H, $J=0.96\text{ Hz}$, H-9); **^{13}C NMR data (100MHz, DMSO- d_6):** δ 161.2, 160.1, 154.6, 153.4, 132.9, 126.4, 118.0, 113.2, 112.5, 111.2, 101.4, 68.7 and 18.1.

4-methyl-7-[(3-methylbut-2-en-1-yl)oxy]-2H-chromen-2-one (A7)



Physical description: White solid

Molecular formula: $\text{C}_{15}\text{H}_{16}\text{O}_3$

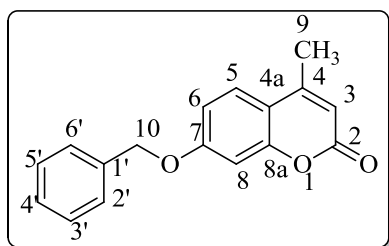
Molecular weight: 244.29 g mol^{-1}

Percentage yield: 104%

R_f value: 0.64

Melting point: 155.7-156.2 °C; **FT-IR data:** $\nu_{\max}(\text{cm}^{-1})$: 1721.19 (C=O stretch), 1615.53 (C=C stretch), 1522.61 (aromatic ring), 1069.94 (C-O stretch); **^1H NMR data (400MHz, DMSO- d_6):** δ 7.64 (d, 1H, $J=8.56\text{Hz}$, H-5), 6.94 (m, 2H, H-6/8), 6.18 (s, 1H, H-3), 5.45-5.42 (m, 1H, H-11), 4.62 (d, 2H, $J=6.72\text{Hz}$, H-10), 2.38 (s, 3H, H-9), 1.73 (d, 6H, $J=9.88\text{ Hz}$, H-13/14); **^{13}C NMR data (100MHz, DMSO- d_6):** δ 161.5, 160.1, 154.7, 153.3, 137.9, 126.3, 119.1, 112.9, 112.5, 110.9, 101.3, 65.1, 25.4 and 18.0.

7-(benzyloxy)-4-methyl-2H-chromen-2-one (A8)



Physical description: White solid

Molecular formula: $\text{C}_{17}\text{H}_{14}\text{O}_3$

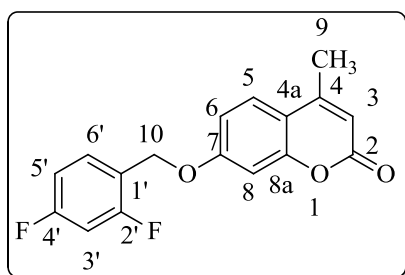
Molecular weight: 266.30 g mol^{-1}

Percentage yield: 85%

R_f value: 0.75

Melting point: 181.0-182.0 °C; **FT-IR data:** $\nu_{\max}(\text{cm}^{-1})$: 2929.82 (C-H stretch), 1716.33 (C=O stretch), 1606.98 (aromatic ring), 1153.48 (C-O stretch); **^1H NMR data (400MHz, DMSO- d_6):** δ 7.44 (d, 1H, $J=8.72\text{Hz}$, H-5), 7.40-7.34 (m, 5H, Ar), 7.06-7.01 (m, 2H, H-6/8), 6.19 (d, 1H, $J=1.08\text{Hz}$, H-3), 5.22 (s, 2H, H-10), 2.38 (d, 3H, $J=1.24\text{Hz}$, H-9); **^{13}C NMR data (100MHz, DMSO- d_6):** δ 161.3, 160.1, 154.6, 153.3, 136.3, 128.5, 128.0, 127.8, 126.4, 113.2, 112.7, 111.2, 101.6, 69.8 and 18.1.

7-[(2,4-difluorobenzyl)oxy]-4-methyl-2H-chromen-2-one (A9)



Physical description: White powder

Molecular formula: C₁₇H₁₂F₂O₃

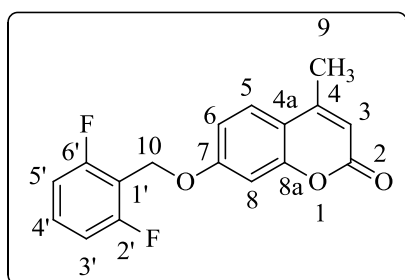
Molecular weight: 302.28 gmol⁻¹

Percentage yield: 68%

R_f value: 0.63

Melting point: 150.3-151.6 °C; **FT-IR data:** $\nu_{\max}(\text{cm}^{-1})$: 3081.91 (C-H stretch), 1706.35 (C=O stretch), 1600.24 (aromatic ring), 1076.89 (C-F stretch); **¹H NMR data (400MHz, CDCl₃):** δ 7.50-6.94 (m, 2H, Ar), 6.93-6.85 (m, 4H, Ar), 6.15 (d, 1H, *J*=0.88 Hz, H-3), 5.14 (s, 2H, H-10), 2.40 (d, 3H, *J*=1.24 Hz, H-9); **¹³C NMR data (100MHz, CDCl₃):** δ 164.4, 164.3, 161.9, 161.2, 155.2, 152.4, 130.9, 125.7, 114.1, 112.5, 111.7, 111.5, 104.2, 103.9, 101.9, 63.7 and 18.6; **¹⁹F NMR data (376.4 MHz, CDCl₃):** 109.1-109.2 (m, 1F), 113.9 (q, 1F). **HRMS data: [m/z]:** 325.0654 (Calculated for C₁₇H₁₂F₂O₃Na, 325.0652).

7-[(2,6-difluorobenzyl)oxy]-4-methyl-2H-chromen-2-one (A10)



Physical description: White powder

Molecular formula: C₁₇H₁₂F₂O₃

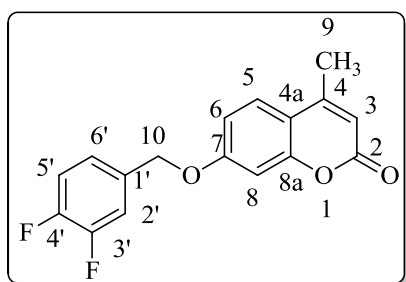
Molecular weight: 302.28 gmol⁻¹

Percentage yield: 77%

R_f value: 0.68

Melting point: 178.3-179.6 °C; **FT-IR data:** $\nu_{\max}(\text{cm}^{-1})$: 3077.39 (C-H stretch), 1697.48 (C=O stretch), 1614.48 (aromatic ring), 1053.51 (C-F stretch); **¹H NMR data (400MHz, CDCl₃):** δ 7.51 (d, 1H, *J*=8.56 Hz, H-5), 7.38-7.33 (m, 1H, Ar), 6.99-6.92 (m, 4H, Ar), 6.15 (d, 1H, *J*=1.16 Hz, H-3), 5.19 (s, 2H, H-10), 2.40 (d, 3H, *J*=1.16 Hz, H-9); **¹³C NMR data (100MHz, CDCl₃):** δ 163.1-163.0, 161.4-161.2, 160.6-160.5, 155.2, 152.5, 131.3-131.1, 125.6, 114.0, 112.7-112.2, 111.9-111.4, 101.9, 58.4 and 18.6; **¹⁹F NMR data (376.4 MHz, CDCl₃):** 114.4 (t, 2F, *J*=6.66 Hz). **HRMS data: [m/z]:** 325.0654 (Calculated for C₁₇H₁₂F₂O₃Na, 325.0652).

7-[(3,4-difluorobenzyl)oxy]-4-methyl-2H-chromen-2-one (A11)



Physical description: Cream white solid

Molecular formula: C₁₇H₁₂F₂O₃

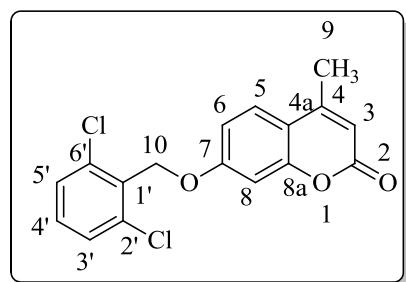
Molecular weight: 302.28 gmol⁻¹

Percentage yield: 64%

R_f value:0.73

Melting point: 73.4-74.8 °C; **FT-IR data:** $\nu_{\max}(\text{cm}^{-1})$: 2935.27 (C-H stretch), 1716.89 (C=O stretch), 1604.39 (aromatic ring), 1154.76 (C-O stretch), 1071.30 (C-F stretch); **¹H NMR data (400MHz, DMSO-*d*₆):** δ 7.53 (d, 1H, *J*=1.92 Hz, H-5), 7.49-7.42 (m, 1H, Ar), 7.35-7.32 (m, 2H, Ar), 7.06-7.01 (m, 2H, H-6/8), 6.20 (d, 1H, *J*=0.96Hz, H-3), 5.20 (s, 2H, H-10), 2.38 (s, 3H, H-9); **¹³C NMR data (100MHz, DMSO-*d*₆):** δ 160.9, 160.0, 154.6, 153.3, 150.4, 148.0, 134.1, 126.5, 124.7, 117.6, 116.9, 113.4, 112.6, 111.3, 101.7, 68.5 and 18.1.

7-[(2,6-dichlorobenzyl)oxy]-4-methyl-2H-chromen-2-one (A12)



Physical description: White solid

Molecular formula: C₁₇H₁₂Cl₂O₃

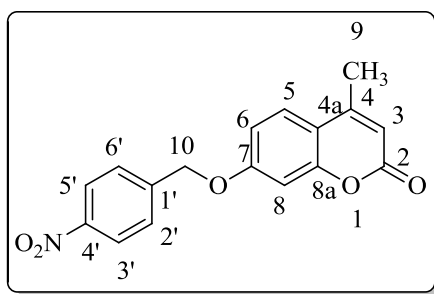
Molecular weight: 335.18 gmol⁻¹

Percentage yield: 93%

R_f value:0.67

Melting point: 170.2-171.5 °C; **FT-IR data:** $\nu_{\max}(\text{cm}^{-1})$: 3068.97 (C-H stretch), 1708.59 (C=O), 1610.07 (aromatic ring), 1135.93 (C-O stretch), 750.75 (C-Cl stretch); **¹H NMR data (400MHz, DMSO-*d*₆):** δ 7.70 (d, 1H, *J*=8.76 Hz, H-5), 7.58-7.48 (m, 3H, Ar), 7.19 (d, 1H, *J*=2.48Hz, H-8), 7.06 (dd, 1H, *J*=2.48, 8.76Hz, H-6), 6.23 (d, 1H, *J*=0.72Hz, H-3), 5.34 (s, 2H, H-10), 2.40 (d, 3H, *J*=0.64 Hz, H-9); **¹³C NMR data (100MHz, DMSO-*d*₆):** δ 161.3, 160.0, 154.7, 153.3, 136.1, 131.8, 130.9, 128.8, 126.6, 113.6, 112.4, 111.4, 101.4, 65.5 and 18.1. **HRMS data: [m/z]:** 357.0074 (Calculated for C₁₇H₁₂Cl₂O₃Na, 357.0061).

4-methyl-7-[(4-nitrobenzyl)oxy]-2H-chromen-2-one (A13)



Physical description: Light yellow solid

Molecular formula: C₁₇H₁₃NO₅

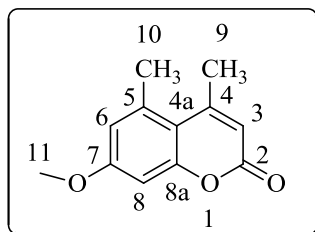
Molecular weight: 311.29 gmol⁻¹

Percentage yield: 70%

R_f value: 0.66

Melting point: 204.0-205.0 °C; **FT-IR data:** $\nu_{\max}(\text{cm}^{-1})$: 3092.94 (C-H stretch), 1715.76 (C=O stretch), 1601.84 (C=C stretch), 1341.08 (Nitro), 1514.97 (aromatic ring); **¹H NMR data (400MHz, CDCl₃):** δ 8.27 (d, 2H, $J=8.8$ Hz, Ar), 7.62 (d, 2H, $J=8.52$ Hz, Ar), 7.54 (d, 1H, $J=8.80$ Hz, H-5), 6.95 (dd, 1H, $J=2.48, 8.72$ Hz, H-6), 6.87 (d, 1H, $J=2.52$ Hz, H-8), 6.16 (d, 1H, $J=1.20$ Hz, H-3), 5.24 (s, 2H, H-10), 2.41 (d, 3H, $J=1.00$ Hz, H-9); **¹³C NMR data (100MHz, CDCl₃):** δ 161.0, 160.9, 155.2, 152.4, 147.8, 143.2, 127.7, 125.8, 123.9, 114.3, 112.7, 112.5, 101.9, 69.0 and 18.7.

7-methoxy-4,5-dimethyl-2H-chromen-2-one (B2)



Physical description: White solid

Molecular formula: C₁₂H₁₂O₃

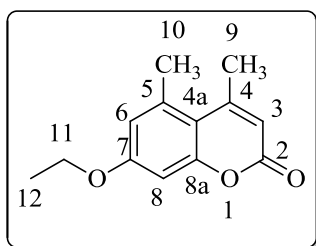
Molecular weight: 204.22 gmol⁻¹

Percentage yield: 74%

R_f value:0.58

Melting point: 134.4-134.8 °C; **FT-IR data:** $\nu_{\max}(\text{cm}^{-1})$: 2943.79 (C-H stretch), 1714.13 (C=O stretch), 1607.01 (aromatic ring); **¹H NMR data (400MHz, DMSO-*d*₆):** δ 6.79 (s, 2H, H-6/8), 6.12 (d, 1H, $J=0.76$ Hz, H-3), 3.86 (s, 3H, H-11), 2.50 (s, 3H, H-9), 2.37 (s, 3H, H-10); **¹³C NMR data (100MHz, DMSO-*d*₆):** δ 159.5, 157.6, 154.6, 153.9, 143.2, 112.7, 109.3, 107.9, 107.4, 56.1, 23.6 and 21.4. **HRMS data:** [m/z]: 227.0683 (Calculated for C₁₂H₁₂O₃Na, 227.0684).

7-ethoxy-4,5-dimethyl-2H-chromen-2-one (B3)



Physical description: White solid

Molecular formula: C₁₃H₁₄O₃

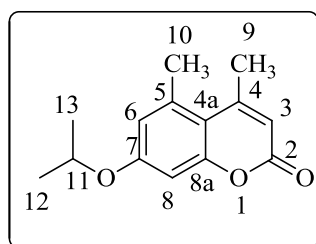
Molecular weight: 218.25 gmol⁻¹

Percentage yield: 68%

R_f value: 0.65

Melting point: 137.7-138.2 °C; **FT-IR data:** $\nu_{\max}(\text{cm}^{-1})$: 2979.95 (C-H stretch), 1726.82 (C=O), 1108.12 (C-O stretch), 1620.04 (C=C), 1607.87 (aromatic ring); **¹H NMR data (400MHz, DMSO-*d*₆):** δ 6.77 (d, 2H, *J*=3.56 Hz, H-6/8), 6.13 (d, 1H, *J*=0.56 Hz, H-3), 4.10 (q, 2H, *J*=6.94 Hz, H-11), 2.53 (d, 3H, *J*=0.88 Hz, H-9), 2.36 (s, 3H, H-10), 1.40 (t, 3H, *J*=6.96 Hz, H-12); **¹³C NMR data (100MHz, DMSO-*d*₆):** δ 159.5, 156.9, 154.6, 154.0, 143.2, 112.8, 109.2, 108.6, 107.4, 64.6, 23.8, 21.4 and 14.4; **HRMS data:** [*m/z*]: 241.0834 (Calculated for C₁₃H₁₄O₃Na, 241.0841).

4,5-dimethyl-7-(propan-2-yloxy)-2H-chromen-2-one (B4)



Physical description: White solid

Molecular formula: C₁₄H₁₆O₃

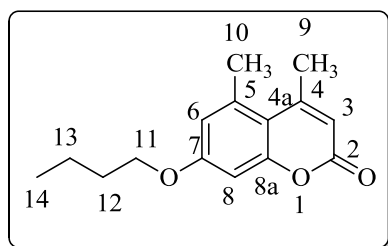
Molecular weight: 232.28 gmol⁻¹

Percentage yield: 57%

R_f value: 0.51

Melting point: 81.3-82.7 °C; **FT-IR data:** $\nu_{\max}(\text{cm}^{-1})$: 2967.34 (C-H stretch), 1716.33 (C=O), 1610.51 (aromatic ring), 1114.36 (C-O stretch); **¹H NMR data (400MHz, DMSO-*d*₆):** δ 6.79 (s, 1H, H-6), 6.74 (s, 1H, H-8), 6.09 (d, 1H, *J*=1.08 Hz, H-3), 4.77 (m, 1H, H-11), 2.52 (d, 3H, *J*=1.08 Hz, H-9), 2.35 (s, 3H, H-10), 1.34 (d, 6H, *J*=6.00 Hz, H12/13); **¹³C NMR data (100MHz, DMSO-*d*₆):** δ 159.5, 155.8, 154.8, 154.1, 143.1, 112.8, 109.5, 108.9, 107.9, 70.7, 24.1, 21.6 and 21.4; **HRMS data:** [*m/z*]: 255.0991 (Calculated for C₁₄H₁₆O₃Na, 255.0997).

7-butoxy-4,5-dimethyl-2H-chromen-2-one (B5)



Physical description: White powder

Molecular formula: C₁₅H₁₈O₃

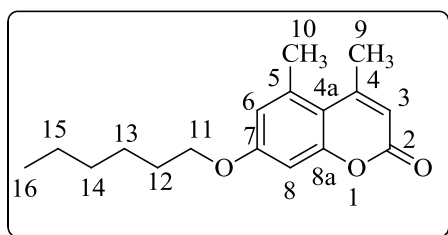
Molecular weight: 246.30 gmol⁻¹

Percentage yield: 68%

R_f value: 0.73

Melting point: 117.9-118.0 °C; **FT-IR data:** $\nu_{\max}(\text{cm}^{-1})$: 2956.78 (C-H stretch), 1716.00 (C=O), 1602.75 (aromatic ring), 1114.65 (C-O stretch); **^1H NMR data (400MHz, DMSO- d_6):** δ 6.77 (d, 2H, $J=2.20$ Hz, H-6/8), 6.10 (s, 1H, H-3), 4.05 (t, 2H, $J=6.32$ Hz, H-11), 2.52 (s, 3H, H-9), 2.35 (s, 3H, H-10), 1.79-1.74 (m, 2H, H-12), 1.49-1.44(m, 2H, H-13), 0.95 (t, 3H, $J=7.36$ Hz, H-14); **^{13}C NMR data (100MHz, DMSO- d_6):** δ 159.5, 157.0, 154.6, 153.9, 143.2, 112.8, 109.2, 108.5, 107.3, 68.5, 30.6, 23.8, 21.4, 18.9 and 13.6; **HRMS data:** [m/z]: 269.1148 (Calculated for $\text{C}_{15}\text{H}_{18}\text{O}_3\text{Na}$, 269.1154).

7-(hexyloxy)-4,5-dimethyl-2H-chromen-2-one (B6)



Physical description: White powder

Molecular formula: $\text{C}_{17}\text{H}_{22}\text{O}_3$

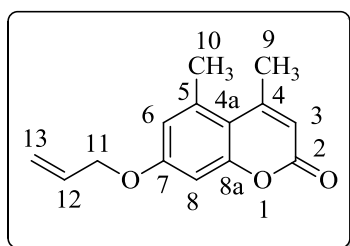
Molecular weight: 274.35 g mol^{-1}

Percentage yield: 56%

R_f value: 0.75

Melting point: 89.5-90.9 °C; **FT-IR data:** $\nu_{\max}(\text{cm}^{-1})$: 2940.29 (C-H stretch), 1724.43 (C=O), 1606.03 (aromatic ring), 1243.87 (C-O stretch); **^1H NMR data (400MHz, DMSO- d_6):** δ 6.75 (s, 2H, H-6/8), 6.09 (d, 1H, $J=0.64$ Hz, H-3), 4.03 (t, 2H, $J=6.36$ Hz, H-11), 2.51 (d, 3H, $J=0.60$ Hz, H-9), 2.35 (s, 3H, H-10), 1.81-1.74 (m, 2H, H-12), 1.47-1.39 (m, 2H, H-15), 1.33-1.29 (m, 4H, H-13/14), 0.88 (t, 3H, $J=6.84$ Hz, H-16); **^{13}C NMR data (100MHz, DMSO- d_6):** δ 159.5, 157.0, 154.6, 153.9, 143.2, 112.8, 109.2, 108.5, 107.3, 68.8, 30.9, 28.4, 25.3, 23.8, 21.9, 21.3 and 13.8; **HRMS data:** [m/z]: 297.1459 (Calculated for $\text{C}_{17}\text{H}_{22}\text{O}_3\text{Na}$, 297.1467).

4,5-dimethyl-7-(prop-2-en-1-yloxy)-2H-chromen-2-one (B7)



Physical description: Cream white solid

Molecular formula: $\text{C}_{14}\text{H}_{14}\text{O}_3$

Molecular weight: 230.26 g mol^{-1}

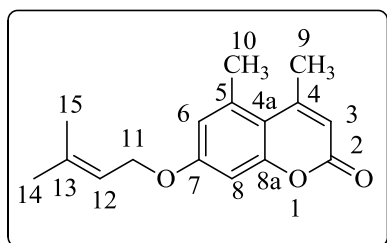
Percentage yield: 89%

R_f value: 0.68

Melting point: 110.9-111.5 °C; **FT-IR data:** $\nu_{\max}(\text{cm}^{-1})$: 2926.36 (C-H stretch), 1716.51 (C=O stretch), 1601.05 (C=C stretch), 1489.94 (aromatic ring); **^1H NMR data (400MHz, DMSO- d_6):** δ 6.79 (d, 2H, $J=1.76$ Hz, H-6,8), 6.16-6.05 (m, 2H, H-3/12), 5.46-5.30 (m, 2H, H-13), 4.67-4.66 (m, 2H, H-11), 2.53 (d, 3H, $J=1.12$ Hz, H-9), 2.35 (s, 3H, H-10); **^{13}C NMR data (100MHz, DMSO- d_6):** δ 159.5, 156.4, 154.6, 153.7, 143.1, 133.0, 118.2, 112.9, 109.5, 109.0,

107.5, 69.7, 23.9 and 21.3; **HRMS data:** [m/z]: 253.0837 (Calculated for $C_{14}H_{14}O_3Na$, 253.0841).

4,5-dimethyl-7-[(3-methylbut-2-en-1-yl)oxy]-2H-chromen-2-one (B8)



Physical description: Cream white solid

Molecular formula: $C_{16}H_{18}O_3$

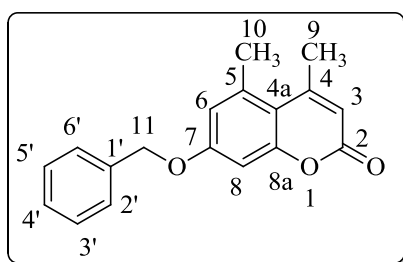
Molecular weight: 258.31 $gmol^{-1}$

Percentage yield: 78%

R_f value: 0.74

Melting point: 85.5-86.9 °C; **FT-IR data:** $\nu_{max}(cm^{-1})$: 2916.17 (C- stretch), 1726.72 (C=O), 1609.20 (aromatic ring), 1244.00 (C-O stretch); **¹H NMR data (400MHz, DMSO-*d*₆):** δ 6.81(s, 1H, H-6), 6.76 (s, 1H, H-8), 6.09 (d, 1H, $J=1.00Hz$, H-3), 5.52-5.48 (m, 1H, H-12), 4.62 (d, 2H, $J=6.68Hz$, H-11), 2.49 (d, 3H, $J=1.16Hz$, H-9), 2.35 (s, 3H, H-10), 1.75 (d, 6H, $J=13.3 Hz$, H-14/15); **¹³C NMR data (100MHz, DMSO-*d*₆):** δ 159.5, 156.8, 154.6, 153.9, 143.1, 137.8, 119.1, 112.8, 109.3, 109.0, 107.5, 65.7, 25.4, 23.7, 21.4 and 18.0; **HRMS data:** [m/z]: 281.1155 (Calculated for $C_{16}H_{18}O_3Na$, 281.1154).

7-(benzyloxy)-4,5-dimethyl-2H-chromen-2-one (B9)



Physical description: White powder

Molecular formula: $C_{18}H_{16}O_3$

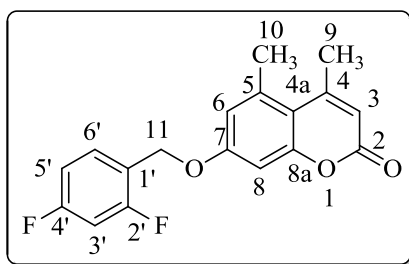
Molecular weight: 280.32 $gmol^{-1}$

Percentage yield: 85%

R_f value: 0.76

Melting point: 141.1-142.3°C; **FT-IR data:** $\nu_{max}(cm^{-1})$: 3054.98 (C-H stretch), 1694.61 (C=O stretch), 1615.01 (aromatic ring), 1245.75 (C-O stretch); **¹H NMR data (400MHz, DMSO-*d*₆):** δ 7.50-7.34 (m, 5H, Ar), 6.91 (s, 1H, H-6), 6.79 (s, 1H, H-8), 6.09 (d, 1H, $J=0.68Hz$, H-3), 5.18 (s, 2H, H-11), 2.44 (d, 3H, $J=0.60Hz$, H-9), 2.36 (s, 3H, H-10). **¹³C NMR data (100MHz, DMSO-*d*₆):** δ 159.5, 156.6, 154.6, 153.8, 143.1, 136.1, 128.5, 128.4, 128.1, 112.9, 109.6, 109.1, 107.6, 70.7, 23.9 and 21.4; **HRMS data** [m/z]: 303.0994 (Calculated for $C_{18}H_{16}O_3Na$, 303.0997).

7-[(2,4-difluorobenzyl)oxy]-4,5-dimethyl-2H-chromen-2-one (B10)



Physical description: White powder

Molecular formula: C₁₈H₁₄F₂O₃

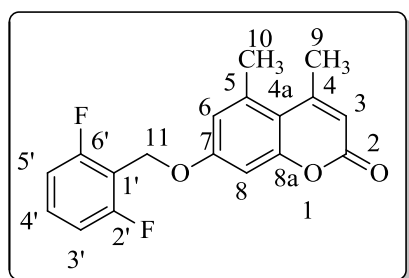
Molecular weight: 316.30 gmol⁻¹

Percentage yield: 84%

R_f value: 0.45

Melting point: 155.3-157.2 °C; **FT-IR data:** $\nu_{\max}(\text{cm}^{-1})$: 2935.33 (C-H stretch), 1713.11 (C=O stretch), 1601.49 (aromatic ring), 1069.48 (C-F stretch); **¹H NMR data (400MHz, DMSO-*d*₆):** δ 7.69-7.67 (m, 1H, Ar), 7.37-7.31 (m, 1H, Ar), 7.18-7.15 (m, 1H, Ar), 6.97 (s, 1H, H-6), 6.83 (s, 1H, H-8), 6.09 (d, 1H, *J*=1.04Hz, H-3), 5.20 (s, 2H, H-11), 2.38 (s, 3H, H-10), 2.36 (d, 3H, *J*=1.12Hz, H-9); **¹³C NMR data (100MHz, DMSO-*d*₆):** δ 163.8, 163.7, 159.4, 156.3, 154.6, 153.6, 143.2, 132.7, 119.5, 113.1, 111.7, 109.8, 109.1, 107.6, 104.2, 64.4, 23.4 and 21.3; **HRMS data [*m/z*]:** 339.0808 (Calculated for C₁₈H₁₄O₃F₂Na, 339.0809).

7-[(2,6-difluorobenzyl)oxy]-4,5-dimethyl-2H-chromen-2-one (B11)



Physical description: White solid

Molecular formula: C₁₈H₁₄F₂O₃

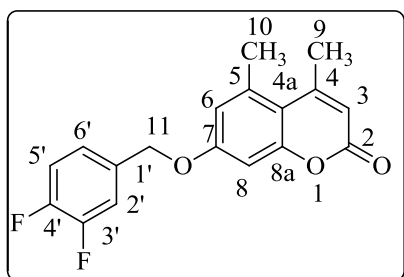
Molecular weight: 316.30 gmol⁻¹

Percentage yield: 78%

R_f value: 0.63

Melting point: 149.9-151.3 °C; **FT-IR data:** $\nu_{\max}(\text{cm}^{-1})$: 2929.41 (C-H stretch), 1719.26 (C=O stretch), 1607.59 (aromatic ring), 1235.00 (C-O stretch), 1105.29 (C-F stretch); **¹H NMR data (400MHz, DMSO-*d*₆):** δ 7.55 (tt, *J*=6.7, 8.4 Hz, H-4'), 7.21 (t, 2H, *J*=8.2 Hz, Ar), 7.02 (s, 1H, H-6), 6.84 (s, 1H, H-8), 6.07 (d, 1H, *J*=0.80 Hz, H-3), 5.23 (s, 2H, H-11), 2.39 (s, 3H, H-10), 2.29 (s, 3H, H-9); **¹³C NMR data (100MHz, DMSO-*d*₆):** δ 159.8-162.3 (d), 159.8, 159.4, 156.1, 154.6, 153.3, 143.3, 131.9-132.1(t), 113.1, 111.97-111.91 (d), 111.78-111.72(d), 110.0, 109.0, 107.5, 58.6, 23.1 and 21.3; **¹⁹F NMR data (376.4 MHz, DMSO-*d*₆):** 114.9 (t, 2F, *J*=7.10Hz, F-2'/6'); **HRMS data [*m/z*]:** 339.0808 (Calculated for C₁₈H₁₄O₃F₂Na, 339.0809).

7-[(3,4-difluorobenzyl)oxy]-4,5-dimethyl-2H-chromen-2-one (B12)



Physical description: White solid

Molecular formula: C₁₈H₁₄F₂O₃

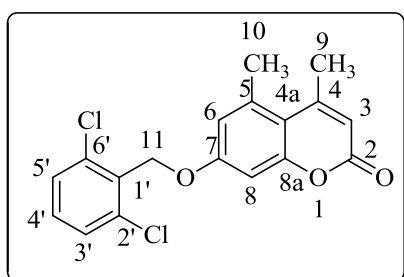
Molecular weight: 316.30 gmol⁻¹

Percentage yield: 121%

R_f value: 0.73

Melting point: 170.8-172.4°C; **FT-IR data:** $\nu_{\max}(\text{cm}^{-1})$: 3369.09 (C-H stretch), 1715.08 (C=O stretch), 1607.44 (aromatic ring), 1068.72 (C-F stretch); **¹H NMR data (400MHz, CDCl₃):** δ 7.24-7.14 (m, 3H, Ar), 6.79 (s, 1H, H-6), 6.58 (s, 1H, H-8), 6.06 (d, 1H, $J=1.20\text{Hz}$, H-3), 5.06 (s, 2H, H-11), 2.49 (d, 3H, $J=0.96\text{ Hz}$, H-9), 2.39 (s, 3H, H-10); **¹³C NMR data (100MHz, CDCl₃):** δ 160.8, 156.5, 155.4, 153.7, 151.8-151.5, 149.2-148.9, 143.1, 132.9, 123.9, 117.7, 116.9, 113.8, 110.9, 108.4, 108.3, 70.0, 24.6 and 21.9; **¹⁹F NMR data (376.4MHz, CDCl₃):** δ 136.6-136.7 (m, 1F), 137.6-137.8 (m, 1F).

7-[(2,6-dichlorobenzyl)oxy]-4,5-dimethyl-2H-chromen-2-one (B13)



Physical description: White solid

Molecular formula: C₁₈H₁₄Cl₂O₃

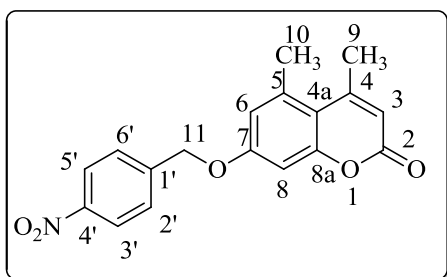
Molecular weight: 349.21 gmol⁻¹

Percentage yield: 85%

R_f value: 0.70

Melting point: 201.7-202.4 °C; **FT-IR data:** $\nu_{\max}(\text{cm}^{-1})$: 2927.42 (C-H stretch), 1721.12 (C=O stretch), 1611.84 (aromatic ring), 1102.86 (C-O stretch), 650.03 (C-Cl stretch); **¹H NMR data (400MHz, DMSO-*d*₆):** δ 7.61 (t, 2H, $J=0.96\text{ Hz}$, Ar), 7.50 (dd, 1H, $J=7.24, 8.84\text{ Hz}$, Ar), 7.07 (s, 1H, H-6), 6.87 (d, 1H, $J=0.40\text{Hz}$, H-8), 6.08 (d, 1H, $J=1.16\text{Hz}$, H-3), 5.34 (s, 2H, H-11), 2.42 (s, 3H, H-10), 2.24 (d, 3H, $J=1.12\text{Hz}$, H-9); **¹³C NMR data (100MHz, DMSO-*d*₆):** δ 159.4, 156.5, 154.6, 153.3, 143.5, 135.9, 131.9, 130.9, 128.9, 113.2, 110.0, 108.8, 107.4, 65.9, 23.1 and 21.4; **HRMS data [*m/z*]:** 371.0221 (Calculated for C₁₈H₁₄O₃Cl₂Na, 371.0218).

4,5-dimethyl-7-[(4-nitrobenzyl)oxy]-2H-chromen-2-one (B14)



Physical description: Light yellow solid

Molecular formula: C₁₈H₁₅NO₅

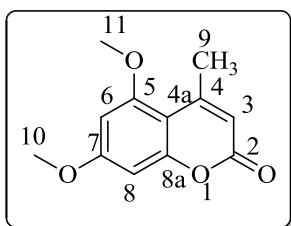
Molecular weight: 325.32 gmol⁻¹

Percentage yield: 72%

R_f value: 0.59

Melting point: 196.3-197.4 °C; **FT-IR data:** $\nu_{\max}(\text{cm}^{-1})$: 2916.07 (C-H stretch), 1714.90 (C=O stretch), 1603.88 (aromatic ring), 1345.94 (nitro), 1078.96 (C-O stretch); **¹H NMR data (400MHz, DMSO-*d*₆):** δ 8.29 (d, 2H, *J*=8.68 Hz, Ar), 7.79 (d, 2H, *J*=8.76 Hz, Ar), 6.91 (s, 1H, H-6), 6.84 (s, 1H, H-8), 6.14 (d, 1H, *J*=1.16 Hz, H-3), 5.38 (s, 2H, H-11), 2.50 (d, 3H, *J*=1.32 Hz, H-9), 2.36 (s, 3H, H-10); **¹³C NMR data (100MHz, DMSO-*d*₆):** δ 159.4, 156.2, 154.7, 153.6, 147.2, 143.9, 143.2, 128.9, 123.7, 113.1, 109.9, 109.2, 107.7, 69.5, 23.9 and 21.4.

5,7-dimethoxy-4-methyl-2H-chromen-2-one (C2)



Physical description: White solid

Molecular formula: C₁₂H₁₂O₄

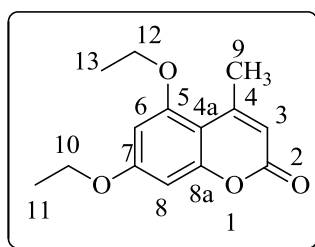
Molecular weight: 220.22 gmol⁻¹

Percentage yield: 61%

R_f value: 0.60

Melting point: 172.0-173.0°C; **FT-IR data:** $\nu_{\max}(\text{cm}^{-1})$: 2936.41 (C-H stretch), 1721.79 (C=O stretch), 1605.55 (aromatic ring), 1080.83 (C-O stretch); **¹H NMR data (400MHz, DMSO-*d*₆):** δ 6.57 (d, 1H, *J*=2.40 Hz, H-6), 6.49 (d, 1H, *J*=2.36 Hz, H-8), 6.01 (d, 1H, *J*=0.88 Hz, H-3), 3.85 (s, 6H, H-10/11), 2.48 (d, 3H, *J*=0.76 Hz, H-9); **¹³C NMR data (100MHz, DMSO-*d*₆):** δ 162.7, 159.7, 158.9, 156.3, 154.2, 110.6, 103.9, 95.6, 93.6, 56.0, 55.9 and 23.6.

5,7-diethoxy-4-methyl-2H-chromen-2-one (C3)



Physical description: White solid

Molecular formula: C₁₄H₁₆O₄

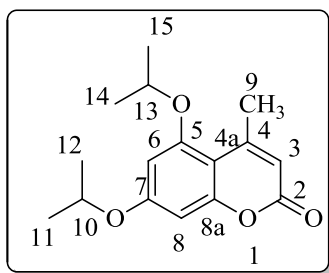
Molecular weight: 248.27 gmol⁻¹

Percentage yield: 56%

R_f value: 0.60

Melting point: 152.0-153.0°C **FT-IR data:** $\nu_{\max}(\text{cm}^{-1})$: 2988.43 (C-H stretch), 1727.86 (C=O), 1606.23 (aromatic ring), 1171.46 (C-O stretch); **$^1\text{H NMR}$ data (400MHz, DMSO- d_6):** δ 6.51 (d, 1H, $J=2.36\text{Hz}$, H-6), 6.41 (d, 1H, $J=2.32\text{Hz}$, H-8), 5.97 (d, 1H, $J=0.92\text{Hz}$, H-3), 4.12-4.05 (m, 4H, H-10/12), 2.49 (s, 3H, H-9), 1.39-1.32 (m, 6H, H-11/13); **$^{13}\text{C NMR}$ data (100MHz, DMSO- d_6):** δ 161.9, 159.7, 158.1, 156.3, 154.2, 110.5, 103.7, 96.2, 93.8, 64.6, 63.9, 23.7, 14.3 and 14.2.

4-methyl-5,7-bis (propan-2-yloxy)-2H-chromen-2-one (C4)



Physical description: Light brown crystals

Molecular formula: $\text{C}_{16}\text{H}_{20}\text{O}_4$

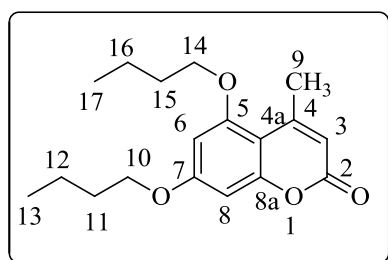
Molecular weight: 276.33 g mol^{-1}

Percentage yield: 57%

R_f value: 0.54

Melting point: 85.2-85.9°C; **FT-IR data:** $\nu_{\max}(\text{cm}^{-1})$: 2976.03 (C-H stretch), 1712.86 (C=O), 1596.84 (aromatic ring), 1074.21 (C-O stretch); **$^1\text{H NMR}$ data (400MHz, DMSO- d_6):** δ 6.51 (d, 1H, $J=2.28\text{Hz}$, H-6), 6.42 (d, 1H, $J=2.24\text{Hz}$, H-8), 5.95 (d, 1H, $J=0.76\text{ Hz}$, H-3), 4.79-4.71 (m, 2H, H-10/13), 2.49 (s, 3H, H-9), 1.31-1.28 (dd, 12H, $J=6.19\text{ Hz}$, H-11/12/14/15); **$^{13}\text{C NMR}$ data (100MHz, DMSO- d_6):** δ 160.9, 159.7, 157.7, 156.5, 154.3, 110.5, 104.2, 97.7, 94.5, 70.8, 70.0, 23.9 and 21.6-21.5. **HRMS data:** [m/z]: 299.1255 (Calculated for $\text{C}_{16}\text{H}_{20}\text{O}_4\text{Na}$, 299.1259).

5,7-dibutoxy-4-methyl-2H-chromen-2-one(C5)



Physical description: Cream white solid

Molecular formula: $\text{C}_{18}\text{H}_{24}\text{O}_4$

Molecular weight: 304.38 g mol^{-1}

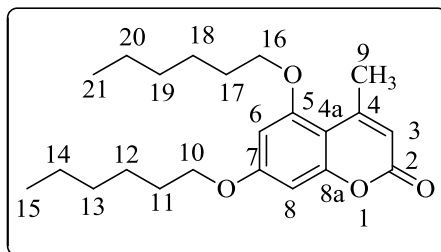
Percentage yield: 55%

R_f value: 0.71

Melting point: 63.6-63.9°C; **FT-IR data:** $\nu_{\max}(\text{cm}^{-1})$: 2932.68 (C-H stretch), 1713.42 (C=O), 1610.08 (aromatic ring), 1239.16 (C-O stretch); **$^1\text{H NMR}$ data (400MHz, DMSO- d_6):** δ 6.51 (s, 1H, H-6), 6.43 (s, 1H, H-8), 5.96 (s, 1H, H-3), 4.04 (q, 4H, $J=6.12\text{ Hz}$, H-10/14), 2.48 (s, 3H, H-9), 1.79-1.66 (m, 4H, H-11/15), 1.48-1.40 (m, 4H, H-12/16), 0.96-0.91 (m, 6H, H-13/17); **$^{13}\text{C NMR}$ data (100MHz, DMSO- d_6):** δ 162.1, 159.7, 158.3, 156.3, 154.1, 110.5,

103.7, 96.1, 93.8, 68.6, 67.8, 30.7-30.5, 23.7, 18.9-18.6 and 13.6 ; **HRMS**[*m/z*]: 327.2192 (Calculated for C₁₈H₂₄O₄Na, 327.1572).

5,7-dihexyloxy-4-methyl-2H-chromen-2-one(C6)



Physical description: Cream white solid

Molecular formula: C₂₂H₃₂O₄

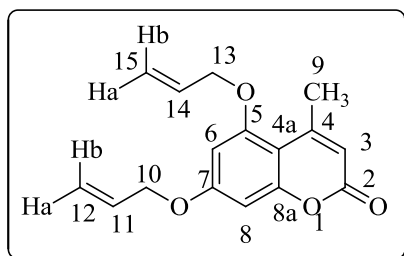
Molecular weight: 360.49 gmol⁻¹

Percentage yield: 83%

R_f value: 0.80

Melting point: 62.1-64.9 °C; **FT-IR data:** $\nu_{\max}(\text{cm}^{-1})$: 2933.20 (C-H stretch), 1718.45 (C=O stretch), 1559.11 (aromatic ring), 1111.71 (C-O stretch); **¹H NMR data (400MHz, DMSO-*d*₆):** δ 6.41 (d, 1H, *J*=2.36 Hz, H-6), 6.27 (d, 1H, *J*=2.36 Hz, H-8), 5.94 (d, 1H, *J*=1.12 Hz, H-3), 3.98 (m, 4H, H-10/16), 2.55 (d, 3H, *J*=1.12 Hz, H-9), 1.88-1.76 (m, 4H, H-11/17), 1.49 (q, 4H, *J*=1.60 Hz, H-12/18), 1.36-1.34 (m, 8H, H-13/14/19/20), 0.91 (t, 6H, *J*=6.96 Hz, H-15/21); **¹³C NMR data (100MHz, DMSO-*d*₆):** δ 162.3, 161.3, 158.6, 156.9, 154.7, 111.1, 104.7, 96.2, 93.7, 69.1, 68.5, 31.5, 29.0, 25.9, 25.6, 24.4, 22.6, 22.5, 14.0 and 13.9; **HRMS data**[*m/z*]: 383.2192 (Calculated for C₂₂H₃₂O₄Na, 383.2198).

4-methyl-5,7-bis(prop-2-en-1-yloxy)-2H-chromen-2-one(C7)



Physical description: Dark yellow solid

Molecular formula: C₁₆H₁₆O₄

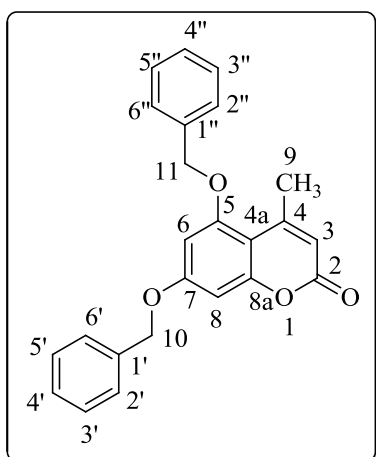
Molecular weight: 272.30 gmol⁻¹

Percentage yield: 59%

R_f value: 0.63

Melting point: 280.0-281.0 °C; **FT-IR data:** $\nu_{\max}(\text{cm}^{-1})$: 2929.87 (C-H stretch), 1718.73 (C=O), 1594.74 (aromatic ring), 1112.76 (C-O stretch); **¹H NMR data (400MHz, DMSO-*d*₆):** δ 6.57(s, 1H, H-6/8), 6.52 (s, 1H, H-6/8), 6.14-5.99 (m, 3H, Ar), 5.43 (dd, 2H, *J*=1.72, 17.32 Hz, H-12b/15b), 5.33-5.28 (m, 2H, H-12a/15a), 4.66 (s, 4H, H-10/13), 2.49 (d, 3H, *J*=1.72 Hz, H-9); **¹³C NMR data (100MHz, DMSO-*d*₆):** δ 161.4, 159.6, 157.7, 156.2, 153.9, 132.9, 132.8, 118.3, 118.1, 110.8, 104.1, 97.0, 94.5, 69.8, 68.8 and 23.8; **HRMS**[*m/z*]: 295.0935 (Calculated for C₁₆H₁₆O₄Na, 295.0946).

5,7-bis(benzyloxy)-4-methyl-2H-chromen-2-one (C8)



Physical description: Cream white solid

Molecular formula: C₂₄H₂₀O₄

Molecular weight: 372.41 gmol⁻¹

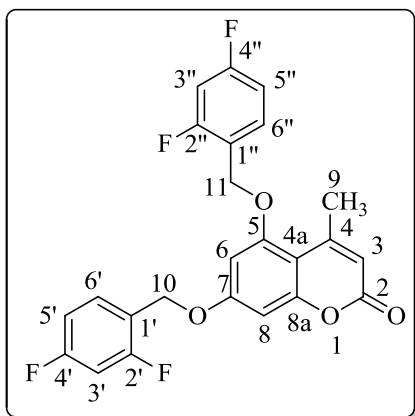
Percentage yield: 60%

R_f value: 0.70

Melting point: 134.0-135.0 °C; **FT-IR data:** $\nu_{\max}(\text{cm}^{-1})$: 2929.48 (C-H stretch), 1712.29 (C=O), 1596.11 (aromatic ring), 1160.04 (C-O stretch); **¹H NMR (400MHz, DMSO-*d*₆):**

δ 7.50-7.33 (m, 10H, Ar), 6.69 (d, 1H, *J*=2.36Hz, H-6/8), 6.67(d, 1H, *J*=2.36Hz, H-6/8), 5.98 (d, 1H, *J*=0.96 Hz, H-3), 5.19 (s, 4H, H-10/11), 2.43 (d, 3H, *J*=0.68 Hz, H-9); **¹³C NMR (100MHz, DMSO-*d*₆):** δ 161.5, 159.6, 157.8, 156.3, 153.9, 136.2, 135.9, 128.5, 128.1, 127.9, 127.3, 110.9, 104.2, 97.3, 94.6, 70.8, 69.9 and 23.8; **HRMS**[*m/z*]: 395.1263 (Calculated for C₂₄H₂₀O₄Na, 395.1259).

5,7-bis[(2,4-difluorobenzyl)oxy]-4-methyl-2H-chromen-2-one(C9)



Physical description: Light yellow solid

Molecular formula: C₂₄H₁₆F₄O₄

Molecular weight: 444.38 gmol⁻¹

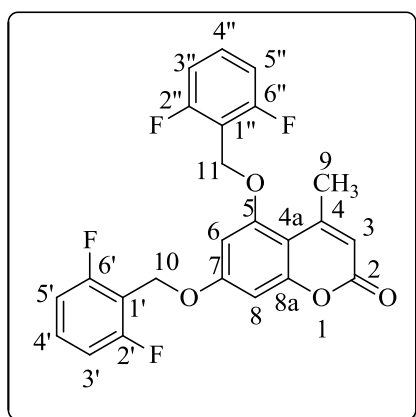
Percentage yield: 70%

R_f value: 0.69

Melting point: 162.9-163.2°C; **FT-IR data:** $\nu_{\max}(\text{cm}^{-1})$: 3112.70 (C-H), 1694.21 (C=O), 1597.53 (aromatic ring), 1079.97 (C-F); **¹H NMR data (400MHz, DMSO-*d*₆):** δ

7.48-7.38 (m, 2H, Ar), 6.95-6.86 (m, 4H, Ar), 6.55 (d, 1H, *J*=2.32 Hz, H-6), 6.46 (d, 1H, *J*=2.40 Hz, H-8), 5.96 (d, 1H, *J*=0.96 Hz, H-3), 5.12 (s, 2H, H-10 or 11), 5.08 (s, 2H, H-10 or 11), 2.42 (d, 3H, *J*=1.08 Hz, H-9); **¹³C NMR data (100MHz, DMSO-*d*₆):** δ 161.3, 160.8, 157.8, 156.9, 153.9, 131.2, 112.0, 111.8, 111.6, 104.3, 104.2, 96.8, 94.9, 64.6, 63.7 and 24.2; **¹⁹F NMR data (376.4 MHz, DMSO-*d*₆):** δ 113.4 (q, *J* = 13.1 Hz, F), 113.3 (q, *J* = 13.1 Hz, F), 109.2-109.1 (m, F), 109.0-108.9 (m, F); **HRMS**[*m/z*]: 467.0874 (Calculated for C₂₄H₁₆O₄F₄Na, 467.0882).

5,7-bis[(2,6-difluorobenzyl)oxy]-4-methyl-2H-chromen-2-one(C10)



Physical description: Light yellow solid

Molecular formula: C₂₄H₁₆F₄O₄

Molecular weight: 444.38 gmol⁻¹

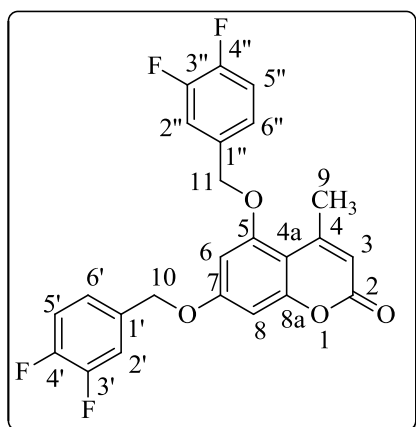
Percentage yield: 64%

R_f value: 0.63

Melting point: 185.0-187.1°C; **FT-IR data:** $\nu_{\max}(\text{cm}^{-1})$: 2896.92 (C-H stretch), 1720.15 (C=O), 1598.86 (aromatic ring), 1161.78 (C-O stretch), 1059.74 (C-F stretch); **¹H**

NMR data (400MHz, DMSO-*d*₆): δ 7.60-7.51 (m, 2H,Ar), 7.23-7.19 (m, 4H,Ar), 6.84 (d, 1H, *J*=2.32Hz, H-6 or 8), 6.79 (d, 1H, *J*=2.32Hz, H-6 or 8), 5.99 (d, 1H, *J*=1.20 Hz, H-3), 5.26 (s, 1H, H-10 or 11), 5.24 (s, 1H, H-10 or 11), 2.28 (d, 3H, *J*=0.56 Hz, H-9); **¹³C NMR data (150MHz, DMSO-*d*₆):** δ 161.7, 161.6, 161.3, 160.7, 160.3, 160.2, 160.1, 159.9, 157.8, 156.9, 156.5, 154.3, 153.9, 131.5, 131.4, 131.1, 131.1, 131.0, 119.1, 119.0, 118.9, 118.8, 118.7, 112.1, 111.8, 111.7, 111.6, 105.5, 104.5, 104.3, 104.2, 103.9, 96.8, 94.9, 64.6, 64.6, 63.8, 63.8 and 24.1; **¹⁹F NMR data(376.4 MHz, DMSO-*d*₆):** δ 114.8-114.9 (m, 4F, F-2',6',2'',6''); **HRMS[m/z]:** 467.0883 (Calculated for C₂₄H₁₆F₄O₄Na, 467.0882).

5,7-bis[(3,4-difluorobenzyl)oxy]-4-methyl-2H-chromen-2-one (C11)



Physical description: Light yellow solid

Molecular formula: C₂₄H₁₆F₄O₄

Molecular weight: 444.38 gmol⁻¹

Percentage yield: 58%

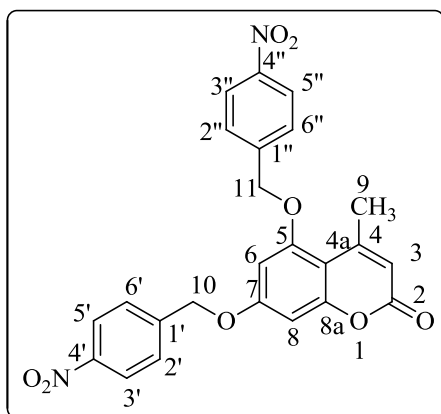
R_f value: 0.74

Melting point: 196.8- 197.3°C; **FT-IR data:** $\nu_{\max}(\text{cm}^{-1})$: 3041.18 (C-H), 1709.99 (C=O), 1602.55 (aromatic ring), 1169.72 (C-O stretch), 1081.54 (C-F stretch); **¹H NMR**

data (400MHz, DMSO-*d*₆): δ 7.43-7.30 (m, 6H, Ar), 6.70 (d, 2H, *J*=2.28Hz, H-6 or 8), 6.68 (d, 2H, *J*=2.28Hz, H-6 or 8), 6.01 (d, 1H, *J*=0.96 Hz, H-3), 5.19 (s, 2H, H-10 or 11), 5.18 (s, 2H, H-10 or 11), 2.43 (d, 3H, *J*=0.64Hz, H-9); **¹³C NMR data (150MHz, DMSO-*d*₆):** δ 150.7, 150.6, 150.6, 150.6, 150.5, 150.5, 150.4, 149.1, 149.1, 149.0, 148.9, 148.9, 148.9, 148.9, 148.8, 134.5, 134.5, 134.5, 134.3, 134.3, 134.2, 125.6, 125.6, 125.6, 125.3, 125.3, 125.2, 125.2, 119.6,

118.2, 118.2, 118.1, 118.0, 117.8, 117.7, 117.5, 117.4, 108.8, 104.9, 97.9, 95.4, 70.0, 69.0 and 24.3; ¹⁹F NMR data (376.4 MHz, DMSO-*d*₆): δ 138.2-138.4 (m, 2F), 139.2-139.5 (m, 2F).

5,7-bis[(4-nitrobenzyl)oxy]-4-methyl-2H-chromen-2-one (C12)



Physical description: Brown solid

Molecular formula: C₂₄H₁₈N₂O₈

Molecular weight: 462.41 gmol⁻¹

Percentage yield: 84%

R_f value: 0.68

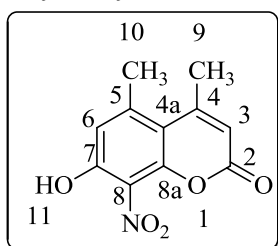
Melting point: 229.9-230.8°C; **FT-IR data:** ν_{max}(cm⁻¹): 3083.06 (C-H), 1743.55 (C=O), 1601.06 (aromatic ring), 1514.74 (NO₂), 1173.43 (C-O), 1108.40 (C-N); **¹H NMR**

data (400MHz, DMSO-*d*₆): δ 7.55-7.41 (m, 8H, Ar), 6.90 (d, 1H, *J*=2.36Hz, H-6 or 8), 6.88 (d, 1H, *J*=2.32Hz, H-6 or 8), 5.99 (d, 1H, *J*=1.20 Hz, H-3), 5.39 (s, 2H, H-10 or 11), 5.33 (s, 2H, H-10 or 11), 2.22 (d, 3H, *J*=1.0 Hz, H-9); **¹³C NMR data (100MHz, DMSO-*d*₆):** δ 161.7, 159.4, 157.8, 156.3, 153.5, 135.4, 132.8, 130.8, 128.7, 111.3, 104.3, 96.7, 94.7, 66.1, 65.6 and 23.0.

3.2.4. Nitration of 4-methylcoumarins.

A flask containing approximately 1.0 gram of 4-methylcoumarin (**B**) dissolved in 8.5 ml of sulfuric acid was kept in an ice bath until the temperature inside the flask was below 1°C. Then 1.6 ml of a nitrating mixture (0.4ml nitric acid and 1.2ml sulfuric acid) was added slowly while taking care that the temperature does not rise above 10°C. After the addition, the flask was allowed to stand at room temperature for 1 hour, and shaken periodically. After completion (TLC), the reaction mixture was poured into crushed ice and the solid product was obtained through filtration. The crude product (**B15**) was recrystallized from ethanol albeit in low yield (32%).

7-hydroxy-4,5-dimethyl-8-nitro-2H-chromen-2-one (B15)



Physical description: Yellow crystals

Molecular formula: C₁₁H₈O₅N

Molecular weight: 235.19 gmol⁻¹

Percentage yield: 32%

R_f value: 0.51

Melting point: 233.3 °C; **FT-IR data:** ν_{\max} (cm^{-1}): 3075.20 (C-H stretch), 1739.62 (C=O stretch), 1598.24 (aromatic ring), 1136.08 (C-O stretch), 1404.03 (Nitro); **^1H NMR data(600MHz, CDCl_3):** δ 12.26 (s, 1H, OH), 6.81(d, 1H, $J=0.76$ Hz, H-6), 6.21 (d, 1H, $J=1.28$ Hz, H-3), 2.73 (s, 3H, H-10), 2.71 (d, 3H, $J=1.24$ Hz, H-9); **^{13}C NMR data (150MHz, CDCl_3):** δ 158.9, 157.9, 156.8, 153.9, 140.9, 131.3, 114.9, 113.1, 109.1, 24.2 and 23.4; **HRMS: [m/z]: [M-H]⁻:** 234.0395 (calculated for $\text{C}_{11}\text{H}_8\text{NO}_5$, 234.0402).

3.3. Antidiabetic and antioxidant activity testing methods

3.3.1. DPPH radical scavenging activity

The total free radical scavenging activity of the tested compounds was determined and compared to that of ascorbic acid using a slightly modified method described by Tuba *et al.* A 0.3 mmol/L solution of DPPH was prepared in methanol and 500 μL of this solution was added to 50 μL of the compounds (dissolved in DMSO) at different concentrations (50-200 $\mu\text{g}/\text{mL}$). These solutions were mixed and incubated in the dark for 30 min at room temperature. Absorbance was then measured at 517 nm against a blank sample lacking scavenger.

3.3.2. Determination of α -glucosidase inhibitory activity of coumarins

The α -glucosidase inhibitory activity was determined according to the method described by Ademiluyi *et al.*, with slight modifications. Briefly, 50 μL of each compound or acarbose dissolved in DMSO at different concentrations (50-200 $\mu\text{g}/\text{mL}$), was incubated with 100 μL of 1.0 U mL^{-1} α -glucosidase solution in 100 mmol L^{-1} phosphate buffer (pH 6.8) at 37 °C for 15 min. Thereafter, 50 μL of pNPG solution (5 mmol L^{-1}) in 100 mmol L^{-1} phosphate buffer (pH 6.8) was added and the mixture was further incubated at 37 °C for 20 min. The absorbance of the released p-nitrophenol was measured at 405 nm and the inhibitory activity was expressed as percentage of a control sample without inhibitors.

3.3.3. Determination of α -amylase inhibitory activity of coumarins

The α -amylase inhibitory activity was determined according to the method described by Shai *et al.*, with slight modifications. A volume of 50 μL of each compound dissolved in DMSO or acarbose at different concentrations (50-200 $\mu\text{g}/\text{mL}$) was incubated with 100 μL of porcine pancreatic amylase (2 U mL^{-1}) in 100 mmol L^{-1} phosphate buffer (pH 6.8) at 37 °C for 20

min. 50 μ L of 1 % starch dissolved in 100 mmol L⁻¹ phosphate buffer (pH 6.8) was then added to the reaction mixture and incubated at 37 °C for 1 h. 100 μ l of DNS colour reagent was then added and boiled for 10 min. The absorbance of the resulting mixture was measured at 540 nm and the inhibitory activity was expressed as percentage of a control sample without inhibitors. All assays were carried out in triplicate.

3.3.4. Statistical analysis

Data were analyzed using a statistical software package (SPSS for Windows, version 23, IBM Corporation, USA) using Tukey's-HSD multiple range post-hoc test. Values were considered significantly different at $p < 0.05$

3.3.5. Homology modelling

Owing to the non-availability of the three dimensional (3D) coordinates of α -glucosidase from *Saccharomyces cerevisiae*, we developed its model using homology modelling technique. First, the amino sequence of α -glucosidase in fasta format was retrieved from UniProt protein data bank (<http://www.uniprot.org/>) using P53341 as an access code. The sequence alignment of the query sequence was performed with the BLAST (Altschule *et al.*, 1990) module in Discovery Studio 4.0 Client (Accelrys), considering the default parameters. Of the total 66 protein hits sampled from blast search, the *Saccharomyces cerevisiae* isolated from isomaltase (pdb code 3AJ7, X-ray resolution 1.3Å) displayed the best match based on its high sequence identity (71.4%) and sequence similarity (87%) with respect to the query sequence (Yamamoto *et al.*, 2010). The X-ray structure of *Saccharomyces cerevisiae* from isomaltase was downloaded from the protein data bank (www.rcsb.com), and utilized as a template to construct the 3D model of α -glucosidase using the "Build Homology Models" protocol implemented in MODELER (Eswar *et al.*, 2006) program in DS. The generated model was energetically minimized using the RMS gradient criteria of value 0.02 kcal mol⁻¹, and finally validated using the Verify Protein (Profiles-3D) module in DS.

3.3.6. Molecular docking method

The structures of all potent compounds (**B2-B3**, **B5-B6**, **B9**, **B11**, **C5** and **C7**) including acarbose (standard drug) were prepared using Chem3D Ultra 8.0. The conformational profile of each compound was explored using "Generate conformations" algorithm in DS. The

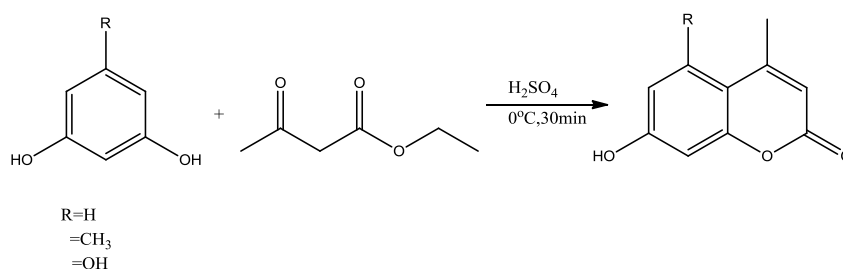
generated conformations were energetically minimized, and the lowest conformation was determined based on the lowest CHARMM energy. The “Prepare Ligands” module was further used to determine the conformers of each compound at physiological pH using their lowest energy conformation as an input. The energy minimization of all conformers was performed in DS, and the one with the lowest energy was selected for docking. The CHARMM force field was considered to develop the partial charges on each atom of the compounds. Before docking, the different binding sites of predicted model of α -glucosidase were determined using “Define and Edit binding Site” protocol in DS. The binding site with the partition level 787.2Å was selected and a binding sphere was created around it. *In silico* docking of all compounds was performed in the binding cavity of the modelled α -glucosidase enzyme using CDocker program (Wuet al., 2003) in DS. The best pose of each compound was selected on the basis of CDocker energy, and utilized further for calculation of the binding energy of the complex. The DS visualizer was used for visualization and analysis (drug receptor interactions etc.) of the complexes.

CHAPTER 4

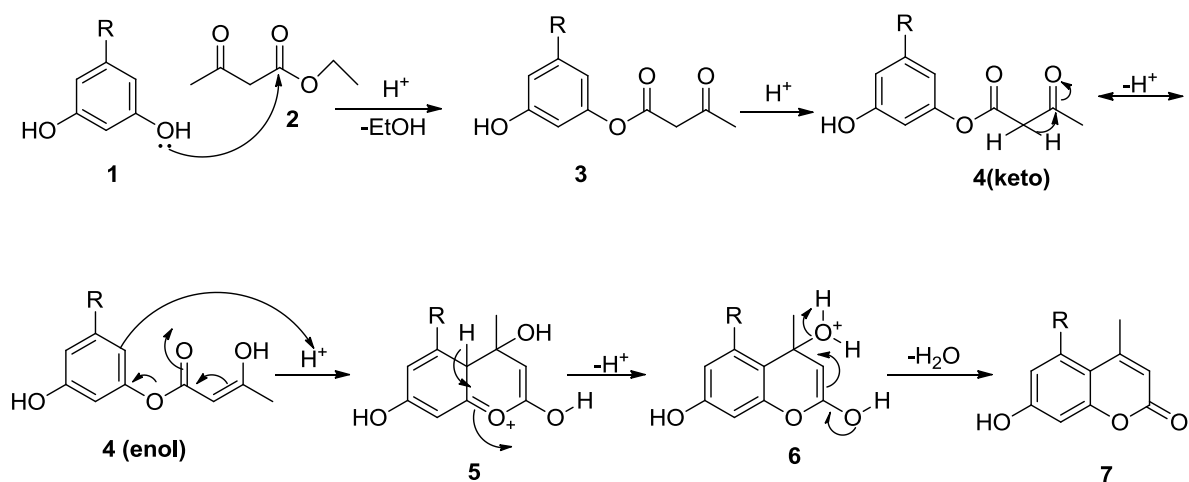
Results and Discussion

4.1 Synthesis of 7-hydroxycoumarins (A-C)

The reactions carried out in this project consisted of two steps, the first step involved the synthesis of hydroxyl derivatives of 4-methylcoumarins (A-C), whereas the second step involved the alkylation or acetylation of the resulting 4-methylcoumarins. Specifically, the reaction between ethyl acetoacetate and a substituted phenol (phloroglucinol, orcinol or resorcinol) was conducted in the first step in the presence of sulfuric acid at 0°C (**Scheme 4.1**) (Sahoo *et al*). The progress of the reaction was monitored using thin layer chromatography (TLC). After completion, the reaction mixture was poured into crushed ice and the solid compounds were obtained, which were further recrystallized using ethanol as a solvent. All the coumarins were obtained in good yields ranging from 70 to 97%. A proposed mechanistic pathway (**Scheme 4.2**) for the reaction involves the nucleophilic attack of hydroxyl group of phenol (**1**) on the activated carbonyl carbon (in the presence of acid) of ethyl acetoacetate (**2**), leading to the formation of an intermediate **3** after condensation (transesterification). The keto-enol tautomerization of intermediate **3** led to the formation of intermediate **4** which upon Michael addition resulted into a cyclic coumarin skeleton (**5**). The aromatization of intermediate **5** led to intermediate **6** which upon acid-induced dehydration resulted in coumarin (**7**). The structural elucidation of isolated products (A-C) was performed using the NMR (^1H and ^{13}C) spectroscopic data and their melting points reported in literature (Table 4.1).



Scheme 4.1. Synthesis of coumarins (A-C) from ethyl acetoacetate and substituted phenols.



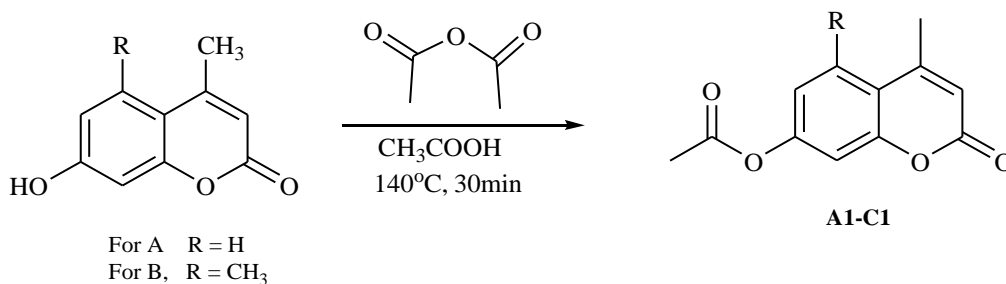
Scheme 4.2. Proposed mechanism of the Pechmann reaction.

Compound	Substitution (R)	R _f value	Yield (%)	Literature melting point (°C)	Reference
A	H	0.44	71	190.0-192.0	Khan <i>et al.</i> , 2003
B	CH ₃	0.54	88	248.0-250.0	Khan <i>et al.</i> , 2003
C	OH	0.25	60	233.3	Mandhane <i>et al.</i> , 2009

Table 4.1: Experimental properties of three different 4-methylcoumarins (**A-C**) synthesized from ethyl acetoacetate and substituted phenols in **Scheme 4.1**.

4.2.1. Synthesis of single O-acetylated coumarins (A1-B1)

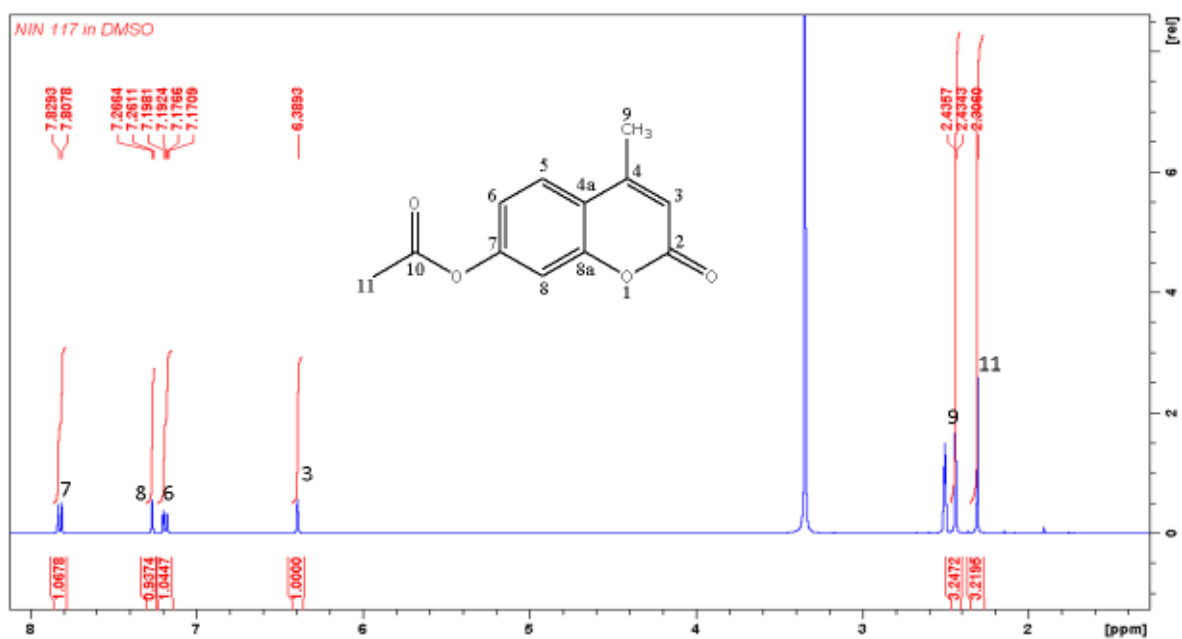
Since, the hydroxyl moiety (at position 7) of the synthesized coumarins (**A** and **B**) has adequately acidic proton (being attached to the electronegative oxygen atom) and can easily acts as a nucleophile without base or in the presence of a mild base, we constructively utilized this moiety (-OH) in the second step to prepare a range of new coumarin analogues by carrying out its O-acetylation/ alkylation reactions. For acetylation reactions, the heating of hydroxy coumarins with alkyl halides, as reported earlier by Sandhya *et al.*, proved to be unsuccessful in our case. However, refluxing a mixture of 7-hydroxycoumarins (**A-C**) and acetic anhydride in glacial acetic acid for 30 minutes led to the isolation of desired compounds with good yields (75-81%) (**Scheme 4.3**).



Scheme 4.3. O-acylation reaction of coumarins (**A** and **B**) bearing single hydroxy group.

All isolated compounds were pure and did not require any further purification. The structural assignments to all O-acetylated coumarins (**A1** and **B1**) were based on the NMR spectral evidence. Compound **A1**, for instance, 4-methyl-2-oxo-2*H*-chromen-7-yl acetate exhibited a characteristic singlet at δ 2.31 ppm corresponding to a methyl group attached to acetyl group, a slightly downfield doublet ($J=0.56\text{Hz}$) at δ 2.44 ppm was assigned for a methyl group attached to β -carbon and a singlet resonating at δ 6.39 ppm was assigned to an olefinic proton attached to α -carbon of pyranone ring (**Figure 4.1a**). Additionally, the J coupling has been very useful to assign the protons of benzene ring. For instance, H5, the most deshielded proton (δ 7.82), appeared as a doublet ($J = 8.6\text{Hz}$) with a typical *ortho* coupling with H6. Similarly, H6 resonates at δ 7.18 ppm as a doublet of doublets (dd, $J = 2.12$ and 8.6 Hz) by coupling with *ortho* (H5) and *meta* (H8) protons, while H8 appeared at δ 7.26 ppm as a doublet ($J = 2.12$) by exhibiting *meta* coupling H6. The structure of **A1** was further corroborated with the help of its ¹³C spectrum (**Figure 4.1b**) whereby the two characteristic shielded singlets resonating at δ 18.1 ppm and 20.8 ppm established the presence of two -CH₃ groups, whereas the two most deshielded peaks resonating at δ 168.8 and 159.6 confirmed the presence of two carbonyl (-C=O) functionalities in the structure in addition to eight peaks ranging between δ value of 110.1 to 153.5 for aromatic/olefinic carbons.

(a)



(b)

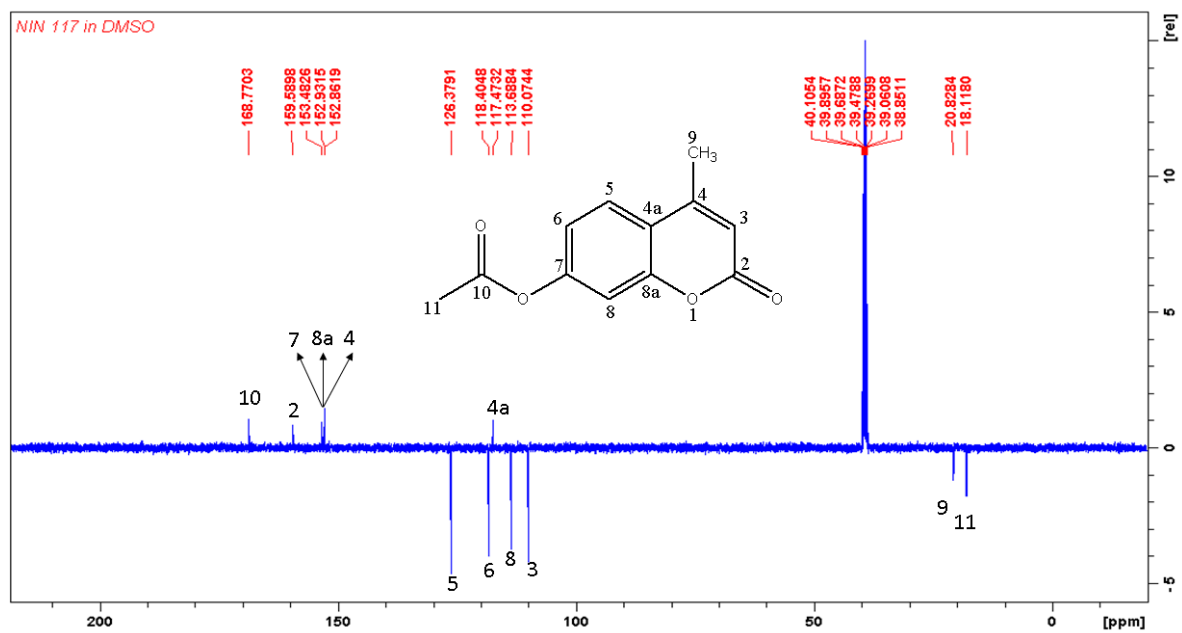
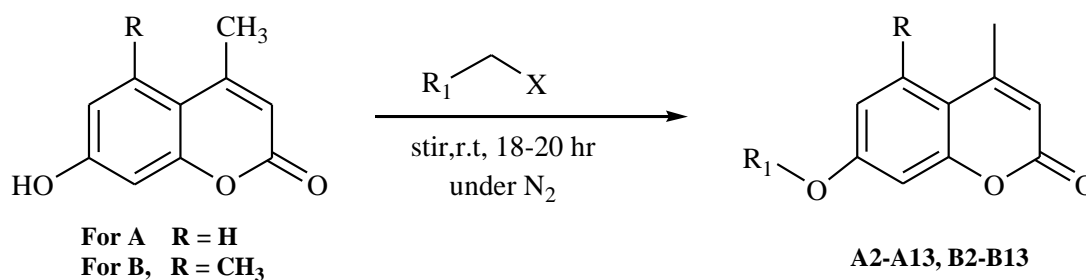


Figure 4.1: ¹H (a) and dept 135 (b) NMR spectrum of 4-methyl-2-oxo-2H-chromen-7-yl acetate (A1)

4.2.2. Synthesis of single O-alkylated coumarins (A2-A13, B2-B13)

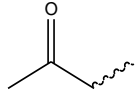
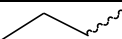
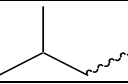
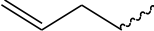
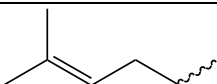
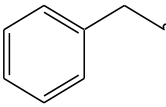
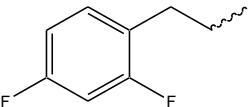
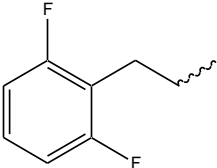
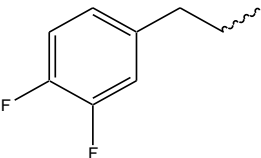
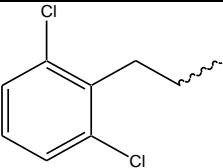
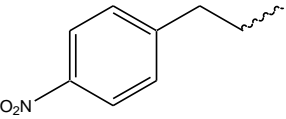
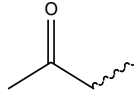
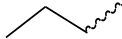
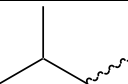
Encouraged by a successful acetylation reaction of coumarins, we decided to synthesize another series of coumarin analogues by O-alkylation of the coumarins (**A-B**) bearing a hydroxy group at position 7. The reported [Yee *et al*] few O-alkylation reactions of coumarins have already been documented in the literature and involves the usage of dry acetone as a solvent and cumbersome isolation procedures. However, we modified the reaction procedure in our work and used DMF as a solvent to carry out the O-alkylation of the coumarins using a wide range of substituted alkyl halides. It was envisaged that the addition of reaction mixture after its completion in crushed ice might yield the pure solid product, as observed in the case of O-acetylation, without any extra purification steps as described previously [Yee *et al*]. Accordingly, the 7-hydroxycoumarins (**A-B**) dissolved in dry DMF and initially activated by K_2CO_3 were allowed to stir with variedly substituted haloalkanes at room temperature under nitrogen atmosphere (**Scheme 4.4**).

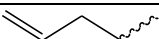
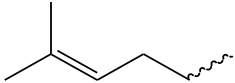
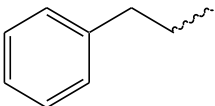
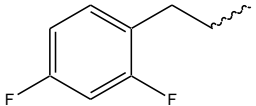
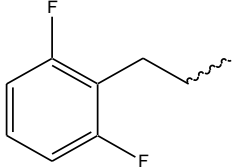
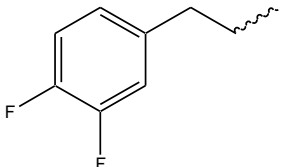
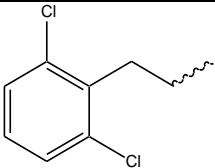
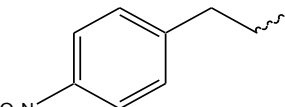


Scheme 4.4. O-alkylation reaction of coumarins (**A** and **B**) bearing single hydroxy group.

The time taken for the completion of the reaction in our study was longer (18-20 hr) than the reported method where the reaction mixture was refluxed at 60°C for 10 hours (Yee *et al*, 2005). The advantages associated with our procedure, however, encompass the simple stirring of reaction mixture and isolation of products with ease. Moreover, the pure coumarin derivatives were obtained in good yields (>50%) without any complicated isolation procedures. The experimental properties of different scaffolds (**A2-A13**, **B2-B13**) that have been synthesized *via* the O-acetylation and O-alkylation of the coumarins are presented in **Table 4.2**.

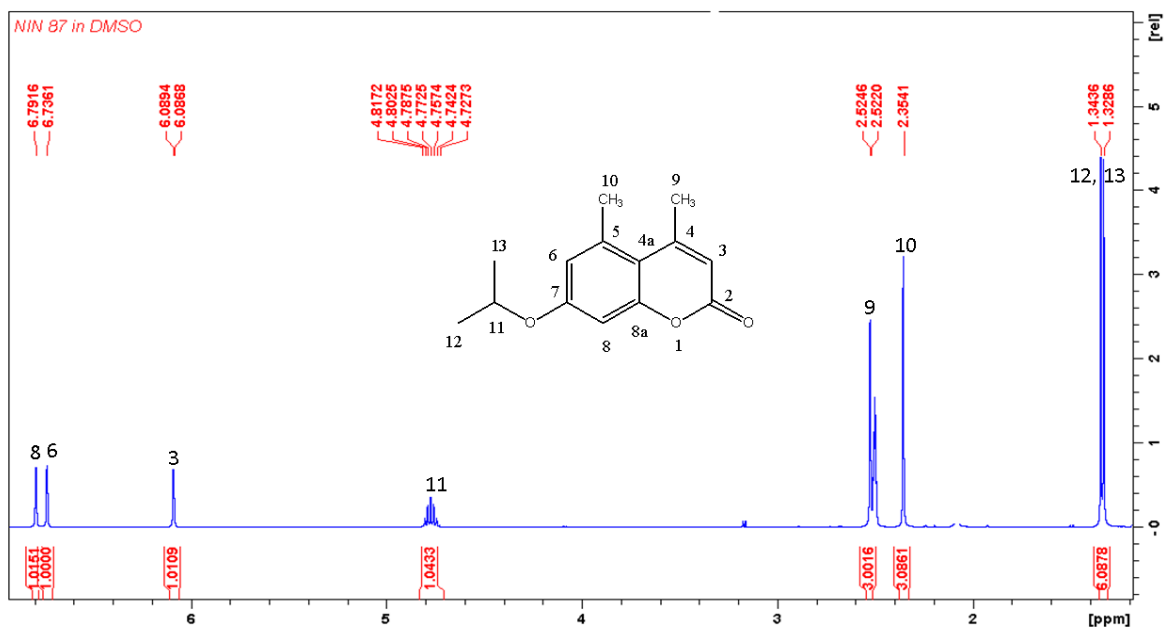
Table 4.2: Shows experimental properties of compounds (A2-A13, B2-B13) synthesized via the acetylation and alkylation reactions of coumarins (A-B).

Cmpd.	Substitution (R ₁)	R _f value	Percentage yield (%)	Melting point (°C)	References
A1		0.48	81	150.0-152.0	Elgogary <i>et al.</i> , 2014
A2		0.66	81	159.0-160.0	Robertson <i>et al.</i> , 1932
A3		0.67	81	106.0-108.0	Khan <i>et al.</i> , 2003
A4		0.68	77	86.0-87.0	Park <i>et al.</i> , 2009
A5		0.73	79	41.0-43.0	Yee <i>et al.</i> , 2005
A6		0.67	90	72.0-75.0	Vianna <i>et al.</i> , 2015
A7		0.64	104	155.7-156.2	Nesmeyanov <i>et al.</i> , 1937
A8		0.75	85	181.0-182.0	Raghavendra <i>et al.</i> , 2011
A9		0.63	68	150.3-151.6	
A10		0.68	77	178.3-179.6	
A11		0.73	64	73.4-74.8	
A12		0.67	93	170.2-171.5	
A13		0.66	70	204.0-205.2	Lévai <i>et al.</i> , 2005
B1		0.51	75	192.0-193.7	
B2		0.58	74	134.4-134.8	
B3		0.65	68	137.7-138.2	
B4		0.51	57	81.3-82.7	

B5		0.73	68	117.9-118.0	
B6		0.75	56	89.5-90.9	
B7		0.68	89	110.9-111.5	
B8		0.74	78	85.5-86.9	
B9		0.76	85	141.1-142.3	
B10		0.45	84	155.3-156.2	
B11		0.63	78	149.9-151.3	
B12		0.73	121	170.8-171.4	
B13		0.70	85	201.7-202.4	
B14		0.59	72	196.3-197.4	

The chemical structures of all O-alkylated coumarins were unequivocally assigned using different spectroscopic techniques including 1D (^1H and ^{13}C), 2D (HMBC, HSQC and COSY), IR and HRMS spectral evidence. The detailed spectral features of each compound are depicted in the experimental section, whereas the salient characteristics are mentioned here.

For example, compound **B4**, interpreted as 4,5-dimethyl-7-(propan-2-yloxy)-2*H*-chromen-2-one exhibited a molecular ion signal at 255.0991 in its HRMS, along with characteristic peaks in its NMR (^1H and ^{13}C) spectra. The ^1H NMR spectrum (**Figure 4.2a**) showed a distinguishing doublet at δ 1.34 ($J = 6\text{Hz}$) corresponding to two methyl (12 and 13) groups



(a)

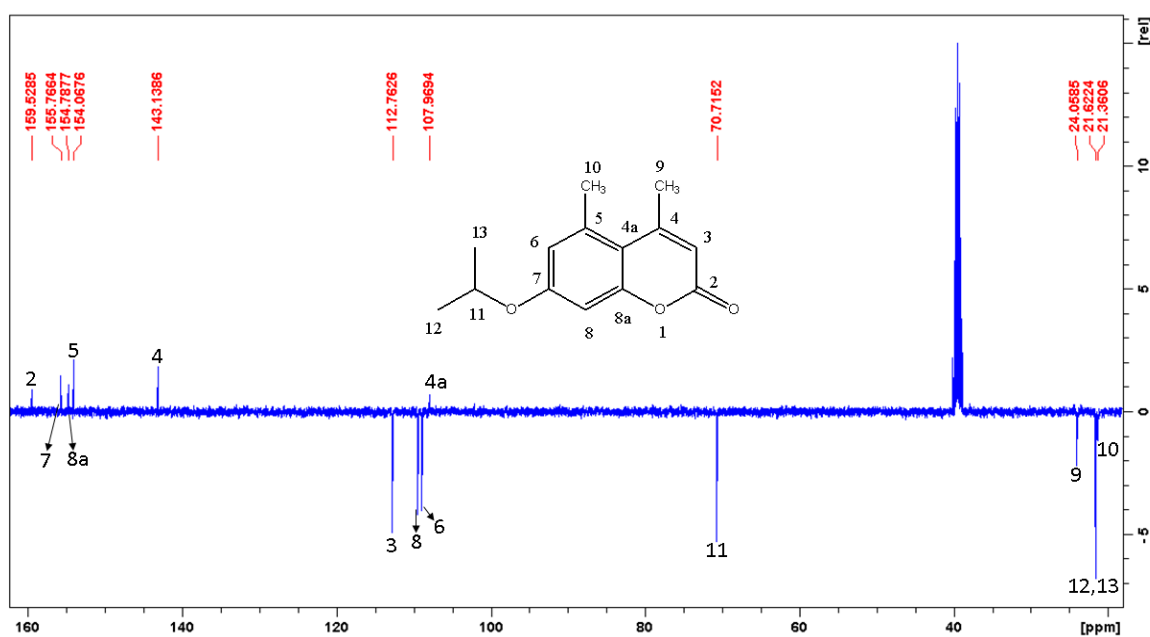


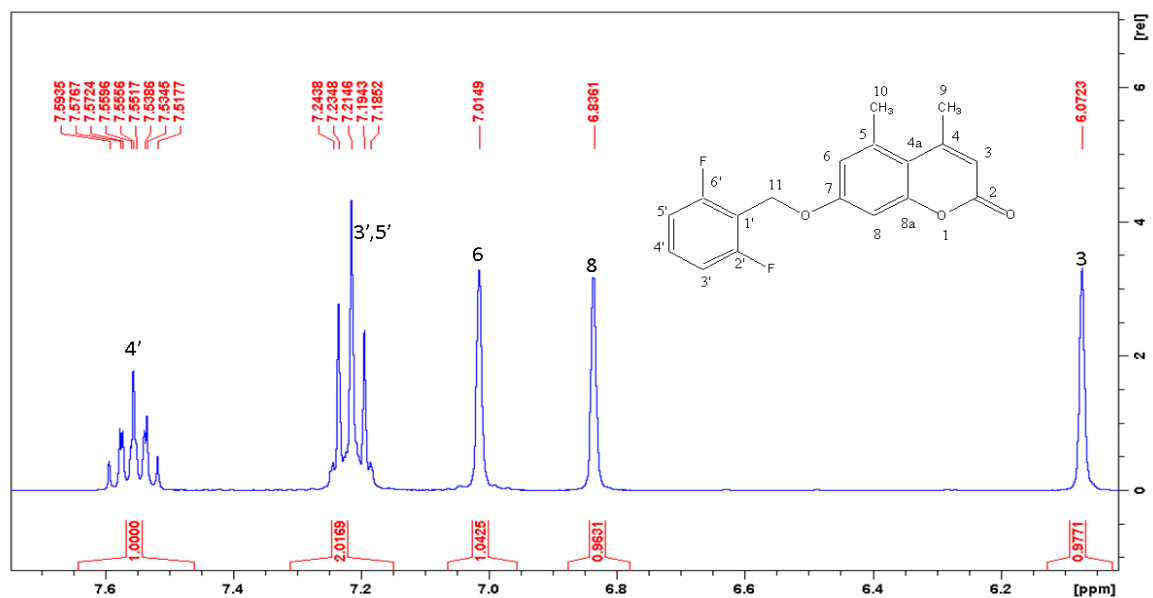
Figure 4.2: ¹H (a) and ¹³C (b) NMR spectrum of 4, 5-dimethyl-7-(propan-2-yloxy)-2H-chromen-2-one (**B4**)

and a deshielded multiplet at δ 4.77 (being attached to oxygen atom) for –CH proton (11) confirming the attachment of isopropyl functionality to the coumarin ring. Additionally, the presence of the requisite number of carbon resonances (**Figure 4.2b**) in the ¹³C NMR spectrum including a characteristic peak at δ 159.5 assigned to carbonyl (=C=O) group of α,β -unsaturated unit further substantiated the assigned structure.

Since, ^{19}F is a NMR active nuclei and has tendency to couple with both the carbon and hydrogen nuclei, the NMR spectrum of fluorinated coumarin derivatives were observed to be complicated and exhibited interesting splitting pattern. For instance, the compound **B11**, bearing 2,6-difluorobenzyl moiety at position 7, in its ^1H spectrum (**Figure 4.3a**) exhibited a characteristic triplet of triplets (tt), a type of dddd, at δ 7.55 for H4' proton owing to its coupling with the two *ortho* protons (H3', H5') and two fluorine atoms (2',6') with J coupling 6.7 and 8.4 Hz, respectively. The two equivalent protons, 3' and 5' were comparatively shielded due to resonance effect of fluorine atoms, and appeared as a triplet (actually a doublet of doublets) at δ 7.21 ppm with the coupling constant of 8.2 Hz.

In the ^{13}C spectrum of **B11** (**Figure 4.3b**), the carbon peaks of benzene ring split into doublets due to C-F coupling with the J value decreasing as the distance increases with respect to the fluorine atom (Momin *et al.*, 2014). The J values have been very useful to assign the carbon resonances of the benzene ring. For instance, the two chemically equivalent carbons (2',6') appeared far downfield (δ 161.1) due to $-I$ effect of fluorine as a doublet (d) with large J coupling value of 247.7 Hz. This large doublet could have been mistaken for two individual carbon resonance in the absence of this knowledge. The *meta* carbons (C3', C5') also resonate as a doublet at δ 111.8 with coupling constants equal to 24.5 Hz, whereas the *para* carbon (C4') resonate as a triplet (actually, dd due to two *meta* F atoms) with the J coupling value of 10.5 Hz. The quaternary carbon (C1') was the most shielded resonance amongst the other carbons of benzene ring that appeared at δ 111.4 as a doublet ($J = 19.1$ Hz). The remaining carbons of coumarin were identified on the basis of 2D NMR spectra (HMBC, HSQC and COSY). For example, the carbons, C2, C3 and C4a were identified by their HMBC correlation with the H3. Similarly, the C6 carbon was differentiated from the C8 carbon by its HBMC correlation with the H10 ($-\text{CH}_3$), whereas the H9 (CH_3) and H10 (CH_3) were differentiated by the HMBC correlation of the former with the H3.

(a)



(b)

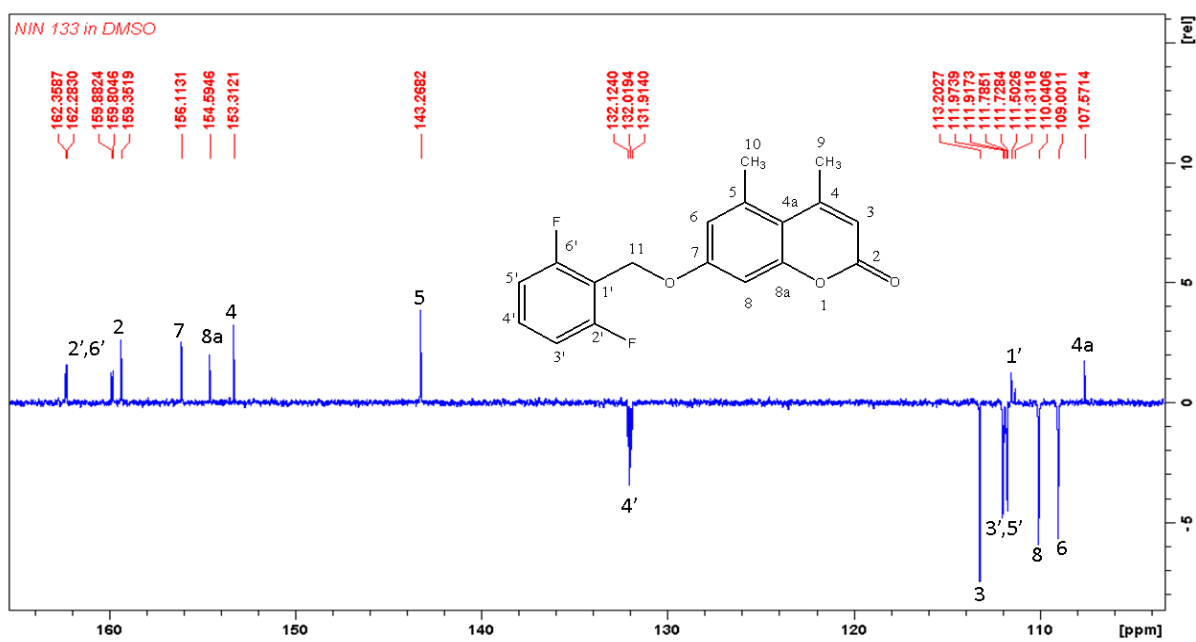
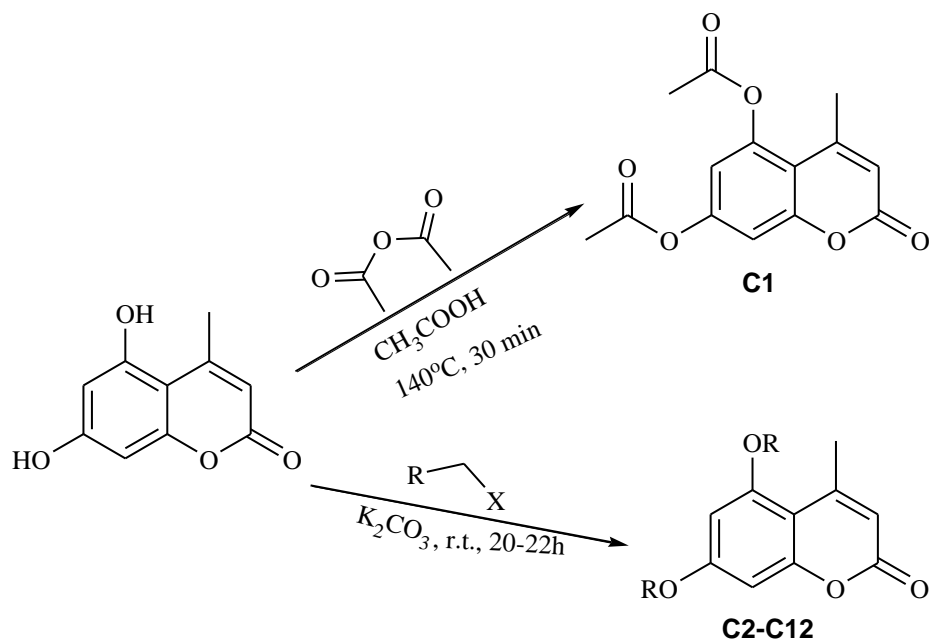


Figure 4.3: ^1H (a) and ^{13}C (b) NMR spectrum (expansion) of [(2,6-difluorobenzyl)oxy]-4,5-dimethyl-2H-chromen-2-one (**B11**)

4.3. Synthesis of double O-acetylated/alkylated coumarins (C1-C12)

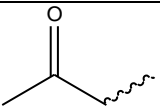
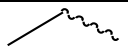
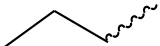
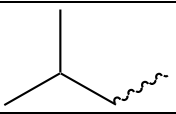
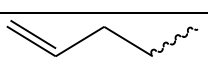
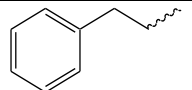
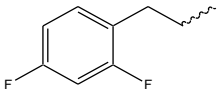
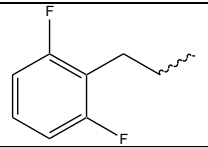
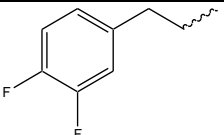
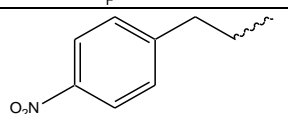
Since, the coumarin **C** contains two –OH groups, it was thought worthwhile to synthesize different functionalized coumarin analogues by O-alkylation/acetylation of both these hydroxyl groups. From chemistry point of view, it was envisaged that the benzene ring of coumarin **C** with *meta* arrangement of the –OH groups would be accommodating enough to afford even bulky moieties without any steric hindrance. To prove this, we first conducted the double acetylation reaction by refluxing coumarin (**C**) with the acetic anhydride in the ratio 1:2, in glacial acetic acid at 140°C for 30 minutes (**Scheme 4.5**). As expected, the addition of reaction mixture in crushed ice afforded pure solid compound that did not require any further purification step in excellent yield (97%, **Table 4.3**).

The synthetic protocol employed for double alkylation involved the treatment of coumarin **C** with 2 equivalents of K_2CO_3 (in DMF) for 10 minutes under nitrogen followed by the addition of appropriate haloalkane in a dropwise fashion at room temperature (**Scheme 4.5**). The reactions took almost the same time as was taken for single O-alkylation (20-22 hr), discussed earlier, affording the solid products after adding the reaction mixture into crushed ice. Again, the pure compounds were obtained with yields ranging between 55 to 84 % (**Table 4.3**).



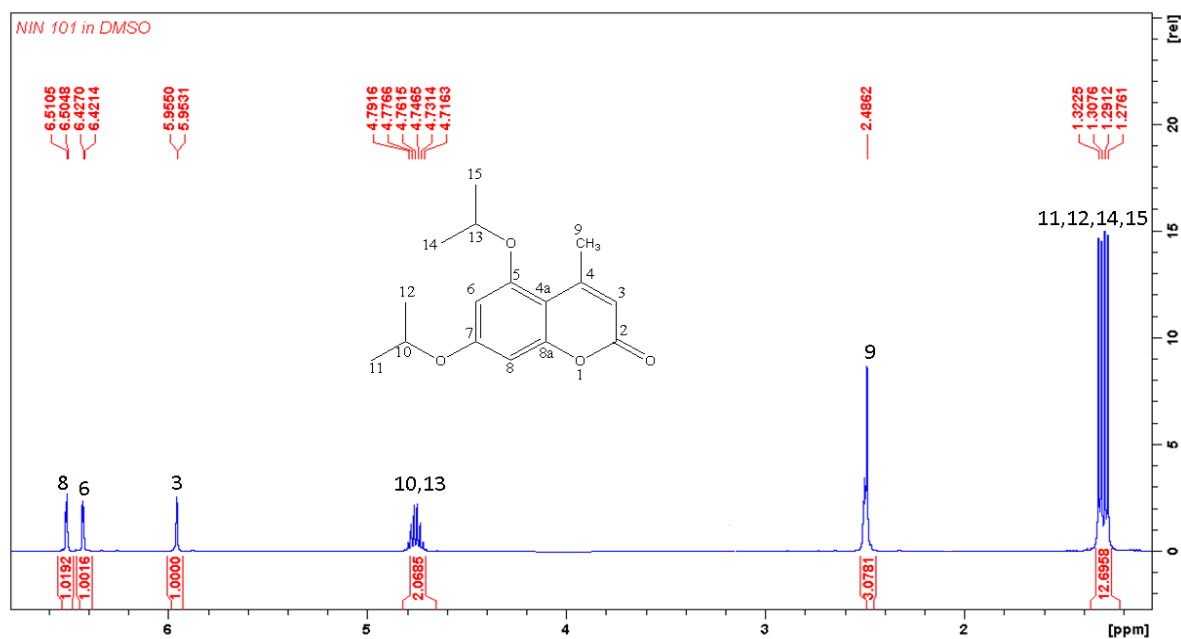
Scheme 4.5. O-acetylation/alkylation reactions of coumarin **C** bearing double hydroxyl groups.

Table 4.3. Shows the experimental properties of compounds synthesized *via* the acetylation and alkylation reactions of coumarin C.

Compound	Substitution (R)	R _f value	Yield (%)	Melting point (°C)	Reference
C1		0.48	97	116.3-117.9	
C2		0.60	61	172.0-173.0	Smitha <i>et al.</i> , 2004
C3		0.60	56	152.0-153.0	Osborne, 1989
C4		0.54	57	85.2-85.9	
C5		0.71	55	63.6-63.9	
C6		0.80	83	62.1-64.9	
C7		0.63	59	280.0-281.0	Goswani <i>et al.</i> , 2006
C8		0.70	60	134.0-135.0	Ahluwalia <i>et al.</i> , 1967
C9		0.69	70	162.9-163.2	
C10		0.63	64	185.0-187.1	
C11		0.74	58	196.8-197.3	
C12		0.68	84	229.9-230.8	

The unambiguous structure elucidation of all compounds was performed on the basis of the detailed spectral data and analytical evidence. As expected, the double alkylation/acetylation of coumarins, in their ¹H NMR spectrum, did not exhibit any appreciable change in chemical shifts or splitting pattern when compared to their structural analogues with the corresponding single substitution. For instance, compound 4-methyl-5, 7-bis (propan-2-yloxy)-2*H*-chromen-2-one (**C4**) with two isopropyl groups, in its ¹H spectrum (**Figure 4.4a**) exhibited two doublets

(a)



(b)

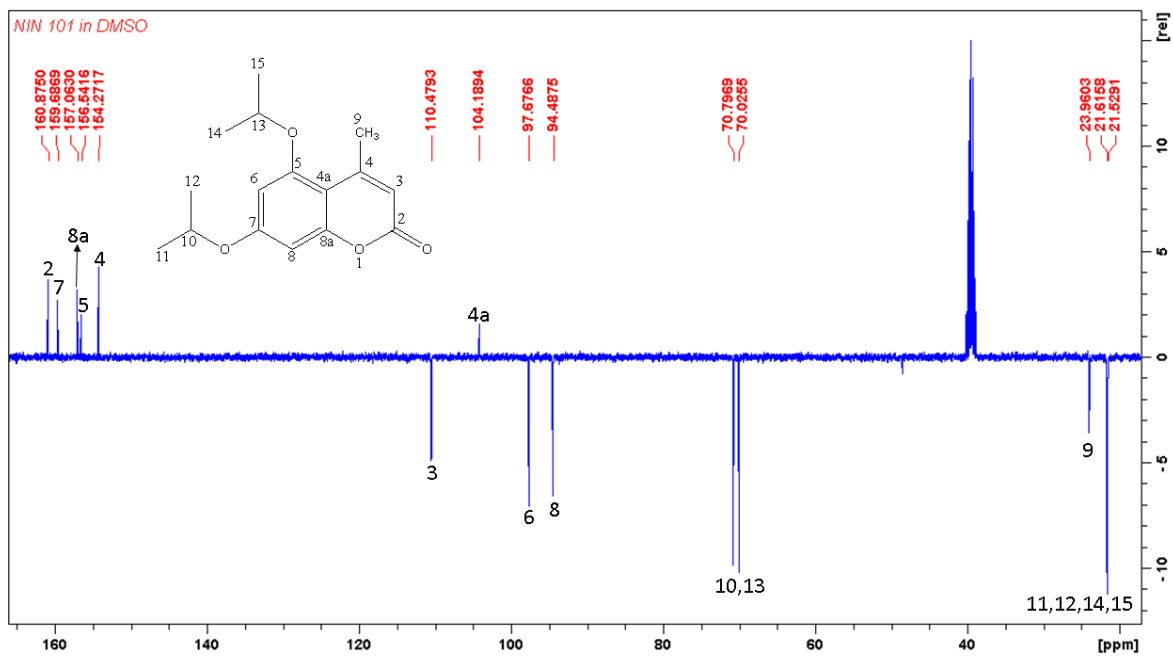
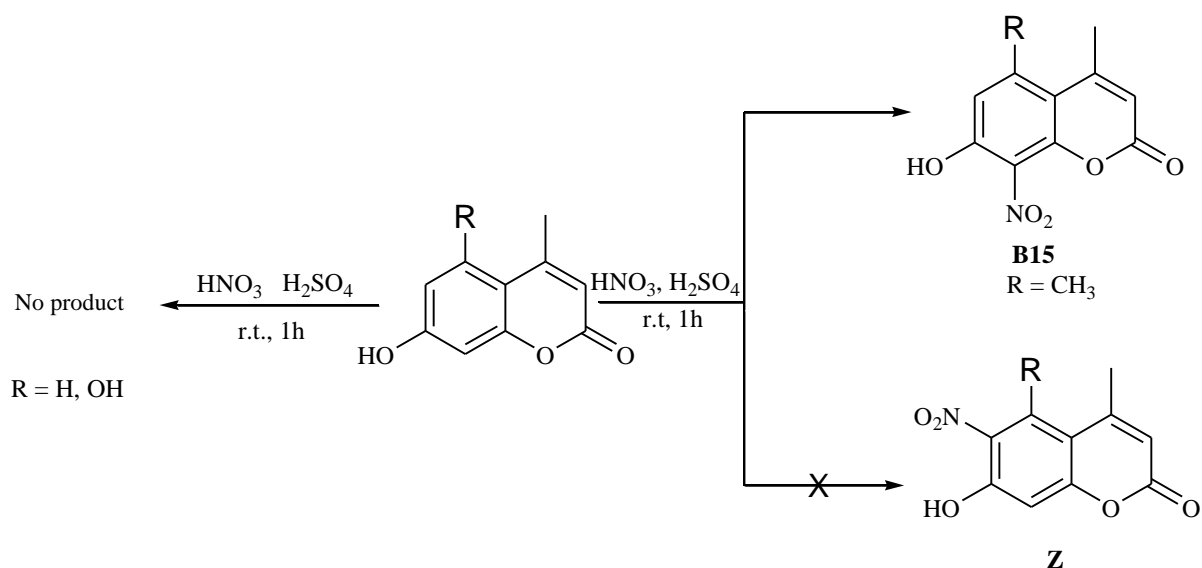


Figure 4.4: ^1H (a) and dept135 (b) NMR spectrum of 4, 5-dimethyl-7-(propan-2-yloxy)-2H-chromen-2-one (C4)

for two sets of -CH₃ groups (11, 12, 14 and 15) at δ 1.31 and 1.28 with the *J* coupling \sim 6.0 Hz, and a multiplet between δ 4.71 to 4.79 accounting for two -CH protons (10 and 13) of isopropyl groups, almost similar chemical shift and *J* pattern as observed in case of its single O-propylated analogue (**B4**). The *meta*-coupling between H6 and H8 protons that was absent in **B4**, however, was present in **C4**. The double alkylation was quite clear in the ¹³C spectrum of **C4** (**Figure 4.4b**) showing characteristic resonances at δ 21.5 (C11/C12), 21.6 (C14/C15), 23.9 (C9), 70.0 (C10), 70.8 (C13) for alkyl groups and other resonances appearing between δ 94.5 to 160.9 corresponding to the remaining nine carbons of the coumarin ring.

4.4. Nitration of coumarins (A-C)

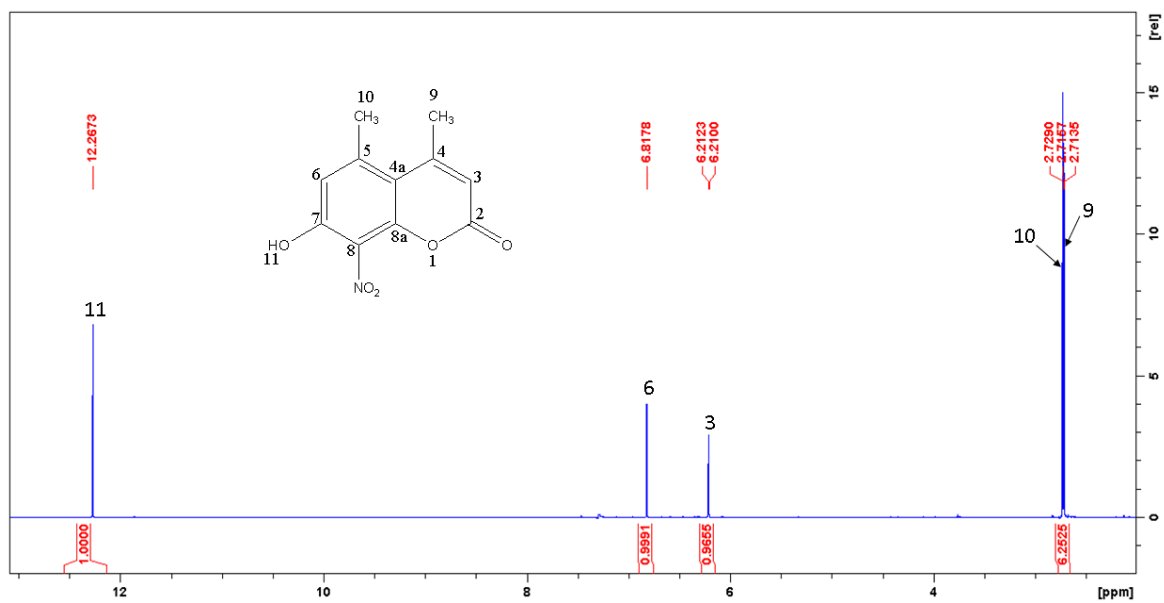
In order to prepare the nitro-substituted coumarins, the electrophilic substitution reaction of coumarins (**A-C**) was performed by treating them with the mixture of nitric acid (HNO₃) and sulfuric acid (H₂SO₄) taken in ratio 1:3, respectively (**Scheme 4.6**). In the case of **B**, after completion of the reaction (monitored using TLC), the solid product was isolated when poured in crushed ice and stirred for 10-15 min. The solid thus obtained had some impurities which were removed by recrystallization from ethanol, yielding crystalline yellow solid with a melting point of 233.3°C in 32% yield. On the other hand, the reaction of coumarin **A** and **C**, led to the formation of intractable mixture from which no desired product could be isolated even after purifying the mixture using column chromatography.



Scheme 4.6: Nitration of 4-methylcoumarins (**A-C**).

The precise structure of compound **B15**, 7-hydroxy-4, 5-dimethyl-8-nitro-2*H*-chromen-2-one, was elucidated based on the NMR spectroscopic data and HRMS. The presence of strong electron-withdrawing group ($-\text{NO}_2$) in the coumarin ring appreciably affected the chemical shifts of its proton nuclei, especially those attached to the benzene ring where the nitro substituent was directly substituted. For instance, in ^1H NMR spectrum of **B15** (**Figure 4.5a**), where the chemical shifts (δ) of H11, H6, H3, H10 and H9 were at 12.26, 6.81, 6.21, 2.73 and 2.71 ppm respectively, showed considerable downfield shift when compared with its parent molecule **B** (**Figure 4.5b**) where the corresponding resonances appeared at δ 10.5, 6.56, 6.04, 2.53 and 2.27 ppm, respectively. The disappearance of a proton (H8) indicated the substitution of aromatic proton with the $-\text{NO}_2$ group. The presence of the $-\text{NO}_2$ group at position 8 was corroborated with the help of HMBC spectra (**Figure 4.6**) where the H6 proton exhibited the HMBC correlation with C4a along with the other two sets of protons, H3 and $-\text{CH}_3$ (at position 9). No such HMBC correlation would have been observed if $-\text{NO}_2$ group was attached at position 6. Moreover, the HMBC relationship between H6 and C8 (quaternary carbon) also supported the nitration of coumarin ring at position 8.

(a) ^1H spectrum of B15



(b) ^1H spectrum of B

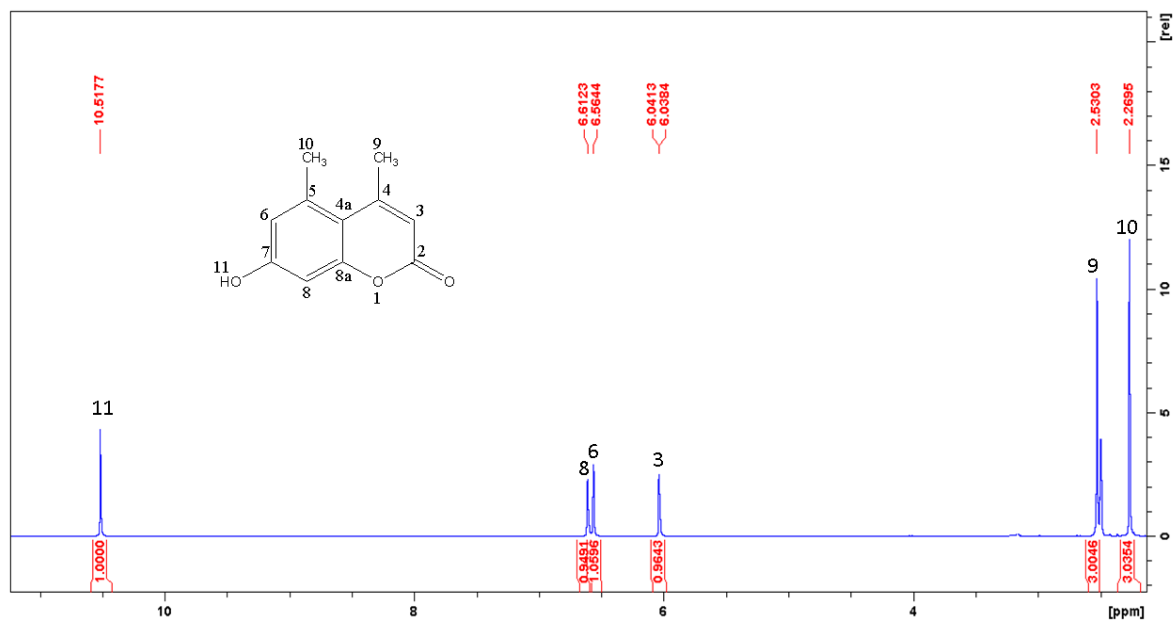


Figure 4.5: ^1H NMR spectrum of B15 (a) and B (b)

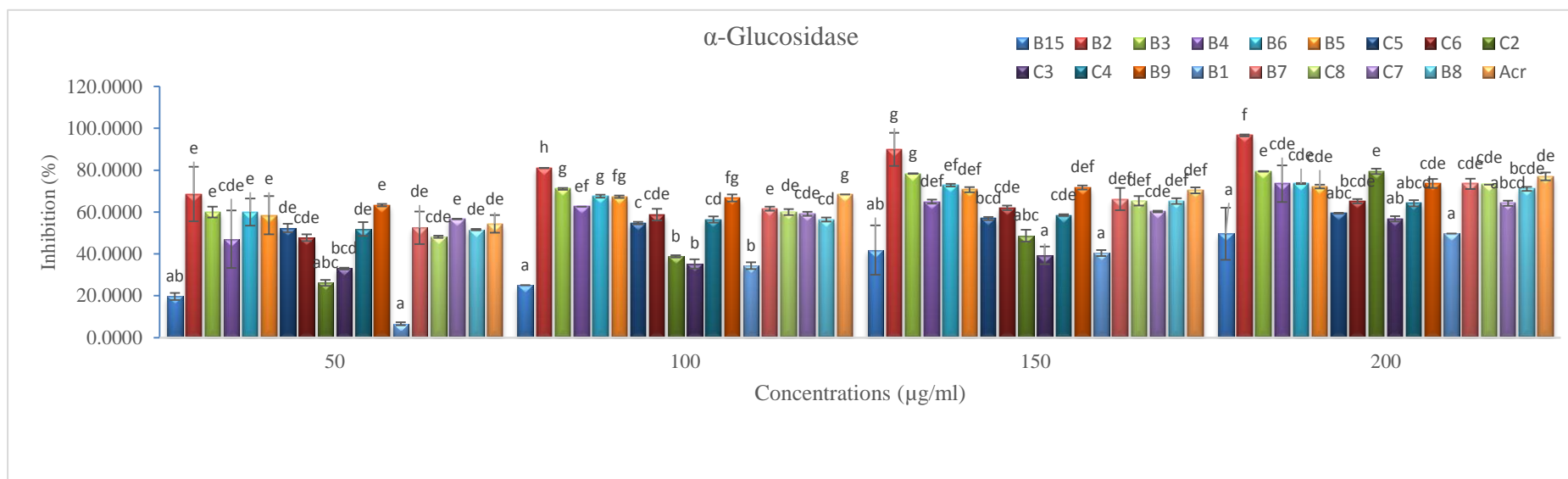
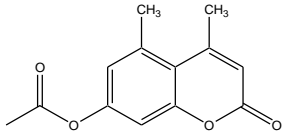
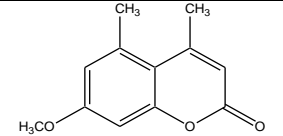
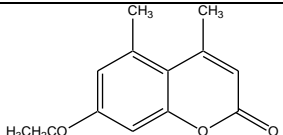
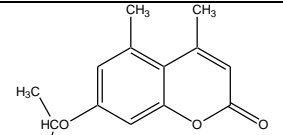
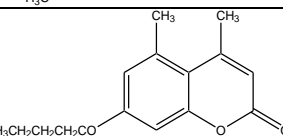
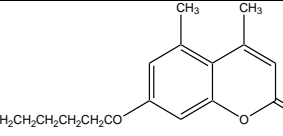
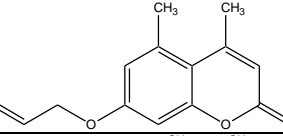
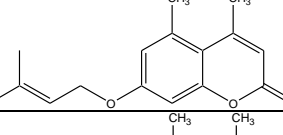
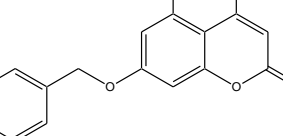
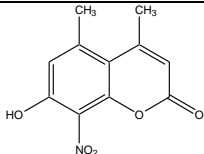
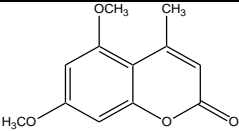
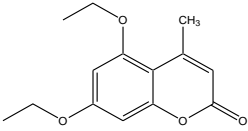
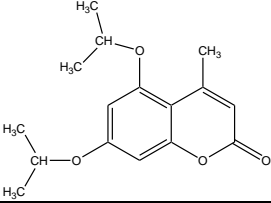
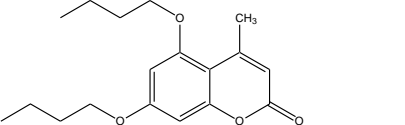
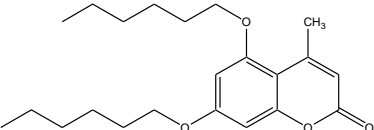
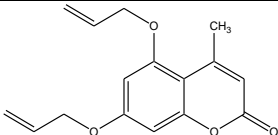
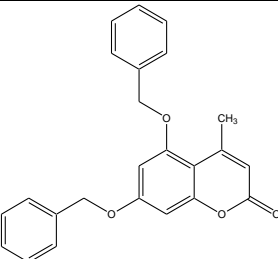


Figure 4.7: *In vitro* α -Glucosidase activity of coumarin derivatives (**B1-B9, B15, and C2-C8**) along with the standard inhibitor (acarbose).

Data are presented as mean \pm SD values of triplicate determinations. a-h different letters stand for significantly different values from each other within a column (Tukey's-HSD multiple range post hoc test, $p < 0.05$, IBM, SPSS, version 23); the same letters stand for non-significant difference

Table: 4.4: *In vitro* IC₅₀ values of antioxidant and α-glucosidase inhibition activities of the acetylated (B1), alkylated (B2-B9 and C2-C7) and nitrated (B15) coumarin analogues along with the reference drugs (Ascorbic acid and Acarbose).

Cmpd.	Structure	DPPH	α-Glucosidase	α-Amylase
		IC ₅₀ (μg/ml)		
B1		74.116±4.821 ^{hi}	194.978±2.365 ^{cd}	269.745±21.19 6 ^c
B2		48.111±3.647 ^{efg}	27.439±9.851 ^{ab}	138.045±1.622 ^a b
B3		5.605±0.113 ^{ab}	28.568±0.056 ^{ab}	117.776±20.01 2 ^{ab}
B4		42.792±2.864 ^{defg}	56.530±28.581 ^{ab} c	113.057±23.69 6 ^{ab}
B5		26.289±12.005 ^{bc} de	34.577±6.046 ^{ab}	171.324±4.266 ^b c
B6		29.485±6.572 ^{cde}	28.121±4.897 ^{ab}	141.745±15.19 1 ^{ab}
B7		33.471±1.998 ^{def}	44.096±20.725 ^{ab} c	114.940±16.00 7 ^{ab}
B8		27.677±0.486 ^{bcde}	49.918±0.583 ^{abc}	87.677±3.779 ^{ab}
B9		83.316±1.045 ⁱ	11.084±0.117 ^a	107.075±12.67 2 ^{ab}

B15		1.855±0.146 ^a	285.375±169.76 2 ^d	453.591±80.0 8 1 ^d
C2		53.456±3.927 ^{fgh}	116.420±2.291 ^{bc} d	170.663±12.9 93 ^{bc}
C3		75.279±5.724 ^{hi}	208.518±31.518 cd	265.701±50.8 67 ^c
C4		20.435±3.537 ^{abcd}	51.252±6.939 ^{abc}	154.520±12.9 93 ^{ab}
C5		24.324±0.117 ^{abcd}	32.488±14.851 ^{ab}	150.903±8.97 1 ^{ab}
C6		2.472±0.845 ^a	56.375±0.672 ^{abc}	98.494±5.994 ^a b
C7		62.670±17.522 ^{ghi}	19.233±3.010 ^a	74.405±1.894 ^a b
C8		7.248±2.846 ^{abc}	56.496±0.358 ^{abc}	95.889±3.717 ^a b
AA	Ascorbic acid	1.184±0.022 ^a	-	-
Acr	Acarbose	-	40.578±5.999 ^{abc}	65.649±5.114 ^a

Data are presented as mean ± SD values of triplicate determinations. a-i Different letters stand for significantly different values from each other within a column (Tukey's-HSD multiple range post hoc test, $p < 0.05$, IBM, SPSS, version 23); the same letters stand for non-significant difference.

Although, the coumarin was common skeleton amongst the tested compounds, a significant variation in their inhibitory potential was observed after introducing different substituents at position 5 and 7 of the main core. For instance, the presence of $-\text{COCH}_3$ group at position 7 of coumarin ring in compound 4,5-dimethyl-2-oxo-2*H*-chromen-7-yl acetate (**B1**) drastically reduces its activity ($\text{IC}_{50} = 194.978 \pm 2.36 \mu\text{g ml}^{-1}$) against the enzyme. On the other hand, compound 7-(benzyloxy)-4, 5-dimethyl-2*H*-chromen-2-one (**B9**) with the benzyl group (Ph-CH_2-) at same position remarkably ($p < 0.05$) increased its activity ($\text{IC}_{50} = 11.084 \pm 0.117 \mu\text{g ml}^{-1}$) four-fold more than the standard inhibitor acarbose ($\text{IC}_{50} = 40.578 \pm 5.999 \mu\text{g ml}^{-1}$). The introduction of O-alkyl hydrocarbon chain at position 7, as in compounds **B2** ($-\text{OCH}_3$), **B3** ($-\text{OCH}_2\text{CH}_3$), **B5** ($-\text{OCH}_2\text{CH}_2\text{CH}_2\text{CH}_3$), **B6** ($-\text{OCH}_2\text{CH}_2\text{CH}_2\text{CH}_2\text{CH}_2\text{CH}_3$) also increased the α -glucosidase inhibition activity of these compounds relative to acarbose. On the contrary, the branching of alkyl chain (in **B4**) or the presence of alkenyl unit at same position (in **B7-B8**) decreased the activity. The nitration of benzene ring of coumarin (in **B15**) also reduced the inhibition activity substantially ($\text{IC}_{50} = 285.375 \pm 169.762 \mu\text{g ml}^{-1}$). In series **C**, the compound 4-methyl-5,7-bis (prop-2-en-1-yloxy)-2*H*-chromen-2-one (**C7**) bearing double propenyl moiety at position 5 and 7 of coumarin ring displayed the most potent α -glucosidase inhibitory activity with IC_{50} value of $19.233 \pm 3.010 \mu\text{g ml}^{-1}$. Similarly, the double O-butylation of coumarin ring (in **C5**) also led to the stronger inhibition of α -glucosidase ($\text{IC}_{50} = 32.488 \pm 14.851 \mu\text{g ml}^{-1}$) better than acarbose. The replacement of the 5, 7-dihydroxy groups with $-\text{methoxy}$ (**C2**), $-\text{ethoxy}$ (**C3**), $-\text{isopropoxy}$ (**C4**), $-\text{hexyloxy}$ (**C6**) or $-\text{benzyloxy}$ (**C8**) resulted in a noticeable decrease in the inhibitory activity. The screening of compounds of set I against α -amylase (**Figure 4.8**) did not yield any promising candidate as all compounds displayed weaker activity with the IC_{50} values ranging between 453.591 ± 80.08 to $74.405 \pm 1.894 \mu\text{g ml}^{-1}$ in comparison to the standard drug acarbose ($\text{IC}_{50} = 65.649 \pm 5.114 \mu\text{g ml}^{-1}$). The antioxidant activity of the compounds of set I was also tested using DPPH assay *in vitro* using ascorbic acid as a reference drug (**Table 4.4, Figure 4.9**). The analysed compounds showed a varying degree of anti-oxidant activity with IC_{50} ranging from 1.855 ± 0.146 to $83.316 \pm 1.045 \mu\text{g ml}^{-1}$. Among the tested compounds, the coumarin 7-hydroxy-4,5-dimethyl-8-nitro-2*H*-chromen-2-one (**B15**), bearing $-\text{NO}_2$ group at position 8 exhibited the highest anti-oxidant activity ($\text{IC}_{50} = 1.855 \pm 0.146 \mu\text{g ml}^{-1}$) comparable to the ascorbic acid ($\text{IC}_{50} = 1.184 \pm 0.022$). The single- or double alkylation/acetylation did not yield any promising anti-oxidant compound as all these compounds exhibited weaker activity (IC_{50} between 2.472 ± 0.845 to $83.316 \pm 1.045 \mu\text{g ml}^{-1}$) with respect to ascorbic acid.

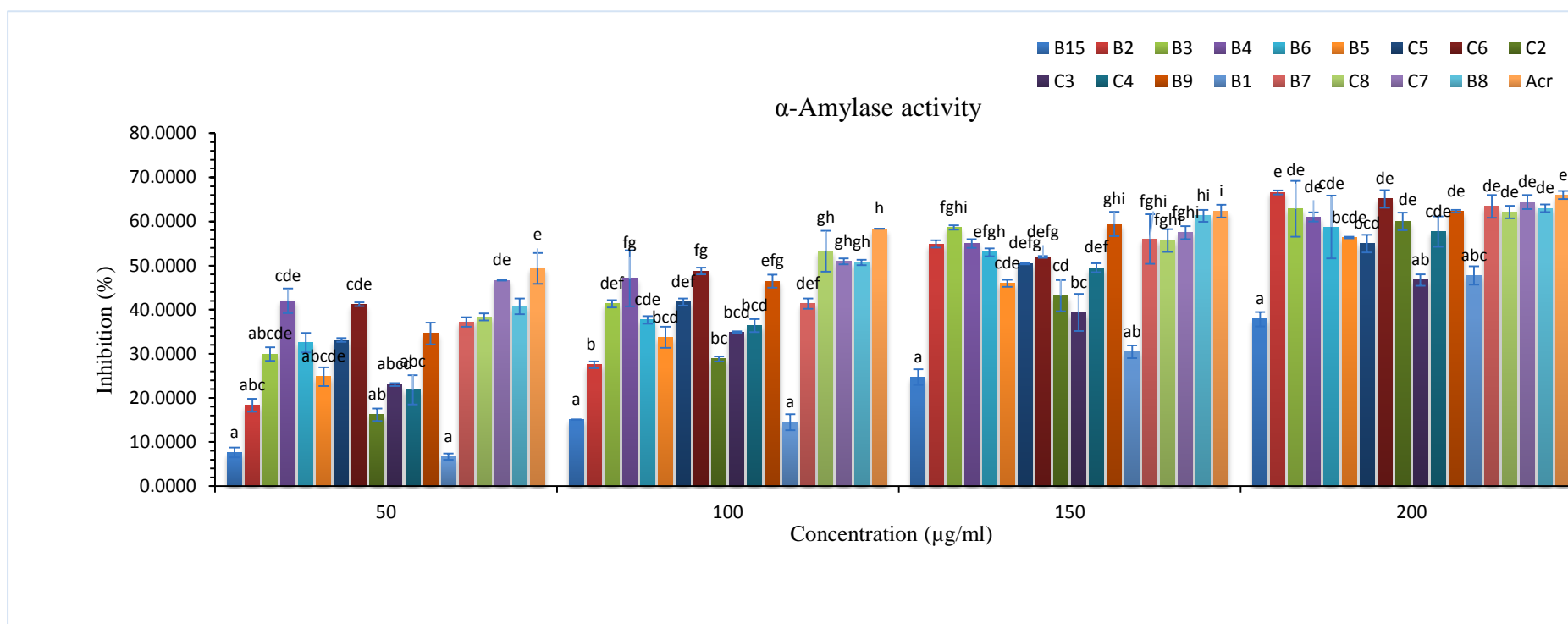


Figure 4.8: *In vitro* α -amylase inhibition activity of coumarin derivatives (**B1-B9, B15, and C2-C8**) along with the standard inhibitor (acarbose).

Data are presented as mean \pm SD values of triplicate determinations. a-i Different letters stand for significantly different values from each other within a column (Tukey's-HSD multiple range post hoc test, $p < 0.05$, IBM, SPSS, version 23); the same letters stand for non-significant difference

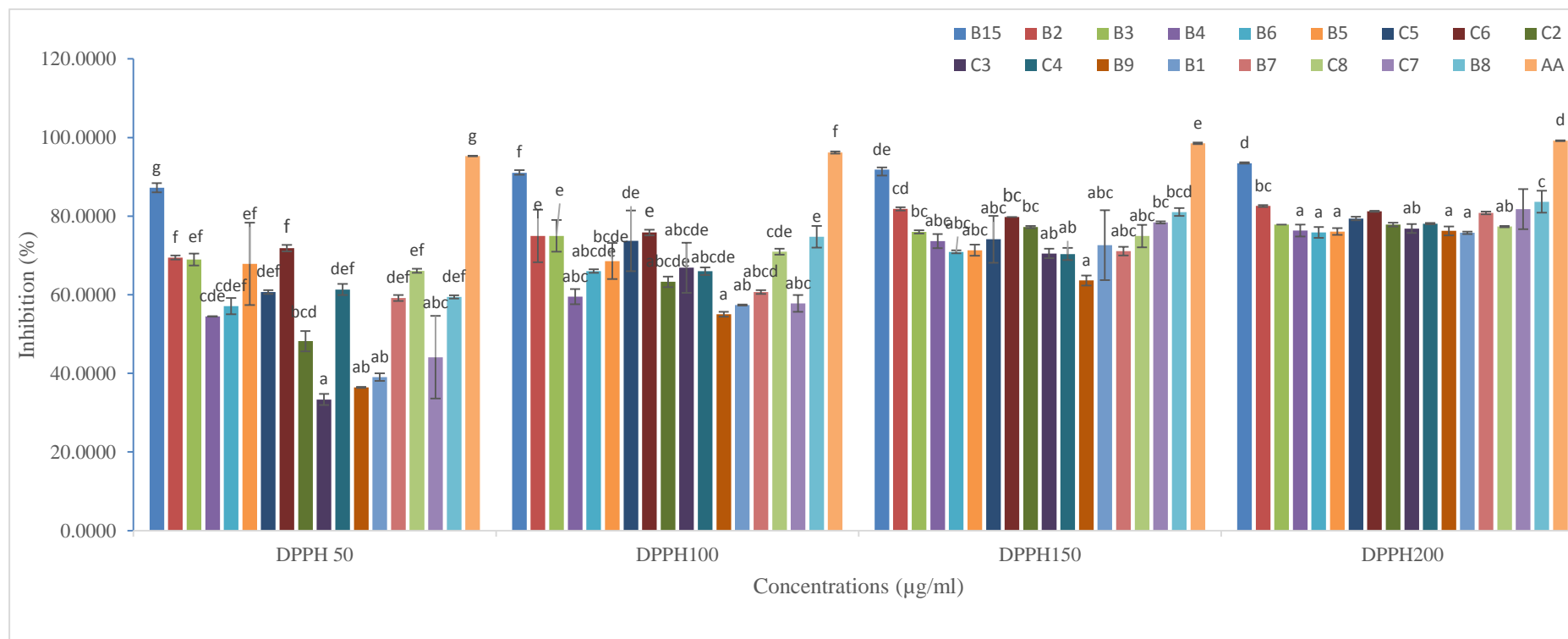
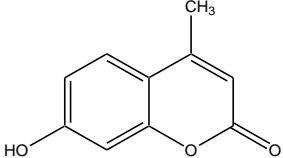
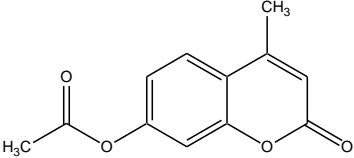
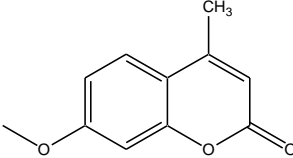
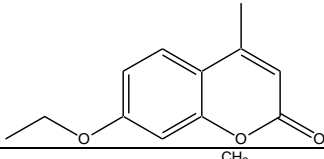
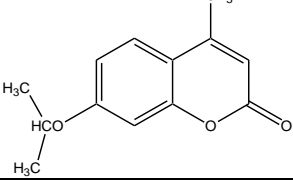
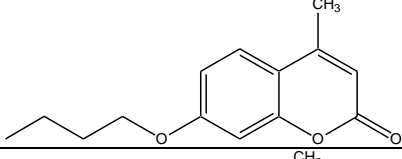
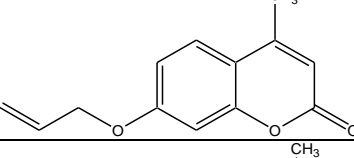
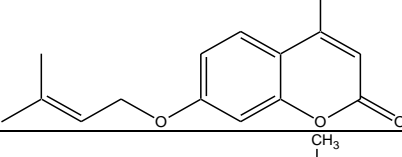
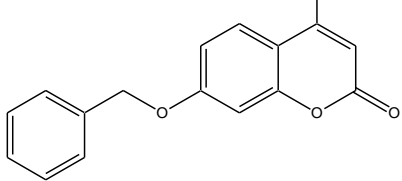


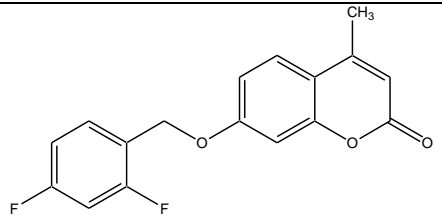
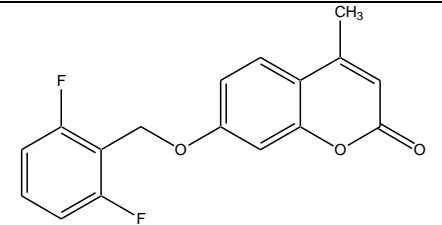
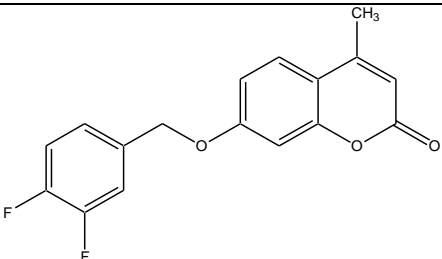
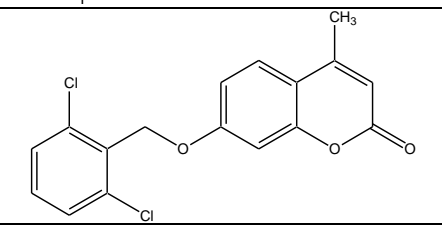
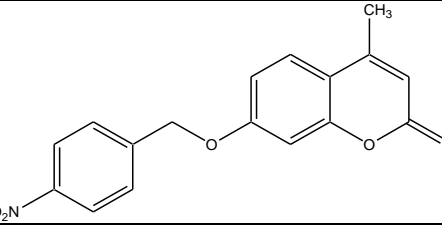
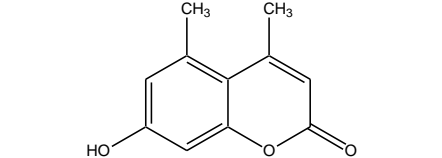
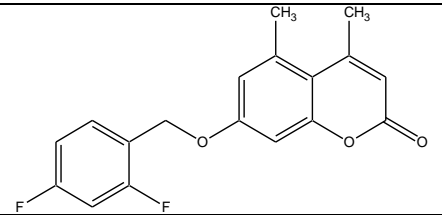
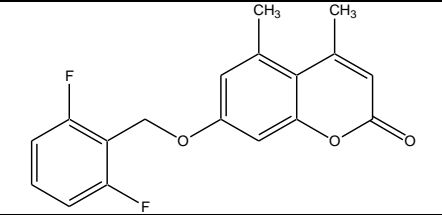
Figure: 4.9: DPPH radical scavenging activity of coumarin derivatives (**B1-B9, B15, and C2-C8**) along with the standard drug (ascorbic acid)

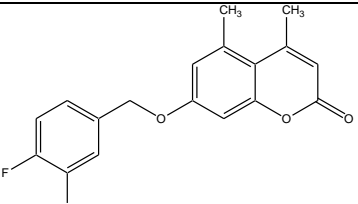
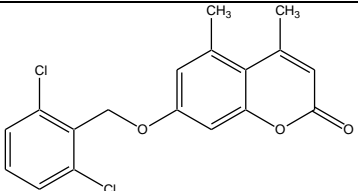
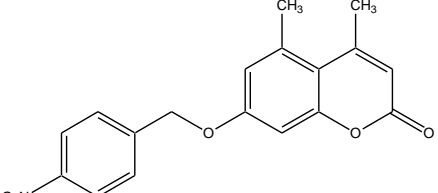
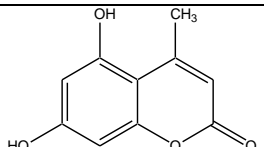
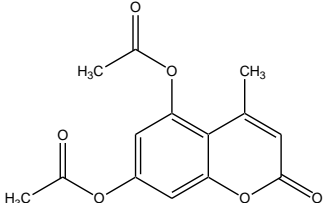
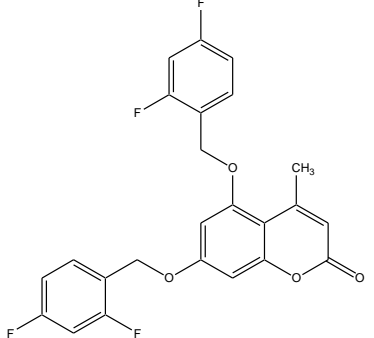
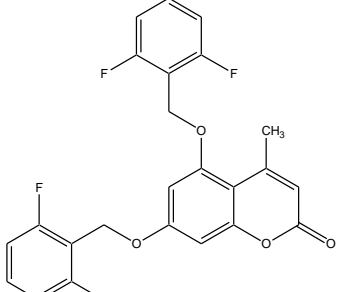
Data are presented as mean \pm SD values of triplicate determinations. a-i Different letters stand for significantly different values from each other within a column (Tukey's-HSD multiple range post hoc test, $p < 0.05$, IBM, SPSS, version 23); the same letters stand for non-significant difference.

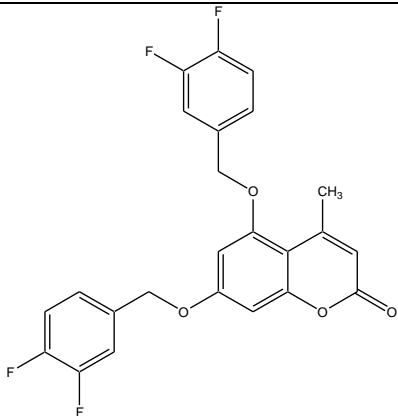
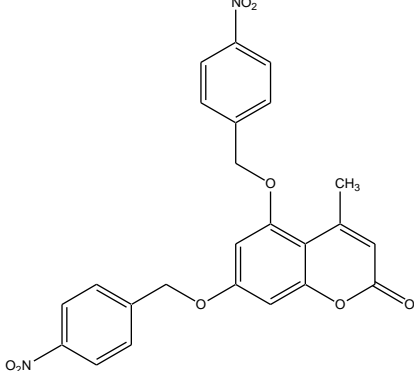
Since, the set I compounds only exhibited potential activity in DPPH inhibition and α -glucose inhibition assays, the remaining 26 compounds of set II were tested only for these two activities *in vitro*. The IC_{50} values for compounds relative to standard drugs are summarized in **Table 4.5**. A closer inspection of **Table 4.5** revealed that all the tested compounds showed weaker anti-oxidant activity ($IC_{50} = 85.38 \pm 7.55 \mu\text{g ml}^{-1}$ to $17.48 \pm 5.43 \mu\text{g ml}^{-1}$) than ascorbic acid ($3.38 \pm 0.92 \mu\text{g ml}^{-1}$). Noticeably, the $-\text{OH}$ substituted coumarins, **A** (32.72 ± 7.65), **B** ($17.48 \pm 5.43 \mu\text{g ml}^{-1}$) and **C** ($28.56 \pm 0.93 \mu\text{g ml}^{-1}$) displayed stronger anti-oxidant activity than their O-alkylated/acetylated analogues suggesting that the presence of hydroxyl groups is important for their antioxidant activity. Another interesting observation of this study was that the presence of electron withdrawing group ($-\text{NO}_2$) group at position 8 in **B15** increased its antioxidant activity ~ 16 -fold more than its hydroxy derivative (**B**). For the α -glucosidase, all the compounds of **A** (except **A4** and **A6**) and **B** series showed improvement in their activity after O-alkylation or acetylation of their precursors (**A** and **B**). For example, the compound **B11** bearing 2, 6-difluorobenzyloxy moiety at position 7 showed the strongest inhibition ($IC_{50} = 21.30 \pm 0.52 \mu\text{g ml}^{-1}$) almost two-fold higher than acarbose ($IC_{50} = 39.36 \pm 1.42 \mu\text{g ml}^{-1}$). On the other hand, **B13**, the chloro analogue of **B11**, displayed comparable ($IC_{50} = 39.68 \pm 2.13 \mu\text{g ml}^{-1}$) activity to acarbose. Similarly, **A11**, bearing 3,4-difluorobenzyloxy group at position 7 exhibited the equivalent activity ($IC_{50} = 39.54 \pm 1.35 \mu\text{g ml}^{-1}$) to acarbose. Conversely, the double O-alkylation/acetylation of **C**, irrespective of the nature or placing of substituents, reduced its ability to inhibit the α -glucosidase. For example, the presence of two 2,6-difluorobenzyloxy on coumarin at position 5 and 7 in **C10**, reduced its α -glucosidase inhibition ability significantly ($IC_{50} = 130.22 \pm 1.5 \mu\text{g ml}^{-1}$) in comparison to its mono alkylated analogue (**B11**). Overall, the results obtained indicated that the O-benylation improves the α -glucosidase inhibition tendency of the coumarin molecule. Similarly, the introduction of $-\text{NO}_2$ group (nitration) on the benzene ring of coumarin significantly increased its antioxidant activity.

Table: 4.5: *In vitro* IC₅₀ values of antioxidant and α-glucosidase inhibition activities of the coumarin analogues (**A1-A13**, **B10-B14**, **C1** and **C9-C12**), their precursors (**A-C**) and the reference drugs (Ascorbic acid and Acarbose).

Sample	Compounds	IC ₅₀ (μg/ml)	
		DPPH	α-Glucosidase
A		32.72±7.65 [†]	148.63±21.89 ^{abc}
A1		62.77±0.79 [†]	51.46± 0.65 ^{ab}
A2		62.54±0.36 [†]	81.42±6.787 ^{ab}
A3		40.55±2.79 [†]	58.40±0.43 ^{ab}
A4		43.40±2.78 [†]	256.94± 12.12 ^c
A5		71.55±2.35 [†]	53.54±0.31 ^{ab}
A6		72.97±1.99 [†]	206.75± 73.40 ^{bc}
A7		67.25±3.12 [†]	79.22±2.61 ^{ab}
A8		65.56±0.52 [†]	53.97± 3.972 ^{ab}

A9		$57.73 \pm 11.79^\dagger$	79.97 ± 17.14^{ab}
A10		$60.02 \pm 4.94^\dagger$	63.66 ± 7.77^{ab}
A11		$47.29 \pm 1.11^\dagger$	39.54 ± 1.35^a
A12		$68.48 \pm 5.72^\dagger$	63.47 ± 1.97^{ab}
A13		$72.29 \pm 6.17^\dagger$	59.56 ± 3.49^{ab}
B		17.48 ± 5.43^{ab}	145.24 ± 29.22^{abc}
B10		$71.17 \pm 3.19^\dagger$	80.26 ± 1.17^{ab}
B11		$53.43 \pm 4.73^\dagger$	21.30 ± 0.52^a

B12		$68.29 \pm 7.10^\dagger$	59.39 ± 6.85^{ab}
B13		$54.51 \pm 12.8^\dagger$	39.68 ± 2.13^a
B14		$67.79 \pm 3.22^\dagger$	99.82 ± 13.2^{abc}
C		28.56 ± 0.93^{abc}	39.612 ± 6.001^a
C1		$63.66 \pm 0.82^\dagger$	61.65 ± 11.07^{ab}
C9		$47.26 \pm 0.68^\dagger$	103.39 ± 5.27^{abc}
C10		$64.61 \pm 0.97^\dagger$	130.22 ± 1.5^{abc}

C11		$43.74 \pm 5.05^{\dagger}$	71.37 ± 7.33^{ab}
C12		$85.38 \pm 7.55^{\dagger}$	65.66 ± 3.81^{ab}
AA		3.38 ± 0.92^a	-
Acr		-	39.36 ± 1.42^a

4.6. Docking results

The glucosidase enzymes catalyses the release of glucose by cleaving the glycosidic bond in different oligosaccharides and thus regulate the glucose level in the body in addition to several associated biological functions. The α -glucosidase, a glucosidase enzyme, has widely received the attention of pharmaceutical companies and researchers to develop novel and potent anti-diabetic agents owing to its role in the breakdown of glycosidic bond in maltose sugar (Borges de Melo *et al.*, 2006). The inhibition of α -glucosidase not only suppresses the carbohydrate digestion but also decrease postprandial hyperglycaemia, and has proven to be very effective strategy in developing novel drugs for the treatment of obesity and diabetes mellitus type II (Scott *et al.*, 2000; Cheng *et al.*, 2004). Since, our compounds showed good inhibition against α -glucosidase even superior to the standard inhibitor under *in vitro* conditions, it was considered worthwhile to investigate the binding ability of compounds with the protein and to explore their binding modes and nature of interactions in the host (enzyme) cavity.

Although, the X-ray coordinates of α -glucosidase isolated from different bacterial sources are available in the protein data bank (www.rcsb.com), the crystal structure of the α -glucosidase from yeast *Sacchromyces cerevisiae*, used in our study, has not been solved yet. On the other hand, the reports showing the construction of 3D models of α -glucosidase from yeast source using homology modelling have been documented in the literature (Khan *et al.*, 2014; Guerreiro *et al.*, 2013). However, none of these modelled structures are available online for scientific community. Hence, we used homology modelling technique to model the 3D structure of α -glucosidase using the amino acid sequence of *Sacchromyces cerevisiae* that is available on UniProt protein data bank (<http://www.uniprot.org/>) with the access code P53341. The BLAST program (Altschul *et al.*, 1990) available in DS was used to probe suitable protein targets on the basis of their sequence similarity with the query sequence, using default parameters. The X-ray structure of *Sacchromyces cerevisiae* that was obtained from isomaltase (pdb code: 3AJ7, resolution 1.30Å) (Yamamoto *et al.*, 2010) was found to be the best match for the query sequence showing 71.4% sequence identity and 86.9% sequence similarity (**Figure 4.10**). The Build homology models protocol in DS software that implements MODELER program (Eswar *et al.*, 2006) was subsequently employed to construct the 3D structure of α -glucosidase, using the X-ray structure of isomaltase (3AJ7) as a template. The generated model of α -glucosidase was energetically minimized until the RMS gradient of value 0.02 was achieved, and validated using the Verify Protein (Profiles-3D) module, in DS. The final assessment of the constructed

homology model was performed by computing its root mean square deviation (RMSD) with respect to the template protein (3AJ7). The computed RMSD less than 1.5Å confirmed a good structural match between them and validated the α -glucosidase model generated (**Figure 4.11**). The binding sites in the generated model were predicted using the Define and Edit Binding Site module, and the one with the highest 6298 points and partition level 787.2Å was selected for docking purpose by creating a binding sphere around this binding site. The eight most potent compounds that showed the better α -glucosidase inhibition than the reference drug (Acarbose) experimentally were selected for docking experiments *in silico*. Initially, the structures of the compounds were prepared in 3D format and subjected to conformational search, ligand preparation and minimization (at physiological pH) modules to determine the lowest energy conformer (details in method section). Docking simulations were subsequently conducted for the compounds in the binding cavity of the modelled α -glucosidase enzyme, using the CDocker program (Wu *et al.*, 2003) embedded in Discovery Studio (DS, Accelrys). The CDocker is a CHARMM force field (Brook *et al.*, 2009) based algorithm that samples different conformations of the ligand molecule during docking simulation using high temperature molecular dynamics, while keeping the protein conformation fixed. For comparison purpose, the docking of acarbose with the α -glucosidase was also conducted considering the same parameters as used for the compounds synthesized. The binding affinity of each compound was determined on the basis of the binding energy (BE) of the complex that was computed by subtracting the energy of the free ligand and energy of the free protein from the energy of their complex. The lower negative value of BE indicates the favorable binding of the ligand with the protein and *vice-versa*. The computed BE values of all compounds were observed to be negative ranging between -21.0 to -8.1 kcal mol⁻¹, suggesting the favorable binding of all eight compounds with the protein. The standard inhibitor (acarbose) relatively displayed the weaker interaction with the enzyme (BE = -5.8 kcal mol⁻¹) supporting the experimental results whereby all these eight compounds exhibited stronger activity against α -glucosidase than acarbose.

The complexes of compounds with the enzyme were further visualized using DS visualizer to determine the nature of forces responsible for their host-guest relationship, and are pictorially depicted in **Figures 4.12-4.20**. Compound **B2** exhibited two conventional hydrogen bonds (2.2Å, 2.6Å) with His280 and Arg442 of enzyme using its carbonyl oxygen (pyran ring) and oxygen atom (-OCH₃), respectively (**Figure 4.12**). Additionally, the two non-conventional hydrogen bonds with Glu277 and Asp352 and multiple hydrophobic interactions with different amino acids (Phe158, Phe159, Phe178, and Arg315) of enzyme were also observed. **B3**

(**Figure 4.13**), the ethyl analogue of **B2** displayed two concurrent hydrogen bonds (2.6 Å, 2.7 Å) with Arg442 (proton donor) through its carbonyl oxygen (proton acceptor) attached to pyran ring, however, missed the interaction with His280 as observed in case of **B2** (**Figure 4.14**). The –CH₂ group (of ethoxy moiety) of **B3** also formed two non-conventional hydrogen bonds with Asp411, while the remaining alkyl groups attached to coumarin ring formed a network of hydrophobic forces with several amino acids of α -glucosidase. Compound **B6** bearing a long six carbon alkyl chain missed several interactions as were seen in case of **B2** and **B3**, however, managed to stabilize its geometry in the active site of enzyme through hydrophobic interactions with Phe158, His280, Phe303 and Asp411 along with a strong electrostatic interaction (cation- π type) with Arg442 (**Figure 4.14**). Similarly, the compound with three-membered hydrocarbon chain at position 5 (**B5**) also interacted with the enzyme *via* two hydrogen bonds (2.2 Å, 2.8 Å) with His280 (proton donor) and Asn415 (proton donor) and hydrophobic interactions with Phe158, Phe303 and Arg315. (**Figure 4.15**). The most potent anti-diabetic compound **B9** ($IC_{50} = 11.084 \pm 0.117 \mu\text{g/mol}$, **Table 4.4**) engaged with the enzyme through a strong conventional hydrogen bond (2.1 Å) formed between the carbonyl oxygen of pyran ring and the –imidazolic nitrogen of His280 (**Figure 4.16**). Additionally, the benzylic group of **B9** displaying a non-conventional hydrogen bond with Glu277 and the coumarin architecture forming hydrophobic network with Arg315 and Phe158 were observed. Moreover, it also displayed a strong electrostatic interaction (cation- π type) between the π -electron cloud of its benzene ring (benzyl group) and positively charged –NH₂ group of Arg442. Another potent antidiabetic agent **B11** ($IC_{50} = 21.3 \pm 0.52 \mu\text{g/mol}$, **Table 4.5**) interacted with the enzyme by establishing two concurrent hydrogen bonds with His280 (2.9 Å) and His246 (2.5 Å) (proton acceptor) through the fluorine atom (proton acceptor), and another hydrogen bond with Gln353 (2.2 Å) through carbonyl oxygen (proton acceptor), in addition to a network of hydrophobic interactions with Arg442, Phe158, Arg315, Pro312 and His240 (**Figure 4.17**).

Compound **C5** (**Figure 4.18**) exhibited a hydrogen bond (2.3 Å) with –NH group (proton donor) of His280 using its ether oxygen (proton acceptor), and another hydrogen bond (2.8 Å) with –NH₂ group (proton acceptor) of Asn415 utilizing its keto group (proton acceptor) of pyran ring, in addition to hydrophobic interactions with His246, Phe158 and Arg315 (**Figure 8**). Similarly, **C7** formed a hydrogen bond (2.2 Å) with His280 through its ether oxygen in addition to establishing several hydrophobic interactions with the α -glucosidase (Arg315, Phe158, His240 and Ph178) utilizing its coumarin ring and side chains (**Figure 4.19**). The standard inhibitor, acarbose (**Figure 4.20**), interacted through hydrogen bonding formed between its hydroxyl

groups and five amino residues (His280, Asp411, Arg315, Pro312 and Glu307) of α -glucosidase along with hydrophobic forces (Phe178, Phe159, Pro312 and Glu277).

Overall, the docking results revealed that the presence of electronegative atoms (oxygen) in the synthesized coumarins was very significant in establishing the hydrogen bonding network with the protein. Similarly, the participation of alkyl/aryl chains and coumarin framework in generating non-bonded interactions (hydrophobic and electrostatic) with the α -glucosidase enzyme played significant role in their host-guest relationship. Docking analysis also identified few key amino acid residues such as His280, Arg315, Phe158, Glu277, Glu215 and Arg442, which were actively involved in the interactions and played important role in locking the geometries of the compounds in the binding site of α -glucosidase. The binding of acarbose to the similar amino acid residues (His280, Arg315, Glu277) as that of the coumarins synthesized indicated their anti-diabetic activity possibly through the same mechanism of action.

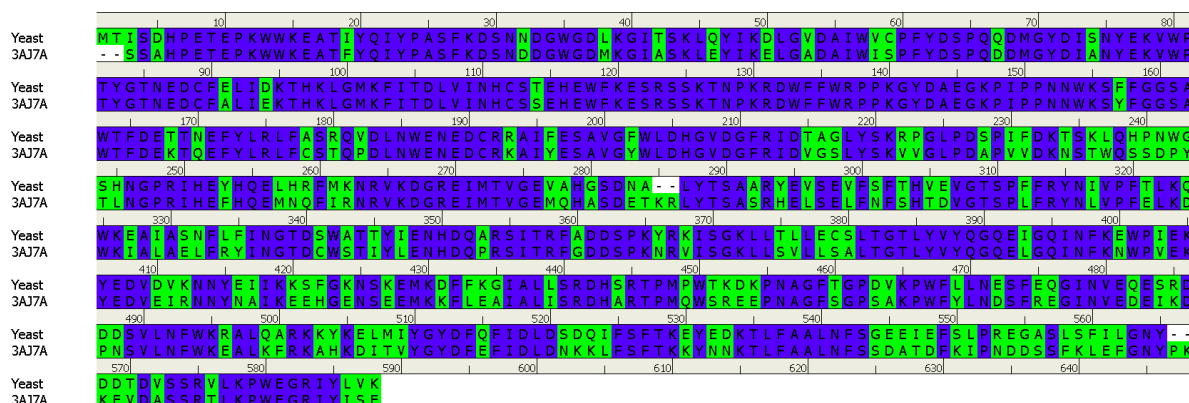


Figure 4.10: Sequence alignment of α -glucosidase from *S. cerevisiae* (uniprot access code: P53341) with the *S. Cerevisiae* from isomaltase (pdb code: 3AJ7). Sequence overlaps are highlighted in blue whereas the conservative substitutions are highlighted in green.

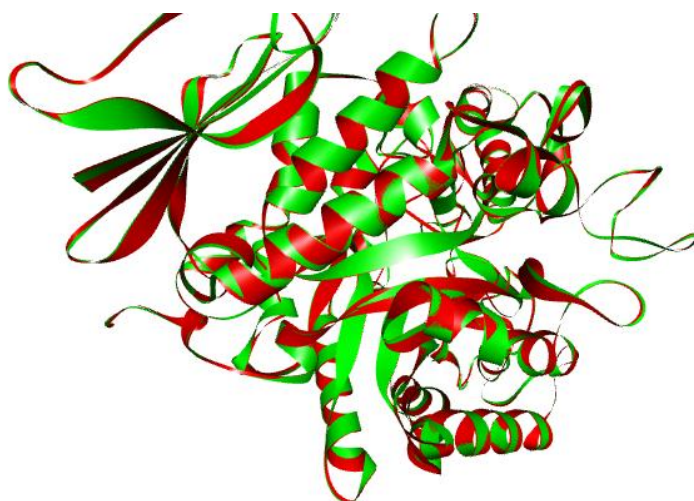


Figure 4.11: Overlay of the predicted homology model of α -glucosidase (shown in red flat ribbons format) with the *Sacchromyces cerevisiae* isomaltase (shown in green flat ribbon format), with the computed RMSD $<1.5\text{\AA}$.

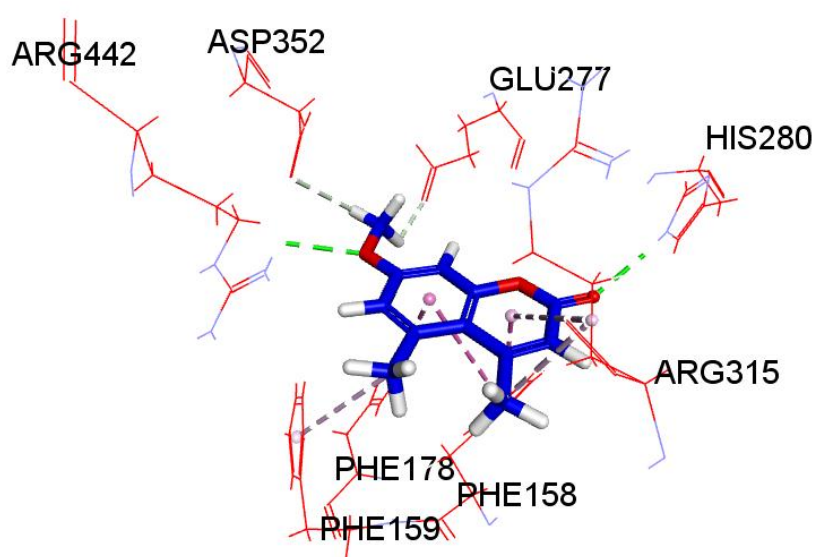


Figure 4.12: Docked complex of **B2** (blue sticks) with the α -glucosidase. Only interacting amino acids (red lines) of enzyme are shown for clarity purpose. Conventional hydrogen bonds as green dotted lines, non-conventional hydrogen bonds as grey dotted lines and hydrophobic interactions are depicted as magenta dotted lines.

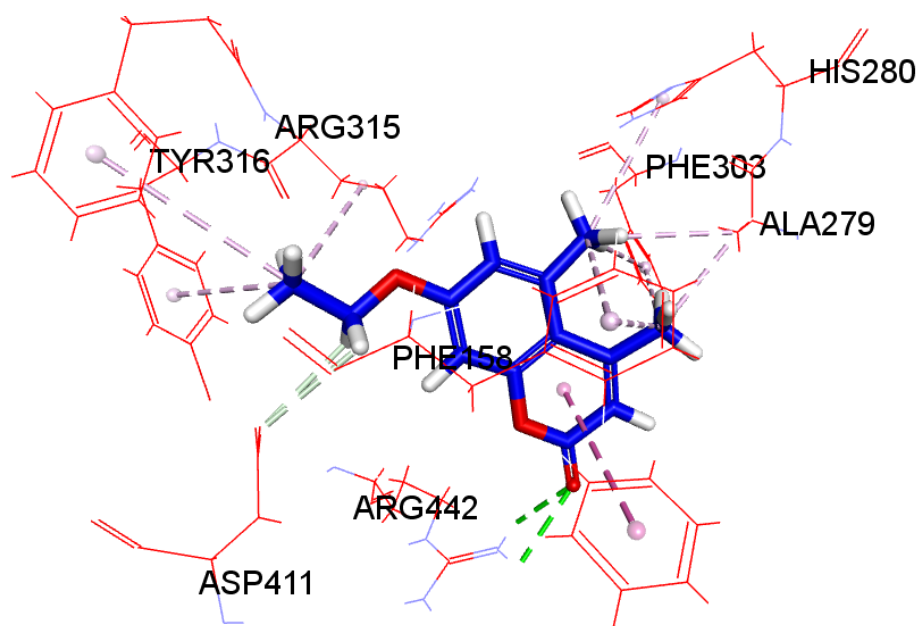


Figure 4.13: Docked complex of **B3** with the α -glucosidase. Only interacting amino acids (red lines) of enzyme are shown for clarity purpose. Conventional hydrogen bonds as green dotted lines, non-conventional hydrogen bonds as grey dotted lines and hydrophobic interactions are depicted as magenta dotted lines.

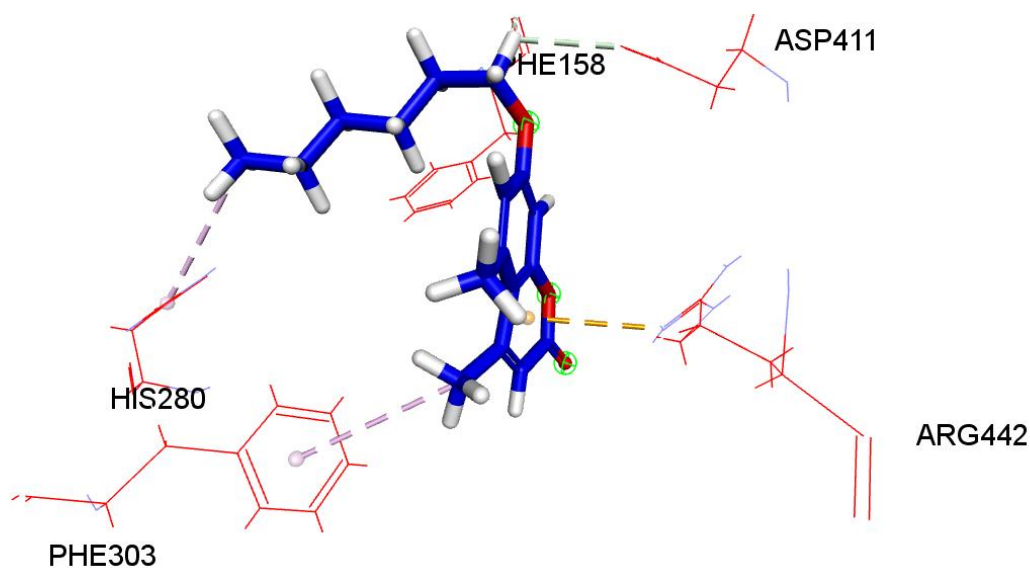


Figure 4.14: Docked complex of **B6** with the α -glucosidase. Only interacting amino acids (red lines) of enzyme are shown for clarity purpose. Conventional hydrogen bonds as green dotted lines, non-conventional hydrogen bonds as grey dotted lines, electrostatic as yellow dotted line and hydrophobic interactions are depicted as magenta dotted lines.

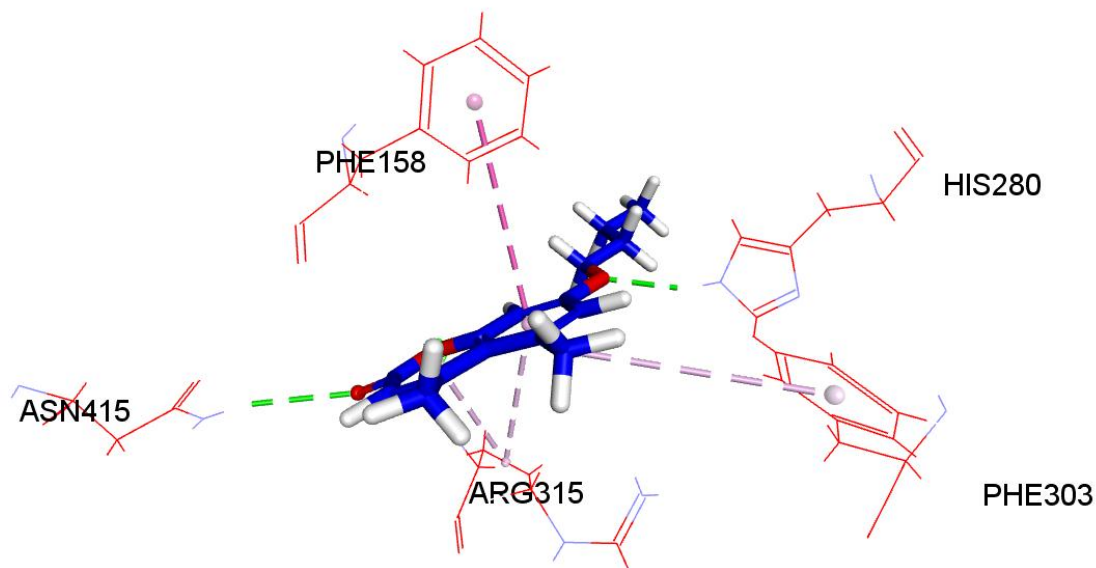


Figure 4.15: Docked complex of **B5** with the α -glucosidase. Only interacting amino acids (red lines) of enzyme are shown for clarity purpose. Conventional hydrogen bonds as green dotted lines, non-conventional hydrogen bonds as grey dotted lines and hydrophobic interactions are depicted as magenta dotted lines.

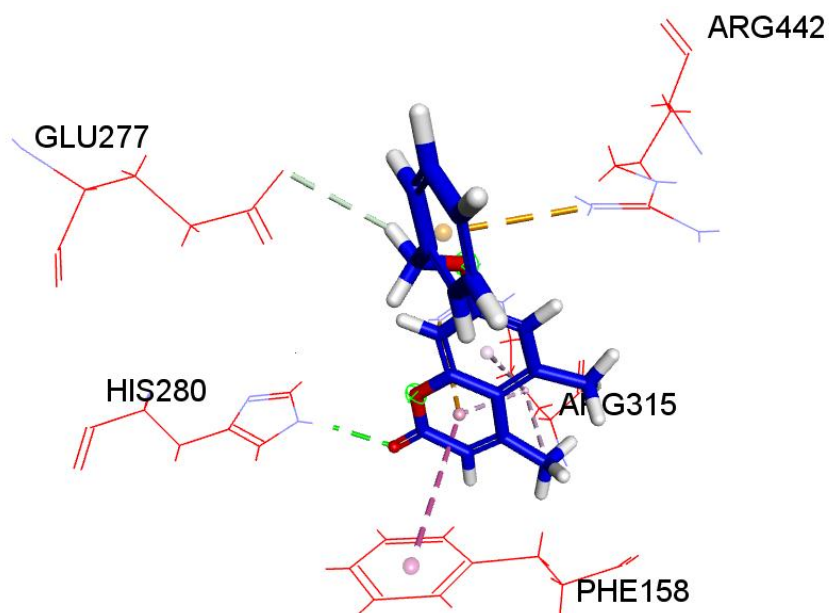


Figure 4.16: Docked complex of **B9** with the α -glucosidase. Only interacting amino acids (red lines) of enzyme are shown for clarity purpose. Conventional hydrogen bonds as green dotted lines, non-conventional hydrogen bonds as grey dotted lines, electrostatic as yellow dotted lines and hydrophobic interactions are depicted as magenta dotted lines.

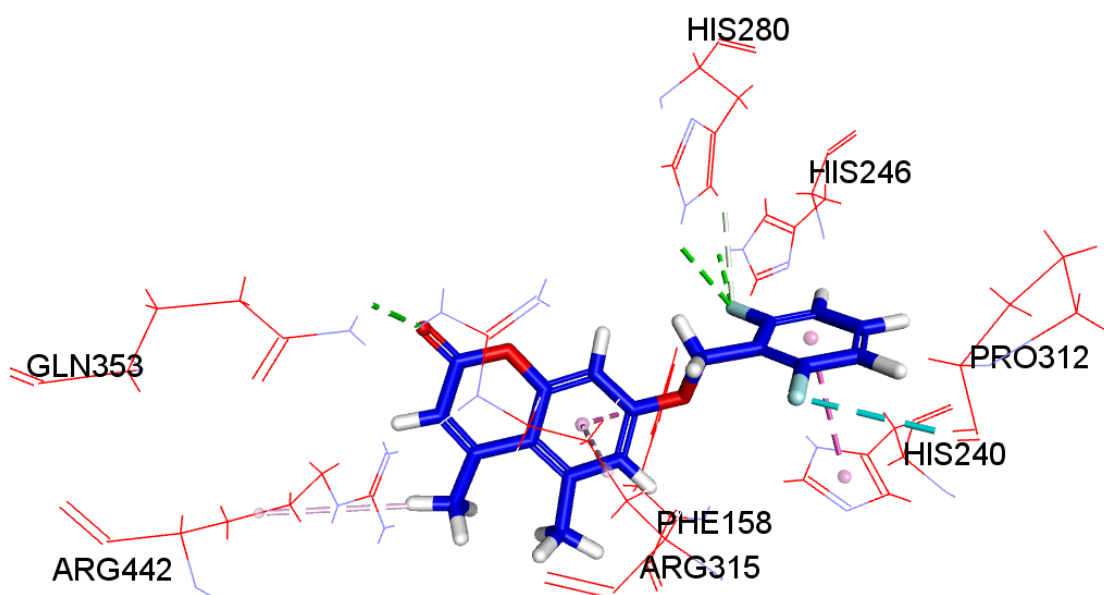


Figure 4.17: Docked complex of **B11** with the α -glucosidase. Only interacting amino acids (red lines) of enzyme are shown for clarity purpose. Conventional hydrogen bonds as green dotted lines, non-conventional hydrogen bonds as grey dotted lines and hydrophobic interactions are depicted as magenta dotted lines.

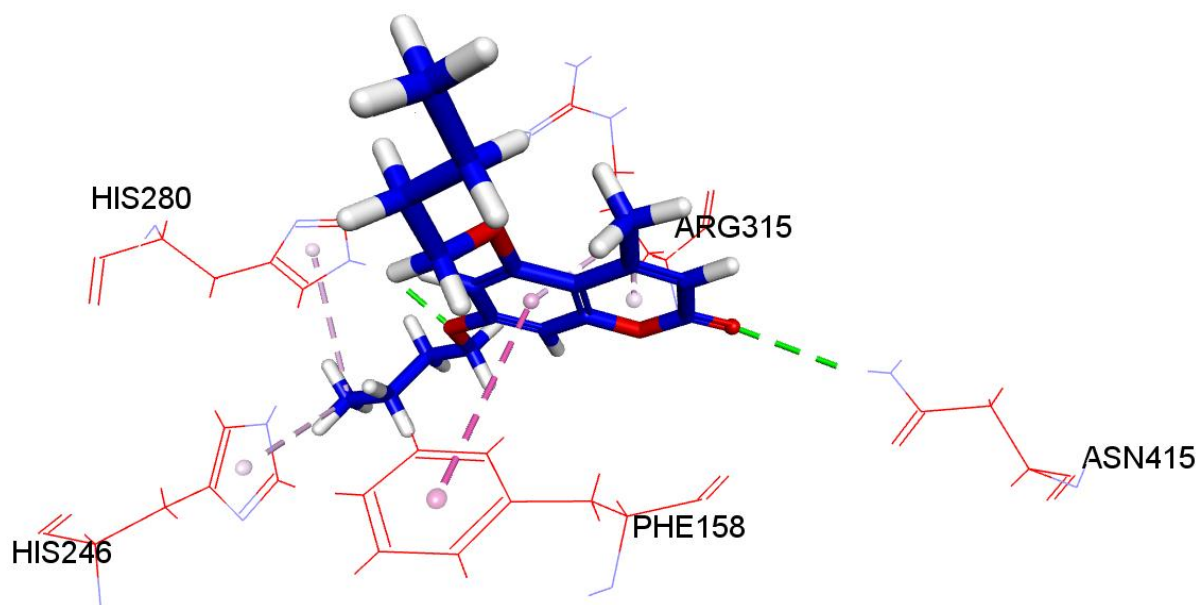


Figure 4.18: Docked complex of **C5** with the α -glucosidase. Only interacting amino acids (red lines) of enzyme are shown for clarity purpose. Conventional hydrogen bonds as green dotted lines, non-conventional hydrogen bonds as grey dotted lines and hydrophobic interactions are depicted as magenta dotted lines.

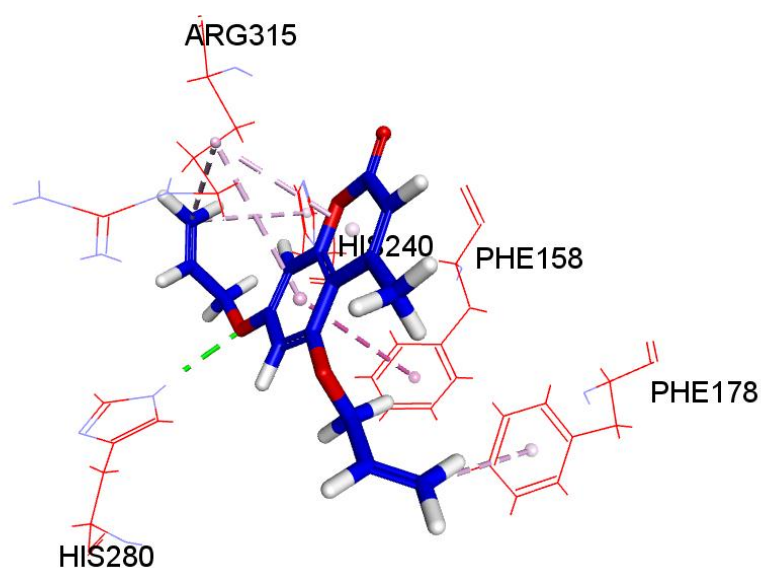


Figure 4.19: Docked complex of C7 with the α -glucosidase. Only interacting amino acids (red lines) of enzyme are shown for clarity purpose. Conventional hydrogen bonds as green dotted lines, non-conventional hydrogen bonds as grey dotted lines and hydrophobic interactions are depicted as magenta dotted lines.

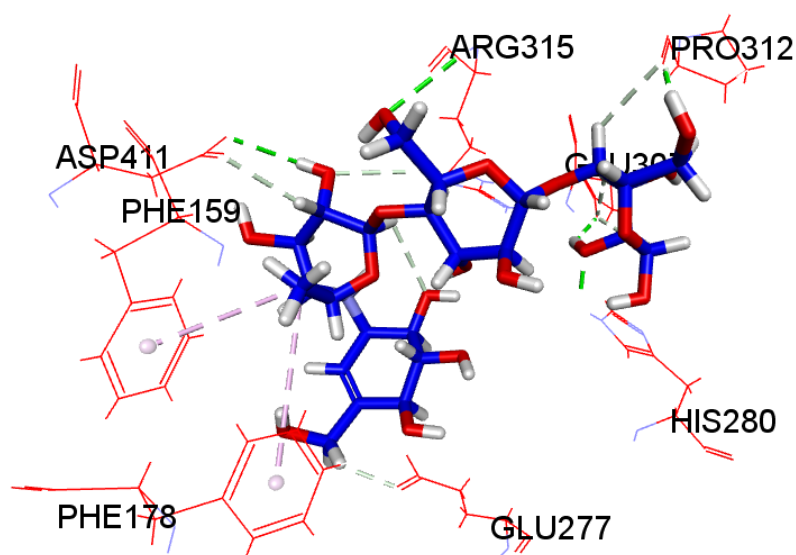


Figure 4.20: Docked pose of acarbose in the binding pocket of α -glucosidase. Only interacting amino acids (red lines) of enzyme are shown for clarity purpose. Conventional hydrogen bonds as green dotted lines, non-conventional hydrogen bonds as grey dotted lines and hydrophobic interactions are depicted as magenta dotted lines.

Chapter 5

Conclusion and Recommendations

We successfully synthesized a range of functionalized coumarin analogues by carrying out the O-alkylation and O-acylation of three coumarins bearing hydroxyl group (s). Of the total 43 compounds synthesized in this study, 27 are novel and have not previously been reported. The starting hydroxyl coumarins were synthesized from different substituted phenols *via* the Pechmann reaction and were subsequently acetylated using acetic anhydride. The O-alkylation of hydroxyl coumarins was accomplished with variedly substituted haloalkanes in the presence of base. Additionally, an unprecedented nitration of coumarin **B** was also performed in this study. The unambiguous structural elucidation of synthesized compounds was accomplished with the help of different spectroscopic techniques such as NMR (1D and 2D), FT-IR and HRMS. Interesting chemical shifts and splitting patterns were observed in case of fluorinated coumarins where fluorine atom being NMR active was engaged in coupling with both proton and carbon nuclei.

The antioxidant and antidiabetic activities of all coumarins (both O-acetylated/acylated) were tested under *in vitro* conditions. The antidiabetic activity was tested *via* inhibition of α -glucosidase and α -amylase enzymes, key proteins in regulating the glucose level in body; while the antioxidant activity was tested by DPPH assay. Based on IC₅₀ data, the single O-alkylated coumarins were observed to be stronger inhibitors of α -glucosidase with respect to their double O-alkylated analogues. Coumarin (**B9**) bearing O-benzyloxy group at position 7 displayed the highest activity against α -glucosidase, almost four-fold higher than the standard inhibitor acarbose. Although, the presence of 2, 6-difluorobenzyl (**B11**) moiety at same position reduced its activity, the compound was still more active (two-fold) than acarbose. The introduction of alkyl chain in this series of compounds (**B2-B6**) also improved their activity relative to acarbose. Conversely, the double O-alkylation/acetylation of coumarins, irrespective of the nature or placing of substituents, reduced their ability to inhibit the α -glucosidase. For instance, the coumarin (**C10**) flanked by two 2,6-difluorobenzyloxy groups at position 5 and 7 displayed weaker α -glucosidase inhibition in comparison to its structural analogue with single benzyloxy chain (**B11**). Only, the double O-propenylation (**C7**) and O-butylation (**C5**) resulted into stronger α -glucosidase inhibitors compared to acarbose. The presence of nitro group in the coumarin ring, in contrast, decreased the α -glucosidase inhibition significantly. None of the tested coumarins showed promising activity against α -amylase.

The *in vitro* antioxidant potential of the coumarins of set I was also tested using DPPH assay. The coumarin (**B15**) bearing $-\text{NO}_2$ group showed the highest anti-oxidant activity amongst the synthesized compounds, almost comparable to the ascorbic acid. All the remaining tested compounds showed weaker activity in comparison to ascorbic acid. These results demonstrate the significance of $-\text{OH}$ groups in antioxidant activity of polyphenols. The chemical transformation of $-\text{OH}$ groups to alkoxy or acetyloxy groups considerably decreased the antioxidant activity of coumarins.

Finally, *in silico* docking simulations of few representative coumarins with the modelled α -glucosidase revealed the importance of hydrogen bonding and non-bonded interactions (hydrophobic and electrostatic) with their host-guest relationship. The heteroatoms (oxygen) were found to be useful in establishing hydrogen bonding, whereas the coumarin framework was observed to be important in forming hydrophobic interactions with the catalytic site of α -glucosidase. Moreover, the amino acids *viz.* His280, Arg315, Phe158, Glu277, Glu215 and Arg442, of α -glucosidase were predicted to be important for locking the conformations of compounds in the catalytic site of α -glucosidase. Overall, the present study demonstrates the potential of coumarin analogues to act as anti-diabetic agents. To the best of our knowledge, this is the first report in which coumarins of this kind have been investigated as inhibitors for α -glucosidase.

Future work can involve placing the substituents preferably different benzyl groups on the pyranone ring of coumarin and observing the effect it has on the inhibition of α -glucosidase. The effect of replacing methyl group at position number 4 with a phenyl group can also be investigated since such coumarins have shown potential activity against various metabolic diseases. With regard to the antioxidant activity, only nitration of coumarin **B** was successful and yielded the compound with comparable antioxidant activity to Ascorbic acid. So, alternative methods can be used for nitration of **A** and **C**, and the resulting compounds can be tested thereafter.

References

- Ademiluyi, A.O.; Oboh, G. **2013**. Soybean phenolic-rich extracts inhibit key-enzymes linked to type 2 diabetes (α -amylase and α -glucosidase) and hypertension (angiotensin I converting enzyme) in vitro. *Experimental and Toxicologic Pathology*.65:305–309. DOI: 10.1016/j.etp.2011.09.005.
- Adolfsson, S.; Arvill, A.; Ahrén, K. **1967**. Stimulation by insulin of accumulation and incorporation into protein of L-[^3H] proline in the intact levator ani muscle from the rat. *Biochimica et Biophysica Acta*. 176-178.
- Aeibi, H. **1984**. Catalase in vitro. *Methods in enzymology*.105:121-126.
- Ahluwalia, V.K.; Sachdev, G.P.; Seshadri, T.R. **1967**. Selective alkylation of 5,7-dihydroxy-4-methyl-coumarin. *Indian Journal of Chemistry*. 5(10):461-463.
- Alam, M.N.; Bristi, N.J.; Ratiquzzaman, M. **2013**. Review on in vivo and in invitro methods evaluation of antioxidant activity. *Saudi Pharmaceutical Journal*. 21: 143-152.
- Al-Amiery, A.A.; Al-Majedy, Y.K.; Kadhum, A.A.H.; Mohamad, A.B. **2015**. Hydrogen Peroxide Scavenging Activity of Novel Coumarins Synthesized Using Different Approaches.*PLoS ONE*. DOI:10.1371/journal.pone.0132175.
- Aleksanyan, D.V.; Artyushin, O.I.; Genkina, G.K.; Vasil'ev, A.A.; Nelyubina, Y.V.; Shepel, N.E.; Klemenkova, Z.S.; Gumileva, L.V.; Kozlov, V.A. **2014**. Synthesis and complexing properties of phosphorylated imines of 8-formyl-7-hydroxycoumarin. *Russian Chemical Bulletin, International edition*. 63: 2309-2316.
- Alipour, M.; Khoobi, M.; Emami, S.; Fallah-Benakohal, S.; Ghasemi-Niri, S.F.; Abdollahi, M.; Foroumadi, A.; Shafiee, A. **2014**. Antinociceptive properties of new coumarin derivatives bearing substituted 3,4-dihydro-2H-benzothiazines.*DARU Journal of Pharmaceutical Sciences*. 22-29.
- Altschul, S.F.; Gish, W.; Miller, W.; Myers, E.W.; Lipman, D.J. **1990**. Basic local alignment search tool. *Journal of Molecular Biology*. 215(3):403-410.
- Amin, K.M.; Rahman, D.E.A.; Al-Eryani, Y.A. **2008**. Synthesis and preliminary evaluation of some substituted coumarins as anticonvulsant agents. *Bioorganic and Medicinal Chemistry*. 16(10):5377-5388.

Amoozadeh, A.; Ahmadzadeh, M.; Kolvari, E. **2013**. Easy access to coumarin derivatives using sulfuric acid as an efficient and reusable catalyst under solvent-free conditions. *Journal of Chemistry*. Vol. 2013, Article ID 767825, 6 pages, <http://dx.doi.org/10.1155/2013/767825>.

Aoki, T.; Hyohdoh, I.; Furuichi, N.; Ozawa, S.; Watanabe, F.; Matsushita, M.; Sakaitani, M.; Ori, K.; Takanashi, K.; Harada, N.; Tomi, Y.; Tabo, M.; Yoshinari, K.; Aoki, Y.; Shimma, N.; Likura, H. **2013**. The sulfamide moiety affords higher inhibitory activity and oral bioavailability to a series of coumarin dual selective RAF/MEK inhibitors. *Bioorganic and Medicinal Chemistry*. 23: 6223-6227.

Apak, R.; Güclü, K.; Özyürek, M.; Celik, S.E. **2008**. Mechanism of antioxidant capacity assays and the CUPRAC (Cupric ion reducing antioxidant capacity) assay. *Microchim Acta*. 160: 413-419.

Asghari, S.; Baharfar, R.; Darabi, S.A.; Mohammadian, R. **2015**. Three component reactions of 7-hydroxy coumarin derivatives, acetylenic esters and aromatic aldehydes in the presence of Net_3 . *Journal of the Brazilian Chemical Society*. 26: 218-223.

Asfari, M.; Janjic, D.; Meda, P.; Li, G.; Halban, P.A.; Wollheim, C.B. **1992**. Establishment of 2-Mercaptoethanol-dependent Differentiated Insulin-secreting cell lines. *Endocrinology*. 130: 168-178.

Asif, M. **2015**. Overview of diverse pharmacological activities of substituted coumarins: Compounds with therapeutic potentials. *American Journal of clinical anesthesiology*. 1: 1-16.

Asif, M. **2015**. Pharmacologically potentials of different substituted coumarin derivatives. *Chemistry International*. 1(1):1-11.

Atmaca, M.; Bilgin, H.M.; Obay, B.D.; Diken, H.; Kelle, M.; Kale, E. **2011**. The hepatoprotective effect of coumarin and coumarin derivatives on carbon tetrachloride-induced hepatic injury by antioxidative activities in rats. *Journal of Physiology and Biochemistry*. 67:569-576.

Augustine, J.K.; Bombrun, A.; Ramappa, B.; Boodappa, C. **2012**. An efficient one-pot synthesis of coumarins mediated by propylphosphoric anhydride (T3P) via the Perkin condensation. *Tetrahedron Letters*. 53: 4422-4425.

Avdeef, A. **2001**. Physicochemical profiling (solubility, permeability and charge state). *Topics in Medicinal Chemistry*. 1(4): 277-351.

Avó, J.; Martins, S.; Jorge Parola, A.; Lima, J.C.; Branco, P.S.; Prates Ramalho, J.P; Pereira, A. **2013**. A family of styrylcoumarins: Synthesis, spectroscopic, Photophysical and Photochemical properties. *Chem Plus Chem*. 78: 789-792.

Bai, Y.; Zhang, F.; Ying, J.; Wu, Y. **2015**. Theoretical investigation of the substituent effects on the electronic and optical properties of 6-substituted coumarin derivatives. *Journal of molecular structure*. 1089:53-58.

Balaji, P.N.; Seleena, S.K.P.; Vidya, G.; Himateja, T.; Neelima, B.; Lakshmiteja, T. **2013**. Synthesis and characterisation of Schiff Bases derived from acetyl coumarin and evaluated for anti-microbial activity. *Research Journal of Pharmaceutical, biological and chemical sciences*. 4(2):9-15.

Ballin, N.Z.; Sørensen, A.T. **2014**. Coumarin content in cinnamon containing food products on the Danish market. *Food Control*. 38: 198-203.

Bedoya, L.M.; Beltrán, M.; Sancho, R.; Olmedo, D.A.; Sánchez-Palomino, S.; del Olmo, E.; López-Pérez, J.L.; Muñoz, E.; Feliciano, A.S.; Alcamí, J. **2005**. 4-Phenylcoumarins as HIV transcription inhibitors. *Bioorganic and Medicinal Chemistry Letters*. 15: 4447-4450.

Benzie, I.F.F.; Strain, J.J. **1996**. The ferric reducing ability of plasma (FRAP) as a measure of 'antioxidant power': The FRAP assay. *Analytical Biochemistry*. 239:70-76.

Benzie, I.F.F.; Strain, J.J. **1999**. [2] Ferric reducing/antioxidant power assay: direct measure of total antioxidant activity of biological fluids and modified version for simultaneous measurement of total antioxidant power and ascorbic acid concentration. *Methods in enzymology*. 299: 15-27.

Black, W.C.; Bayly, C.I.; Davis, D.E.; Desmarais, S.; Falgueyret, J.; Léger, S.; Li, C.S.; Massé, F.; McKay, D.J.; Palmer, J.T.; Percival, M.D.; Robichaud, J.; Tsou, N.; Zamboni, R. **2005**. Trifluoroethylamines as amide isoesters in inhibitors of cathepsin K. *Bioorganic and Medicinal Chemistry Letters*. 15(21): 4741-4744.

Borges de Melo, E.; da Silveira Gomes, A.; Carvalho, I. **2006**. α - and β -Glucosidase inhibitors: chemical structure and biological activity. *Tetrahedron*. 62: 10277-10302.

Borges, F.; Roleira, F.; Milhazes, N.; Santana, L.; Uriarte, E. **2005**. Simple Coumarins and Analogues in Medicinal Chemistry: Occurrence, Synthesis and Biological activity. *Current Medicinal Chemistry*. 12: 887-916.

Brooks, B.R.; Brooks, C.L., 3rd; Mackerell, A.D., Jr.; Nilsson, L.; Petrella, R.J.; Roux, B.; Won, Y.; Archontis, G.; Bartels, C.; Boresch, S.; Caffisch, A.; Caves, L.; Cui, Q.; Dinner, A.R.; Feig, M.; Fischer, S.; Gao, J.; Hodoseck, M.; Im, W.; Kuczera, K.; Lazaridis, T.; Ma, J.; Ovchinnikov, V.; Paci, E.; Pastor, R.W.; Post, C.B.; Pu, J.Z.; Schaefer, M.; Tidor, B.; Venable, R.M.; Woodcock, H.L.; Wu, X.; Yang, W.; York, D.M.; Karplus, M. **2009**. CHARMM: the biomolecular simulation program. *Journal of Computational Chemistry*. 30(10): 1545-1614.

Buckle, D.R.; Cantello, B.C.C.; Smith, H.; Spicer, B.A. **1975**. Antiallergic activity of 4-hydroxy-3-nitrocoumarins. *Journal of Medicinal Chemistry*. 18(4):391-394.

Budzisz, E.; Brzezinska, E.; Krajewska, U.; Rozalski, M. **2003**. Cytotoxic effects, alkylating properties and molecular modelling of coumarin derivatives and their phosphonic analogues. *European Journal of Medicinal Chemistry*. 38:597-603.

Calvino-Casilda, V.; Bañares, M.A.; Lozano Diz, E. **2010**. Real-time Raman monitoring during coumarins synthesis via Pechmann condensation : A tool for controlling the preparation of pharmaceuticals. *Catalysis Today*. 155:279-281.

Canter, F.W.; Curd, F.H.; Robertson, A. **1931**. CLXVI.-Hydroxy-carbonyl compounds. Part III. The preparation of coumarins and 1:4-Benzopyrones from phloroglucinol and resorcinol. *Journal of the Chemical Society*. 1255-1265.

Carotti, A.; Carrieri, A.; Chimichi, S.; Boccalini, M.; Cosimelli, B.; Gnerre, C.; Carotti, A.; Carrupt, P.; Testa, B. **2002**. Natural and Synthetic Geiparvarins are strong and selective MAO-B inhibitors. Synthesis and SAR studies. *Bioorganic and Medicinal Chemistry Letters*. 12: 3551-3555.

Chaudry, I.H.; Sayeed, M.M.; Baue, A.E. **1975**. The effect of insulin on glucose uptake in soleus muscle during Hemorrhagic Shock. *Canadian Journal of Physiology and Pharmacology*. 53: 67-73.

Cheng, A.; Josse, R. **2004**. Intestinal absorption inhibitors for type 2 diabetes mellitus: prevention and treatment. *Drug Discovery Today: Therapeutic Strategies*. 1: 201-206.

Chunduru, V.S.R.; Rao, V.R. **2013**. Synthesis of coumarin substituted triazolothiadiazine derivatives via Ring transformation reaction. *Journal of Heterocyclic Chemistry*. 50:159-164.

Claisen, L. **1925**. About the mechanism of rearrangement of phenol allyl esters. *European Journal of Inorganic Chemistry*. 58(2):275-281.

Colca, J.R. **1995**. Insulin sensitiser drugs in development for the treatment of diabetes. *Expert opinion on investigational drugs*. 4: 27-29.

Crombie, L.; Games, D.E.; McCormick, A. **1967**. Extractives of *Mammea Americana*. L. Part II. The 4-Phenylcoumarins, Isolation and structure of Mammea A/AA, A/A cyclo D, A/BA, A/AB and A/BB. *Journal of the Chemical Society (C)*. 2553-2559.

Cubukcu, B.; Bray, D.H.; Warhurst, D.C.; Mericli, A.H.; Ozhatay, N.; Sariyar, G. **1990**. In vitro antimalarial activity of crude extracts and compounds from *Artemisia abrotanum* L. *Phytotherapy Research*. 5(4):203-204.

Dahlqvist, A. **1964**. Method for assay of intestinal disaccharidases. *Analytical Biochemistry*. 7: 18-25.

Dang, B.T.; Guitton, Y.; Freuze, I.; Grovel, O.; Litaudon, M.; Richomme, P.; Séraphin, D.; Derbé, S. **2015**. Dereplication of *Mammea neurophylla* metabolites to isolate original 4-phenylcoumarins. *Phytochemistry Letters*. 11: 61-68.

De, S.K.; Gibbs, R.A. **2005**. An efficient and practical procedure for the synthesis of 4-substituted coumarins. *Synthesis*. 8:1231-1233.

de Alcantara, F.C.; Lozano, V.F.; Velosa, A.S.V.; dos Santos, M.R.M.; Pereira, R.M.S. **2015**. New coumarin complexes of Zn, Cu, Ni and Fe with antiparasitic activity. *Polyhedron*. 101:165-170.

de Almeida Barros, T.A.; de Freitas, L.A.R.; Filho, J.M.B.; Nunes, X.P.; Giulietti, A.M.; de Souza, G.E.; dos Santos, R.R.; Soares, M.B.P.; Villarreal, C.F. **2010**. Antinociceptive and anti-inflammatory properties of 7-hydroxycoumarin in experimental animal models: potential therapeutic for the control of inflammatory chronic pain. *Journal of Pharmacy and Pharmacology*. 62:205-213.

DeWitte, R.S.; Shakhnovich, E.L. **1996**. SMOG: de novo Design Method Based on Simple, Fast, and Accurate Free Energy Estimates. 1. Methodology and Supporting Evidence. *Journal of American Chemical Society*. 118: 11733-11744.

Dinis, T.C.P.; Madeira, V.M.C.; Almeida, L.M. **1994**. Action of phenolic derivatives (Acetaminophen, Salicylate, and *s*-Aminosalicylate) as inhibitors of membrane lipid peroxidation and as peroxy radical scavengers. *Archives of biochemistry and biophysics*. 315: 161-169.

Doebner, O. **1902**. As to the homologous of sorbic acid, unsaturated acids containing two double bonds. *Report of the German Chemical Society*. 35(1):1136-1147.

Duo, L.; Shuanglian, C.; Fangjian, L.; Qui'an, W. **2015**. Synthesis of long chain fatty acids acylated coumarin glycoside esters with lipase as catalyst. *Chemical Research in Chinese Universities*. 31: 534-538.

Eissa, A.A.M.; Farag, N.A.H.; Soliman, G.A.H. **2009**. Synthesis, biological evaluation and docking studies of novel benzopyranone congeners for their expected activity as anti-inflammatory analgesic and antipyretic agents. *Bioorganic and Medicinal Chemistry*. 17:5059-5070.

Elgogary, S.R.; Hashem, N.M.; Khodeir, M.N. **2014**. Synthesis and photooxygenation of linear and angular furocoumarin derivatives as a hydroxyl radical source: Psoralen, Pseudopsoralen, Isopseudopsoralen, and Allopsoralen. *Journal of Heterocyclic Chemistry*. 00(00). DOI 10.1002/jhet.

el-Saadani, M.; Esterbauer, H.; el-Sayed, M.; Goher, M.; Nassar, A.Y.; Jürgens, G. **1989**. A spectrophotometric assay for lipid peroxides in serum lipoproteins using a commercially available reagent. *The Journal of Lipid Research*. 30:627-630.

Ellman, G.L. **1959**. Tissue sulfhydryl groups. *Archives of Biochemistry and Biophysics*. 82(1):70-77.

Emami, S.; Dadashpour, S. **2015**. Current developments of coumarin based anti-cancer agents in medicinal chemistry. *European Journal of medicinal chemistry*. doi:10.1016/j.ejmech.2015.08.033.

Emami, S.; Foroumadi, A.; Faramarzi, M.A.; Samadi, N. **2008**. Synthesis and antibacterial activity of quinolone-based compounds containing a coumarin moiety. *Archiv der Pharmazie. Chemistry in Life Sciences*. 341:42-48.

Eswar, N.; Webb, B.; Marti-Renom, M.A.; Madhusudhan, M.S.; Eramian, D.; Shen, M.Y.; Pieper, U.; Sali, A. **2006**. Comparative protein structure modeling using Modeller. *Current Protocols in Bioinformatics*. Chapter 5, Unit 5 6.

Ewing, T.J.A.; Makino, S.; Skillman, A.G.; Kuntz, I.D. **2001**. DOCK 4.0: Search strategies for automated molecular docking of flexible molecule databases. *Journal of Computer-Aided Molecular Design*. 15: 411-428.

Fais, A.; Corda, M.; Era, B.; Fadda, M.B.; Matos, M.J.; Quezada, E.; Santana, L.; Picciau, C.; Podda, G.; Delogu, G. **2009**. Tyrosinase inhibitor activity of coumarin-resveratrol hybrids. *Molecules*. 14(7):2514-2520.

Farahi, M.; Karami, B.; Tanuraghaj, H.M. **2015**. Efficient synthesis of a new class of sulfonamide-substituted coumarins. *Tetrahedron Letters*. 56:1833-1836.

Fogliano, V.; Verde, V.; Randazzo, G.; Ritieni, A. **1999**. Method for measuring antioxidant activity and its application to monitoring the antioxidant capacity of wines. *Journal of agricultural and food chemistry*. 47: 1035-1040.

Foley, J.E.; Gliemann, J. **1981**. Accumulation of 2-deoxyglucose against its concentration gradient in rat adipocytes. *Biochimica et Biophysica Acta*. 648: 100-106.

Frère, S.; Thiéry, V.; Besson, T. **2001**. Microwave acceleration of the Pechmann reaction on graphite/montmorillonite K10: application to the preparation of 4-substituted 7-aminocoumarins. *Tetrahedron Letters*. 42(15):2791-2794.

Gadakh, S.K.; Dey, S.; Sudalai, A. **2015**. Rh-catalyzed synthesis of coumarin derivatives from phenolic acetates and acrylates via C-H Bond activation. *The Journal of Organic Chemistry*. 1-21.

Gao, W.; Li, Q.; Chen, J.; Wang, Z.; Hua, C. **2013**. Total synthesis of six 3,4-unsubstituted coumarins. *Molecules*. 18:15613-15623.

Garazd, M.M.; Garazd, Y.L.; Khilya, V.P. **2005**. Neoflavones. 2. Methods for synthesizing and modifying 4-aryl coumarins. *Chemistry of Natural Compounds*. 41:245-270.

Geppert, T.; Bauer, S.; Hiss, J.A.; Conrad, E.; Reutlinger, M.; Schneider, P.; Weisel, M.; Pfeiffer, B.; Altmann, K.; Waibler, Z.; Schneider, G. **2012**. Immunosuppressive Small Molecule Discovered by Structure-Based Virtual Screening for Inhibitors of Protein-Protein Interactions. *Angewandte Chemie International Edition*. 51: 258-261.

Ghani, U. **2015**. Re-exploring promising α -glucosidase inhibitors for potential development into oral anti-diabetic drugs: Finding needle in the haystack. *European Journal of Medicinal Chemistry*. 103: 133-162.

Ghiselli, A.; Serafini, M.; Maiani, G.; Azzini, E.; Ferro-Luzzi, A. **1995**. A fluorescence-based method for measuring total plasma antioxidant capability. *Free radical biology and medicine*. 18: 29-36.

Gliemann, J.; Osterlind, K.; Vinten, J.; Gammeltoft, S. **1972**. A procedure for measurement of distribution spaces in isolated fat cells. *Biochimica et Biophysica Acta*. 286: 1-9.

Goel, R.K.; Maiti, R.N.; Manickam, M.; Ray, A.B. **1997**. Antiulcer activity of naturally occurring pyrano-coumarin and isocoumarins and their effect on prostanoid synthesis using human colonic mucosa. *Indian Journal of Experimental Biology*. 35(10):1080-1083.

Gohlke, H.; Hendlich, M.; Klebe, G. **2000**. Knowledge-based Scoring Function to Predict Protein-Ligand Interactions. *Journal of Molecular Biology*. 295: 337-356.

Golfakhrabadi, F.; Abdollahi, M.; Ardakani, M.R.; Saeidnia, S.; Akbarzadeh, T.; Ahmadabadi, A.N.; Ebrahimi, A.; Yousefbeyk, F.; Hassanzadeh, A.; Khanayi, M. **2014**. Anticoagulant activity of isolated coumarins (suberosin and suberenol) and toxicity evaluation of *Ferulago carduchorum* in rats. *Pharmaceutical Biology*. 52(10):1335-1340.

Goswami, S.; Gupta, V.K.; Gupta, B.D.; Sivakumar, K. **2006**. Synthesis and crystal structure of 5,7-diallyloxy-4-methylcoumarin. *Journal of Chemical Crystallography*. 36(1):77-82.

Goth, A. **1945**. The antibacterial properties of dicoumarol. *Science*. 101:383.

Grazul, M.; Budzisz, E. **2009**. Biological activity of metal ions complexes of chromones, coumarins and flavones. *Co-ordination Chemistry Reviews*. 253: 2588-2598.

Guerreiro, L.R.; Carreiro, E.P.; Fernandes, L.; Cardote, T.A.F.; Moreira, R.; Caldeira, A.T.; Guedes, R.C.; Burke, A.J. **2013**. Five-membered iminocyclitol α -glucosidase inhibitors:

Synthetic, biological screening and in silico studies. *Bioorganic and Medicinal Chemistry*. 21:1911–1917.

Gupta, A.K.D.; Chatterje, R.M.; Das, K.R.; Green, B. **1969**. Coumarins and related compounds. Part IV. Aluminium chloride-catalysed reaction of phenols with methyl acrylate: a new approach to the synthesis of hydroxycoumarins. *Journal of the Chemical Society C*. 29-33.

Gupta, J.K.; Sharma, P.K.; Dudhe, R.; Mondal, S.C.; Chaudhary, A.; Verma, P.K. **2011**. Synthesis and analgesic activity of novel pyrimidine derivatives of coumarin moiety. *Acta Poloniae Pharmaceutica*. 68(5):785-793.

He, X.; Yan, Z.; Hu, X.; Zuo, Y.; Jiang, C.; Jin, L.; Shang, Y. **2014**. FeCl₃-catalyzed cascade reaction : An efficient approach to functionalized coumarin derivatives. *Synthetic communications: An international Journal for Rapid Communication of Synthetic organic chemistry*. 1-20.

Hitotsuyanagi, Y.; Kojima, H.; Ikuta, H.; Tokeya, K.; Itokawa, H. **1996**. Identification and structure-activity relationship studies of Osthol, A cytotoxic principle from *cnidium monnieri*. *Bioorganic and medicinal chemistry Letters*. 6: 1791-1794.

Hoesch, K. **1915**. A new synthesis of aromatic ketones.1. preparation of some phenolic ketone. *European Journal of Inorganic Chemistry*. 48(1):1122-1133.

Honda, M.; Hara, Y. **1993**. Inhibition of Rat Small Intestinal sucrase and α -Glucosidase Activities by Tea Polyphenols. *Bioscience, Biotechnology, and Biochemistry*. 57: 123-124.

Huang, S.; Zou, X. **2010**. Advances and challenges in Protein-Ligand Docking. *International Journal of Molecular Sciences*. 11: 3016-3034.

Hwu, J.R.; Singha, R.; Hong, S.C.; Chang, Y.H.; Das, A.R.; Vliegen, I.; Clercq, E.D.; Neyts, J. **2008**. Synthesis of new benzimidazole-coumarin conjugates as anti-hepatitis C virus agents. *Antiviral Research*. 77:157-162.

Imran, M.; Abida; Khan, S.A. **2015**. Synthesis and antimicrobial activity of some 2-Amino-4-(7-Substituted/Unsubstituted Coumarin-3-yl)-6-(Chlorosubstitutedphenyl) Pyrimidines. *Tropical Journal of Pharmaceutical Research*. 14(7):1265-1272.

International Diabetes Federation (IDF).**2014**. Global diabetes scorecard-tracking progress for action. Brussels: IDF.

Iqbal, P.F.; Bhat, A.R.; Azam, A. **2009**. Antiamoebic coumarins from the root bark of *Adina cordifolia* and their new thiosemicarbazone derivatives. *European Journal of Medicinal Chemistry*. 44(5):2252-2259.

Jain, M.; Surin, W.R.; Misra, A.; Prakash, P.; Singh, V.; Khanna, V.; Kumar, S.; Siddiqui, H.H.; Raj, K.; Barthwal, M.K.; Dikshit, M.**2013**. Antithrombotic activity of a newly synthesized coumarin derivative 3-(5-Hydroxy-2,2-dimethyl-chroman-6-yl)-N-{2-[3-(5-hydroxy-2,2-dimethyl-chroman-6-yl)-propionylamino]-ethyl}-propionamide.*Chemical Biology & Drug Design*. 81:499-508.

Jameel, E.; Umar, T.; Kumar, J.; Hoda, N. **2015**. Coumarin: A privileged scaffold for the design and development of antineurodegenerative agents. *Chemical biology and drug design*. 87(1):21-38.

Jiménez-Orozco, F.A.; Rosales, A.A.R.; Vega-López, A.; Domínguez-López, M.L.; García-Mondragon, M.J.; Maldonado-Espinoza, A.; Lemini, C.; Mendoza-Patiño, N.; Mandoki, J.J. **2011**. Differential effects of esculetin and daphnetin on in vitro cell proliferation and in vivo estrogenicity. *European Journal of Pharmacology*. 668:35-41.

Jones, J.E. **1924**. On the determination of molecular fields. II. From the equation of state of a gas. *Proceedings of the Royal Society A*. 106: 463-477.

Jorensen, W.L. **1991**. Rusting of the lock and key model for protein-ligand binding. *Science*. 24: 954-955.

Kabouche, A.; Kabouche, Z.; Öztürk, M.; Kolak, U.; Topcu, G. **2007**. Antioxidant abietane diterpenoids from saliva barrelieri. *Food Chemistry*. 102: 1281-1287.

Kalita, P.; Kumar,R. **2012**. Solvent-free coumarin synthesis via Pechmann reaction using solid catalysts. *Microporous and Mesoporous materials*. 149:1-9.

Kalkhambkar, R.G.; Kulkarni, G.M.; Kamanavalli, C.M.; Premkumar, N.; Asdaq, S.M.B.; Sun, C.M. **2008**. Synthesis and biological activities of some new fluorinated coumarins and 1-aza coumarins. *European Journal of Medicinal Chemistry*. 43(10): 2178-2188.

Kazeem, M.I.; Davies, T.C. **2016**. Anti-diabetic functional foods as sources of insulin secreting, insulin sensitizing and insulin mimetic agents. *Journal of functional foods*. 20: 122-138.

Khan, K.M.; Rahim, F.; Wadood, A.; Kosar, N.; Taha, M.; Lalani, S.; Khan, A.; Fakhri, M.I.; Junaid, M.; Rehman, W.; Khan, M.; Perveen, S.; Sajid, M.; Choudhary, M.I. **2014**. Synthesis and molecular docking studies of potent α -glucosidase inhibitors based on biscoumarin skeleton. *European Journal of Medicinal Chemistry*. 81: 245-252.

Khan, K.M.; Saify, Z.S.; Begum, S.; Noor, F.; Khan, M.Z.; Hayat, S.; Choudhary, M.I.; Perveen, S.; Attar-Ur-Rahman, Zia-Ullah. **2003**. Synthesis and biological screening of 7-hydroxy-4-methyl-2*H*-chromen-2-one, 7-hydroxy-4,5-dimethyl-2*H*-chromen-2-one and their some derivatives. *Natural Product Research*. 17(2):115-125.

Khodabakhshi, S. **2012**. Barium dichloride as a powerful and inexpensive catalyst for the Pechmann condensation without using solvent. *Organic Chemistry International*. 2012, Article I.D. 306162, 5 pages, <http://dx.doi.org/10.1155/2012/306162>.

Khoobi, M.; Emami, S.; Dehghan, G.; Foroumadi, A.; Ramazani, A.; Shafiee, A. **2011**. Synthesis and free radical scavenging activity of coumarin derivatives containing a 2-Methylbenzotiazoline motif. *Archiv der Pharmazie. Chemistry in Life Sciences*. 344:588-594.

Kikuzaki, H.; Usuguchi, J.; Nakatani, N. **1991**. Constituents of Zingiberaceae. I. Diarylheptanoids from the Rhizomes of Ginger (*Zingiber officinale* Roscoe). *Chemical and Pharmaceutical Bulletin*. 39: 120-122.

Kinnula, V.L., Crapo, J.D., **2004**. Superoxide dismutases in malignant cells and human tumors. *Free Radical Biology and Medicine*. 36: 718–744.

Kitchen, D.B.; Decornez, H.; Furr, J.R.; Bajorath, J. **2004**. Docking and scoring in virtual screening for drug discovery: methods and applications. *Nature reviews drug discovery*. 3: 935-949.

Knoevenagel, E. **1898**. Condensation of malonic acid with aromatiachen aldehydes by ammonia and amines. *Reports of the German Chemical Society*. 31(3):2596-2619.

Kontogiorgis, C.A.; Hadjipavlou-Litina, D.J. **2005**. Synthesis and anti-inflammatory activity of coumarin derivatives. *Journal of Medicinal Chemistry*. 48: 6400-6408.

Kooy, N.W.; Royall, J.A.; Ishchiropoulous, H.; Beckman, J.S. **1994**. Peroxynitrite-mediated oxidation of dihydrorhodamine 123. *Free radical biology and medicine*. 16: 149-156.

v. Kostanecki, St.; Rózycki, A. **1901**. About a mode of formation of chromonderivatens. *European Journal of inorganic chemistry*. 34(1): 102-109.

Kostova, I.; Bhatia, S.; Grigorov, P.; Balkansky, S.; Parmar, V.S.; Prasad, A.K.; Saso, L. **2011**. Coumarins as antioxidants. *Current Medicinal Chemistry*. 18:3929-3951.

Krishna, C.; Bhargavi, M.V.; Rao, C.P.; Krupadanam, G.L.D. **2015**. Synthesis and antimicrobial assessment of novel coumarins featuring 1,2,4-oxadiazole. *Medical Chemistry Research*. 24:3743-3751.

Kuehnle, H.F. **1996**. New therapeutic agents for the treatment of NIDDM. *Experimental and Clinical endocrinology and diabetes*. 104: 93-101.

Kumar, S.; Saini, A.; Sandhu, J.S. **2007**. LiBr-mediated, solvent free van Pechmann reaction: facile and efficient method for the synthesis of 2H-chromen-2-ones. *ARKIVOC*. (XV), 18-23.

Kumar, A.; Voet, A.; Zhang, K.Y.J. **2012**. Fragment Based drug design: From experimental to computational approaches. *Current Medicinal Chemistry*. 19:5128-5147.

Kumar, J.A.; Tiwari, A.K.; Ali, A.Z.; Rao, R.R.; Raju, B.C. **2011**. Synthesis and α -glucosidase inhibitory, DPPH scavenging activity of substituted 2-Oxo-2H-chromen-7-yl-dihydrogen Phosphate derivatives. *Journal of Heterocyclic Chemistry*. 48: 1251-1257.

Kunchandy, E.; Rao, M.N.A. **1990**. Oxygen radical scavenging activity of curcumin. *International Journal of Pharmaceutics*. 58: 237-240.

Kuntz, I.D.; Blaney, J.M.; Oatley, S.J.; Langridge, R.; Ferrin, T.E. **1982**. A Geometric Approach to Macromolecule-Ligand Interactions. *Journal of Molecular Biology*. 161: 269-288.

Lacy, A.; O'Kennedy, R. **2004**. Studies on coumarins and coumarin-related compounds to determine their therapeutic role in the treatment of cancer. *Current Pharmaceutical Design*. 10:3797-3811.

Lanoot, B.; Vancanneyt, M.; Cleenwerck, I.; Wang, L.; Li, W.; Liu, Z.; Swings, J. **2002**. The search for synonyms among streptomycetes by using SDS-PAGE of whole-cell proteins. Emendation of the species *Streptomyces aurantiacus*, *Streptomyces cacaoi* subsp. *cacaoi*,

Streptomyces caeruleus and *Streptomyces violaceus*. *International Journal of systematic and evolutionary Microbiology*. 52:823-829.

Laufer, M.C.; Hausmann, H.; Hölderich, W.F. **2003**. Synthesis of 7-hydroxycoumarins by Pechmann reaction using nafion resins/silica nanocomposites as catalysts. *Journal of catalysis*. 218(2):315-320.

Laurie, A.T.R.; Jackson, R.M. **2005**. Q-SiteFinder: an energy-based method for the prediction of protein-ligand binding sites. *Bioinformatics*. 21: 1908-1916.

Leal, L.K.; Ferreira, A.A.; Bezerra, G.A.; Matos, F.J.; Viana, G.S. **2000**. Antinociceptive, anti-inflammatory and bronchodilator activities of Brazilian medicinal plants containing coumarin: a comparative study. *Journal of Ethnopharmacology*. 70(2):151-159.

Lee, S.O.; Choi, S.Z.; Lee, J.H.; Chung, S.H.; Park, S.H.; Kang, H.C.; Yang, E.Y.; Cho, H.J.; Lee, K.R. **2004**. Antidiabetic coumarin and cyclitol compounds from *Peucedanum japonicum*. *Archives of Pharmacal Research*. 27(12):1207-1210.

Lee, Y.Y.; Lee, S.; Jin, J.L.; Yun-Choi, H.S. **2003**. Platelet anti-aggregatory effects of coumarins from the roots of *Angelica genuflexa* and *A.gigas*. *Archives of Pharmacal Research*. 26(9):723-726.

Lengauer, T.; Rarey, M. **1996**. Computational methods for biomolecular docking. *Current opinion in Structural Biology*. 6: 402-406.

Lévai, A.; Jekö, J. **2005**. An efficient procedure for the preparation of 4-methyl-2-thiocoumarins by the reaction of 4-methylcoumarins with Lawesson's Reagent. *Journal of Heterocyclic Chemistry*. 42:739-742.

Levinthal, C.; Wodak, S.J.; Kahn, P.; Dadivanian, A.K. **1975**. Hemoglobin Interaction in Sickle Cell Fibers. 1. Theoretical Approaches to the Molecular Contacts. *Proceedings of the National Academy of Science of the United States of America*. 72: 1330-1334.

Li, Y.; Wang, C.; Ye, M.; Yao, G.; Wang, H. **2015**. Novel Coumarin –Containing Aminophosphonates as Antitumor Agent: Synthesis, Cytotoxicity, DNA-Binding and Apoptosis Evaluation. *Molecules*. 20: 14791-14809.

Li, Z.; Pan, M.; Su, X.; Dai, Y.; Fu, M.; Cai, X.; Shi, W.; Huang, W.; Qian, H. **2016**. Discovery of Novel Pyrrole-Based Scaffold as Potent and Orally Bioavailable Free Fatty acid Receptor 1

Agonists for the treatment of Type 2 diabetes. *Bioorganic and Medicinal Chemistry*. DOI: <http://dx.doi.org/10.1016/j.bmc.2016.03.014>.

Li, Z.; Qiu, Q.; Xu, X.; Wang, X.; Jiao, L.; Su, X.; Pan, M.; Huang, W.; Qian, H. **2016**. Design, Synthesis and structure-activity relationship studies of New Thiazole-Based Free fatty acid receptor 1 Agonists for the treatment of Type 2 diabetes. *European Journal of Medicinal Chemistry*. DOI:10.1016/j.ejmech.2016.02.040.

Lima, C.R.; Vasconcelos, C.F.B.; Costa-Silva, J.H.; Maranhão, C.A.; Costa, J.; Batista, T.M.; Carneiro, E.M.; Soares, L.A.L.; Ferreira, F.; Wanderley, A.G. **2012**. Anti-diabetic activity of extract from *Persea americana* Mill. leaf via the activation of protein kinase B (PκB/Aκt) in streptozotocin-induced diabetic rats. *Journal of Ethnopharmacology*. 141(1):517-525.

Link, K.P. **1959**. The discovery of dicumarol and its sequels. *Circulation*. 19(1):97-107.

Liu, X.S.; Brutlag, D.L.; Liu, J.S. **2002**. An algorithm for finding protein-DNA binding sites with applications to chromatin-immunoprecipitation microarray experiments. *Nature biotechnology*. 20: 835-839.

Mamun-or-Rashid, A.N.M.; Hossain, S Md.; Hassan, N.; Dash, B.K.; Sapon, A Md.; Sen, M.K. **2014**. A review on medicinal plants with antidiabetic activity. *Journal of Pharmacognosy and Phytochemistry*. 3(4):149-159.

Mandhane, P.G.; Joshi, R.S.; Ghawalkar, A.R.; Jadhay, G.R.; Gill, C.H. **2009**. Ammonium Metavanadate: A Mild and efficient catalyst for the synthesis of coumarins. *Bulletin of the Korean Chemical Society*. 30(12):2969-2972.

Manhas, M.S.; Ganguly, S.N.; Mukherjee, S.; Jain, A.K.; Bose, A.K. **2006**. Microwave initiated reactions: Pechmann coumarin synthesis, Biginelli reaction, and acylation. *Tetrahedron Letters*. 47:2423-2425.

Manzocco, L.; Nicoli, M.C.; Anese, M. **1998**. Antioxidant properties of tea extracts as affected by processing. *Lebens-mittel-Wissen-schaft Und-Technolgie*. 31: 694-698.

Marcocci, L.; Maguire, J.J.; Droy-Lefaix, M.T.; Packer, L. **1994**. The nitric oxide-scavenging properties of Ginkgo Biloba Extract EGb 761. *Biochemical and Biophysical research communications*. 201: 748-755.

Màrquez, N.; Sancho, R.; Bedoya, L.M.; Alcamí, J.; López-Pérez, J.L.; Feliciano, A.S.; Fiebich, B.L.; Munoz, E. **2005**. Mesuol, a natural occurring 4-phenylcoumarin, inhibits HIV-1 replication by targeting the NF- κ B pathway. *Antiviral research*. 66:137-145.

Mashraqui, S.H.; Vashi, D.; Mistry, H.D. **2004**. Efficient synthesis of 3-substituted coumarins. *Synthetic communications*. 34:3129-3134.

Masuda, K.; Okamoto, Y.; Tsuura, Y.; Kato, S.; Miura, T.; Horikoshi, H.; Ishida, H.; Seino, Y. **1995**. Effects of Troglitazone (CS-045) on insulin secretion in isolated rat pancreatic islets and HIT cells: an insulintropic mechanism distinct from glibenclamide. *Diabetologia*. 38: 24-30.

Matos, M.J.; Vazquez-Rodriguez, S.; Fuentes-Edfuf, C.; Santos, Y.; Muñoz-Crego, A.; Uriarte, E.; Santana, L. **2012**. Synthesis of novel amino/ nitro substituted 3-arylcoumarins as antibacterial agents. <http://www.usc.es/congresos/ecsoc/>

McCord, J.M.; Fridovich, I. **1969**. Superoxide dismutase, an enzymic function for erythrocytes. *The Journal of biological chemistry*. 244(22):6049-6055.

Medimagh-Saidana, S.; Romdhane, A.; Daami-Remadi, M.; Jabnoun-Khiareddine, H.; Touboul, D.; Jannet, H.B.; Hamza, M. A. **2015**. Synthesis and antimicrobial activity of novel coumarin derivatives from 4-methylumbelliferone. *Medicinal Chemistry Research*. 24: 3247-3257.

Miglietta, A.; Bocca, C.; Gabriel, L.; Rampa, A.; Bisi, A.; Valenti, P. **2001**. Antimicrotubular and cytotoxic activity of geiparvarin analogues, alone and in combination with paclitaxel. *Cell Biochemistry and Function*. 19(3): 181-189.

Miller III, B.R.; Roitberg, A.E. **2013**. Trypanosoma cruzi trans-sialidase as a drug target against Chagas disease (American trypanosomiasis). *Future Medicinal Chemistry*. 5: 1889-1900.

Momin, M.; Ramjugernath, D.; Koorbanally, N.A. **2014**. Structure elucidation of a series of fluoro-2-styrylchromones and methoxy- 2-styrylchromones using 1D and 2D NMR spectroscopy. *Magnetic Resonance in Chemistry*. 52: 521-529.

Morgenthaler, M.; Schweizer, E.; Hoffmann-Röder, A.; Benini, F.; Martin, R.E.; Jaeschke, G.; Wagner, B.; Fischer, H.; Bendels, S.; Zimmerli, D.; Schneider, J.; Diedrich, F.; Kansy, M.; Müller, K. **2007**. Predicting and tuning Physicochemical properties in lead optimization: Amine Basicities. *ChemMedChem*. 2(8):1100-1115.

Morris, G.M.; Goodsell, D.S.; Halliday, R.S.; Huey, R.; Hart, W.E.; Belew, R.K.; Olson, A.J. **1998**. Automated Docking using a Lamarckian genetic algorithm and an empirical binding free energy function. *Journal of Computational Chemistry*. 19: 1639-1662.

Muegge, I.; Martin, Y.C. **1999**. A general and fast scoring function for Protein-Ligand Interactions: A Simplified Potential Approach. *Journal of Medicinal Chemistry*. 42: 791-804.

Müller, G.; Wied, S. **1993**. The sulfonyl urea drug, glimepiride, stimulates glucose transport, glucose transporter translocation, and dephosphorylation in insulin-resistant rat adipocytes in vitro. *Diabetes*. 42: 1852-1867.

Müller, K.; Faeh, C.; Diederich, F. **2007**. Fluorine in pharmaceuticals: Looking beyond intuition. *SCIENCE*. 317:1881-1886.

Murakami, A.; Kuki, W.; Takahashi, Y.; Yonci, H.; Nakamura, Y.; Ohto, Y.; Ohigashi, H.; Koshimizu, K. **1997**. Auraptene, a citrus coumarin, inhibits 12-O-Tetradecanoylphorbol-13-acetate-induced tumor promotion in ICR mouse skin, possibly through suppression of superoxide generation in leukocytes. *Japanese Journal of Cancer Research*. 88:443-452.

Naik, B.; Desai, K.R. **2006**. Novel approach for rapid and efficient synthesis of heterocyclic Schiff bases and azetidiones under microwave irradiation. *Indian Journal of Chemistry*. 45(B):267-271.

Nair, R.V.; Fisher, E.P.; Safe, S.H.; Cortez, C.; Harvey, R.G.; Di Giovanni, J. **1991**. Novel coumarins as potential anticarcinogenic agents. *Carcinogenesis*. 12(1): 65-69.

Nakai, K.; Kurahashi, T.; Matsubara, S. **2015**. Nickel-catalyzed dual C–C σ bond activation to construct carbocyclic skeletons. *Tetrahedron*. DOI:10.1016/j.tet.2015.02.064.

Nazemi, A.H.; Asadi, G.A.; Ghorbani, R. **2015**. Herbicidal activity of coumarin when applied as a pre-plant incorporated into soil. *Notulae Scientia Biologicae*. 7(2):239-243.

Neelgundmath, M.; Dinesh, K.R.; Mohan, C. D.; Li, F.; Dai, X.; Siveen, K.S.; Paricharak, S.; Mason, D.J.; Fuchs, J.E.; Sethi, G.; Bender, A.; Rangappa, K.S.; Kotresh, O.; Basappa. **2015**. Novel Synthetic coumarins that targets NF- κ B in Hepatocellular carcinoma. *Bioorganic and Medicinal Chemistry Letters*. 25:893-897.

Nesmeyanov, A.N.; Vompe, A.F.; Zarevich, T.S.; Smolin, D.D. **1937**. Syntheses in the series of 7-hydroxycoumarin derivatives. *Zhurnal Obshchei Khimii*. 7:2767-2773.

Neuvirth, H.; Raz, R.; Schreiber, G. **2004**. ProMate: A structure Based Prediction Program to Identify the location of Protein-Protein Binding Sites. *Journal of Molecular Biology*. 338: 181-199.

Nguyen, P.; Zhao, B.T.; Kim, O.; Lee, J.H.; Choi, J.S.; Min, B.S.; Woo, M.H. **2016**. Anti-inflammatory terpenylated coumarins from the leaves of *Zanoxylum schinifolium* with α -glucosidase inhibitory activity. *Journal of Natural Medicines*. 70: 276-281.

Nikolaeva, O.G.; Karlutova, O.Y.; Cheprasov, A.S.; Metelitsa, A.V.; Dorogan, I.V.; Dubonosov, A.D.; Bren, V.A. **2015**. Synthesis of bis-spiroprans based on 6,8-diformyl-5,7-dihydroxy-4-methylcoumarin and photochromic properties thereof. *Chemistry of Heterocyclic Compounds*. 51:229-233.

Noro, T.; Oda, Y.; Miyase, T.; Ueno, A.; Fukushima, S. **1983**. Inhibitors of Xanthine Oxidase from the flowers and buds of *Daphne genkwa*. *Chemical and Pharmacological Bulletin*. 31: 3984-3987.

Ohkawa, H.; Ohishi, N.; Yagi, K. **1979**. Assay for lipid peroxides in animal tissues by thiobarbituric acid reaction. *Analytical Biochemistry*. 95(2):351-358.

Olsen, J.A.; Banner, D.W.; Seiler, P.; Obst Sander, U.; D'Arcy, A.; Stihle, M.; Müller, K.; Diederich, F. **2003**. A fluorine scan of thrombin inhibitors to map the fluorophilicity/fluorophobicity of an enzyme active site: evidence for C-F....C=O interactions. *Angewandte Chemie International Edition*. 42(22): 2507-2511.

Osborne, A.G. **1989**. ¹³C NMR spectral studies of some methoxycoumarin derivatives. A Re-assignment for Citropten (Limettin) and an examination of peri-proximity effects for the methyl-methoxy and methoxy-methyl couples. *Magnetic Resonance in Chemistry*. 27:348-354.

Ottolenghi, A. **1959**. Interaction of ascorbic acid and mitochondrial lipides. *Archives of biochemistry and biophysics*. 79: 355-363.

Ou, B.; Huang, D.; Hampsch-Woodili, M.; Flanagan, J.A.; Deemer, E.K. **2002**. Analysis of antioxidant activities of common vegetables employing oxygen radical absorbance capacity (ORAC) and ferric reducing antioxidant power (FRAP) Assays: A comparative study. *Journal of agricultural and food chemistry*. 50: 3122-3128.

Ou, S.; Kwok, K.; Li, Y.; Fu, L. **2001**. In Vitro Study of possible role of dietary fiber in lowering postprandial serum glucose. *Journal of Agricultural and Food Chemistry*. 49: 1026-1029.

Oxford Handbook of Infectious Diseases and Microbiology. OUP Oxford. **2009**. p. 56. ISBN 9780191039621.

Pan, L.; Li, X.; Yan, Z.; Guo, H.; Qin, B. **2015**. Phytotoxicity of umbelliferone and its analogs: Structure-activity relationships and action mechanisms. *Plant Physiology and Biochemistry*. 97: 272-277.

Park, B.K.; Kitteringham, N.R.; O'Neill, P.M. **2001**. Metabolism of fluorine-containing drugs. *Annual review of pharmacology and toxicology*. 41:443-470.

Park, S.; Kubota, Y.; Funabiki, K.; Matsui, M. **2009**. Survey of liquid coumarin dyes and their fluorescence properties. *Chemistry Letters*. 38(2):162-163.

Patil, S.A.; Prabhakara, C.T.; Halasangi, B.M.; Toragalmath, S.S.; Badami, P.S. **2015**. DNA cleavage, antibacterial, antifungal and anthelmintic studies of Co(II), Ni(II) and Cu(II) complexes of coumarin schiff bases: Synthesis and spectral approach. *Spectrochimica Acta Part A: Molecular and Biomolecular spectroscopy*. 137:641-657.

Paulini, R.; Müller, K.; Diederich, F. **2005**. Orthogonal multipolar interactions in structural chemistry and biology. *Angewandte Chemie International Edition*. 44(12): 1788-1805.

Pechmann, H.V. **1884**. New education, the coumarins. Synthesis of Daphnetins.I. *Reports of the German Chemical Society*. 17(1):929-936.

Pedersen, J.Z.; Oliveira, C.; Incerpi, S.; Kumar, V.; Fiore, A.M.; Vito, P.D.; Prasad, A.K.; Malhotra, S.V.; Parmar, V.S.; Saso, L. **2007**. Antioxidant activity of 4-methylcoumarins. *Journal of Pharmacy and Pharmacology*. 59:1721-1728.

Peng, X.; Damu, G.L.V.; Zhou, C. **2013**. Current developments of coumarin compounds in medicinal chemistry. *Current Pharmaceutical Design*. 19:3884-3930.

Pérez, M.; García, M.; Ruiz, D.; Autino, J.C.; Romanelli, G.; Blustein, G. **2016**. Antifouling activity of green-synthesized 7-hydroxy-4-methylcoumarin. *Marine Environmental Research*. 113: 134-140.

Perkin, W.H. **1868**. On the artificial production of coumarin and formation of its homologues. 53-63. <http://pubs.rsc.org/doi:10.1039/JS8682100053>.

Phadtare, S.B.; Jarag, K.J.; Shankarling, G.S. **2013**. Greener protocol for one pot synthesis of coumarin styryl dyes. *Dyes and Pigments*. 97:105-112.

Plewczynski, D.; Łaźniewski, M.; Augustyniak, R.; Ginalski, K. **2011**. Can we trust docking Results? Evaluation of seven commonly used programs on PDBbind Database. *Journal of Computational Chemistry*. 32: 742-755.

Ponndorf, W. **1925**. The reversible exchange of the oxidation stages between aldehydes or ketones on the one hand and primary or secondary alcohols on other hand. *Journal of Applied Chemistry*. 38(201):138-143.

Prieto, P.; Pineda, M.; Aguilar, M. **1999**. Spectrophotometric quantitation of antioxidant capacity through the formation of a phosphomolybdenum complex: Specific application to the determination of Vitamin E. *Analytical Biochemistry*. 269: 337-341.

Prior, R.L.; Hoang, H.; Gu, L.; Wu, X.; Bacchiocca, M.; Howard, L.; Hampsch-Woodili, M.; Huang, D.; Ou, B.; Jacob, R. **2003**. Assays for hydrophilic and lipophilic antioxidant capacity (oxygen radical absorbance capacity (ORAC_{FL})) of plasma and other biological and food samples. *Journal of agricultural and food chemistry*. 51: 3273-3279.

Prousis, K.C.; Avlonitis, N.; Heropoulos, G.A.; Calogeropoulou, T. **2014**. FeCl₃-catalysed ultrasonic-assisted, solvent-free synthesis of 4-substituted coumarins. A useful complement to the Pechmann reaction. *Ultrasonics Sonochemistry*. 21:937-942.

Pu, W.; Lin, Y.; Zhang, J.; Wang, F.; Wang, C.; Zhang, G. **2014**. 3-Arylcoumarins: Synthesis and potent anti-inflammatory activity. *Bioorganic and Medicinal Letters*. 24:5432-5434.

Rajabi F.; Feiz, A.; Luque, R. **2015**. An efficient synthesis of coumarin derivatives using a SBA-15 supported Cobalt (II) Nanocatalyst. *Catalysis Letters*. 145: 1621-1625.

Quezada, E.; Delogu, G.; Picciau, C.; Santana, L.; Podda, G.; Borges, F.; Garcia-Morales, V.; Viña, D.; Orallo, F. **2010**. Synthesis and vasorelaxant and platelet antiaggregatory activities of a new series of 6-Halo-3-phenylcoumarins. *Molecules*. 15:270-279.

Raghavendra, P.; Veena, G.; Kumar, G.A.; Kumar, E.R.; Sangeetha, N.; Sirivennela, B.; Smarani, S.; Kumar, H.P.; Suthakaran, R. **2011**. Microwave synthesis and anti-inflammatory

evaluation of some new imidazole quinolone analogs. *Rasayan Journal of Chemistry*. 4(1):91-102.

Razavi, S.F.; Khoobi, M.; Nadri, H.; Sakhteman, A.; Moradi, A.; Emami, S.; Foroumadi, A.; Shafiee, A. **2013**. Synthesis and evaluation of 4-substituted coumarins as novel acetylcholinesterase inhibitors. *European Journal of Medicinal Chemistry*. 64: 252-259.

Reformatsky, S. **1954**. New synthetic diatomic monobasic acids from the ketones. *European journal of inorganic chemistry*. 20(1):1210-1211.

Riris, I.D. **2014**. Identification of chemistry bioactivity structure of A-glucosidase inhibitor from ethanol extract of the stem bark Raru(*Vatica Pauciflora* Blume). *Journal of Applied Chemistry*. 7: 35-40.

Robak, J.; Gryglewski, R.J. **1988**. Flavonoids scavengers of superoxide anions. *Biochemical Pharmacology*. 37: 837-841.

Robertson, A.; Waters, R.B.; Jones, E.T. **1932**. Hydroxycarbonyl compounds: VII. Coumarins and 1,4-benzopyrones derived from m-cresol. *Journal of the chemical society*. 1681-1688.

Rodriguez-Domínguez, J.C.; Kirsch, G. **2006**. Sulfated zirconia, a mild alternative to mineral acids in the synthesis of hydroxycoumarins. *Tetrahedron Letters*. 47(19):3279-3281.

Roth, B.D.; Ortwine, D.F.; Hoefle, M.F.; Stratton, C.D.; Sliskovic, D.R.; Wilson, M.W.; Newton, R.S. **1990**. Inhibitors of cholesterol biosynthesis.1. trans-6-(2-Pyrrol-1-ylethyl)-4-hydroxypyran-2-ones, a novel series of HMG-CoA reductase inhibitors.1. Effects of structural modifications at the 2- and 5-positions of the pyrrole nucleus. *Journal of Medicinal Chemistry*.33(1):21-31.

Ruch, R.J.; Cheng, S.; Klaunig, J.E. **1989**. Prevention of cytotoxicity and inhibition of intercellular communication by antioxidant catechins isolated from Chinese green tea. *Carcinogenesis*. 10: 1003-1008.

Sabou, R.; Hoelderich W.F.; Ramprasad, D.; Weinand, R. **2005**. Synthesis of 7-hydroxy-4-methylcoumarin via the Pechmann reaction with Amberlyst ion-exchange resins as catalysts. *Journal of catalysis*. 232(1):34-37.

Sahoo, S.S.; Shukla, S.; Nandy, S.; Sahoo, H.B. **2012**. Synthesis of novel coumarin derivatives and its biological evaluations. *European Journal of experimental Biology*. 2:899-908.

Saleh, A.M.; Madany, M.M.Y. **2015**. Coumarin pre-treatment alleviates salinity stress in wheat seedlings. *Plant Physiology and Biochemistry*. 88:27-35.

Salemme, F.R. **1976**. An hypothetical structure for an Intermolecular Electron transfer Complex of Cytochromes c and b₅. *Journal of molecular biology*. 102: 563-568.

Sandhya, B.; Mathew, V.; Lohitha, P.; Ashwini, T.; Shravani, A.A.; Reddy, B.M.; Rangaraju, G. **2010**. Synthesis characterization and pharmacological activities of coumarin derivatives. *International Journal of Chemical and Pharmaceutical sciences*. 1(1):16-25.

Santerre, R.F.; Cook, R.A.; Crisel, R.M.D.; Sharp, J.D.; Schmidt, R.J.; Williams, D.C.; Wilson, C.P. **1981**. Insulin synthesis in a clonal cell line of simian virus 40-transformed hamster pancreatic beta cells. *Proceedings of the national academy of science of the United States of America*. 78: 4339-4343.

Sardari, S.; Mori, Y.; Morita, K.; Micetich, R.G.; Nishibe, S.; Daneshtalab, M. **1999**. Synthesis and antifungal activity of coumarins and angular furanocoumarins. *Bioorganic and medicinal Chemistry*. 7: 1933-1940.

Sashidhara, K.V.; Kumar, A.; Chatterjee, M.; Rao, K.B.; Singh, S.; Verma, A.K.; Palit, G. **2011**. Discovery and synthesis of novel 3-phenylcoumarin derivatives as antidepressants agents. *Bioorganic and Medicinal Chemistry Letters*. 21: 1937-1941.

Sashidhara, K.V.; Modukuri, R.K.; Choudhary, D.; Bhaskara Rao, K.; Kumar, M.; Khedgikar, V.; Trivedi, R. **2013**. Synthesis and evaluation of new coumarin-pyridine hybrids with promising anti-osteoporotic activities. *European Journal of Medicinal Chemistry*. 70:802-810.

Sashidhara, K.V.; Modukuri, R.K.; Singh, S.; Rao, K.B.; Teja, G.A.; Gupta, S.; Shukla, S. **2015**. Design and synthesis of new series of coumarin-aminopyran derivatives possessing potential anti-depressant-like activity. *Bioorganic and Medicinal Chemistry Letters*. 25: 337-341.

Schönberg, A.; Latif, N. **1954**. Furochromones and coumarins.XI. The molluscicidal activity of bergapten, isopimpinillin and xanthotoxin. *Journal of the American Chemical Society*. 76(23):6208.

Scott, L.; Spencer, C.; **2000**. Miglitol: a review of its therapeutic potential in type 2 diabetes mellitus. *Drugs*. 59: 521–549.

Seeram, N.P.; Henning, S.M.; Niu, Y.; Lee, R.; Scheulier, H.S.; Heber, D. **2006**. Catechin and caffeine content of green tea dietary supplements and correlation with antioxidant capacity. *Journal of agricultural and food chemistry*. 54: 1599-1603.

Shai, L.J.; Masoko, P.; Mokgotho, M.P.; Magano, S.R.; Mogale, A.M.; Boaduo, N.; Eloff, J.N. **2010**. Yeast alpha glucosidase inhibitory and antioxidant activities of six medicinal plants collected in Phalaborwa, South Africa. *South African Journal of Botany*. 76: 465–470. DOI: 10.1016/j.sajb.2010.03.002

Shen, Q.; Shao, J.; Peng, Q.; Zhang, W.; Ma, L.; Chan, A.S.C.; Gu, L. **2010**. Hydroxycoumarin derivatives: Novel and potent α -Glucosidase inhibitors. *Journal of Medicinal Chemistry*. 53: 8252-8259.

Sing, P.R.; Singh, D.U.; Samant, S.D. **2004**. Sulphamic acid-An efficient and cost effective solid acid catalyst for the Pechmann Reaction. *Synlett*. 11:1909-1912.

Singal, P.K.; Kapur, N.; Dhillon, K.S.; Beamish, R.E.; Dhalla, N.S. **1982**. Role of free radicals in catecholamine-induced cardiomyopathy. *Canadian Journal of Physiology and Pharmacology*. 60(11):1390-1397.

Singh, L.V.; Priyanka; Singh, V.; Katiyar, D. **2015**. Design, Synthesis and biological evaluation of some new coumarin derivatives as potential antimicrobial agents. *Medicinal Chemistry*. 11:128-134.

Singh, T.; Biswas, D.; Jayaram, B. **2011**. AADS-An Automated Active Site Identification, Docking, and Scoring Protocol for Protein Targets Based on Physicochemical Descriptors. *Journal of chemical information and modelling*. 51: 2515-2527.

Smart, B.E. **2001**. Fluorine substituent effects (on bioactivity). *Journal of Fluorine Chemistry*. 109(1):3-11.

Smart, B.E. in *Organofluorine Chemistry. Principles and commercial applications*. Banks, B.E.; Smart, B.E.; Tatlow, J.C. ed; Plenum Press; New York; **1994**, 57-88.

Smitha, G.; Reddy, S. Ch. **2004**. ZrCl₄-catalyzed Pechmann Reaction: Synthesis of coumarins under solvent-free conditions. *Synthetic communications*. 34(21):3997-4003.

Suzuki, A. **1991**. Synthetic studies via the cross-coupling reaction of organoboron derivatives with organic halides. *Pure and applied chemistry*. 63(3):419-422.

Taha, M.; Ismail, N.H.; Javaid, K.; Imran, S.; Anouar, E.H.; Wadood, A.; Wahab, A.; Ali, M.; Khan, K.M.; Saad, S.M.; Rahim, F.; Choudary, M.I. **2015**. Evaluation of 2-indolcarbohydrazones as potent α -glucosidase inhibitors in silico studies and DFT based stereochemical predictions. *Bioorganic Chemistry*. 63: 24-35.

Tahanpesar, E.; Sarami, L. **2015**. Synthesis of substituted coumarins catalysed by sawdust-SO₃H. An efficient and environmentally benign solid acid catalyst under solvent-free conditions. *Russian Journal of General Chemistry*. 85: 2135-2140.

Thorat, K.; Patil, L.; Limaye, D.; Kadam, V. **2012**. Invitro models for antidiabetic activity assessment. *International Journal of Research in Pharmaceutical and biomedical Sciences*. 3: 730-733.

Tietze, L.F. **1996**. Domino reactions in organic synthesis. *Chemical Reviews*.96:115-136.

Tuba, A.K.; Gulcin, I. **2008**. Antioxidant and radical scavenging properties of curcumin, *Chemico-Biological Interactions*. 174: 27–37. DOI: 10.1016/j.cbi.2008.05.003.

Tundis, R.; Loizzo, M.R.; Menichini, F. **2010**. Natural products as alpha-amylase and alpha-glucosidase inhibitors and their hypoglycaemic potential in the treatment of diabetes: an update. *Mini - Reviews in Medicinal Chemistry*. 10(4): 315-331.

Tyagi, B.; Mishra, M.K.; Jasra, R.V. **2007**. Synthesis of 7-substituted 4-methyl coumarins by Pechmann reaction using nano-crystalline sulfated-zirconia. *Journal of Molecular Catalysis A: Chemical*. 276:47-56.

Valizadeh, H.; Shockravi, A. **2005**. An efficient procedure for the synthesis of coumarin derivatives using TiCl₄ as catalyst under solvent-free conditions. *Tetrahedron Letters*. 46:3501-3503.

Valkov, E.; Sharpe, T.; Marsh, M.; Greive, S.; Hyvönen, M. **2012**. Targeting Protein-Protein Interactions and Fragment-Based Drug Discovery. *Top current chemistry*. 317: 145-180.

van Niel, M.B.; Collins, I.; Beer, M.S.; Broughton, H.B.; Cheng, S.K.F.; Goodacre, S.C.; Heald, A.; Locker, K.L.; MacLeod, A.M.; Morrison, D.; Moyes, C.R.; O'Connor, D.; Pike, A.; Rowley, M.; Russell, M.G.N.; Sohal, B.; Stanton, J.A.; Thomas, S.; Verrier, H.; Watt, A.P.; Castro, J.L. **1999**. Fluorination of 3-(3-(Piperidin-1-yl)propyl) indoles and 3-(3-(Piperazin-1-

yl)propyl) indoles Gives selective Human 5-HT_{1D} receptor ligands with improved pharmacokinetic profiles. *Journal of Medicinal Chemistry*. 42(12): 2087-2104.

Verdia, P.; Santamarta, F.; Tojo, E. **2011**. Knoevenagel Reaction in [MMIm][MSO₄]: Synthesis of coumarins. *Molecules*. 16:4379-4388.

Verdonk, M.L.; Cole, J.C.; Hartshorn, M.J.; Murray, C.W.; Taylor, R.D. **2003**. Improved Protein-Ligand Docking Using GOLD. *PROTEINS: Structure, Function, and Genetics*. 52: 609-623.

Vianna, D.R.; Ruschel, L.; Dietrich, F.; Figueiró, F.; Morrone, F.B.; Canto, R.F.S.; Corrello, F.; Velho, A.; Crestani, A.; Teixeira, H.; von Poser, G.L.; Battastini, A.M.O.; Eifler-Lima, V.L. **2015**. 4-Methylcoumarins with Cytotoxic activity against T24 and RT4 human bladder cancer cell lines. *Medicinal Chemistry Communications*. 6: 905-911.

Vilsmeier, A.; Haack A. **1927**. About the action of halogen phosphorus to alkyl formanilides. A new method for the preparation of secondary and tertiary p-alkylamino-benzaldehyde. *European Journal of Inorganic Chemistry*. 60(1):119-122.

Virsoia, V.; Shaikh, M.S.; Manvar, A.; Desai, B.; Parecha, A.; Loriya, R.; Dholariya, K.; Patel, G.; Vora, V.; Upadhyay, K.; Denish, K.; Shah, A.; Coutinho, E.C. **2010**. Screening for in vitro antimycobacterial activity and three-dimensional quantitative structure-activity relationship (3D-QSAR) study of 4-(arylamino) coumarin derivatives. *Chemical Biology and Drug design*. 76(5): 412-424.

Vogel, A. **1820**. Preparation of benzoic acid from the tonka bean and from the Meliloten or stone clover – flowers. *Annals of Physics*. 64(2):161-166.

Wadsworth J.r., W.S.; Emmons, W.D. **1961**. The utility of phosphonate carbanions in olefin synthesis. *Journal of the American Chemical Society*. 83(7):1733-1738.

Walsh, T.J.; Standiford, H.C.; Reboli, A.C.; John, J.F.; Mulligan, M.E.; Ribner, B.S.; Montgomerie, J.Z.; Goetz, M.B.; Mayhall, C.G.; Rimland, D. **1993**. Randomized double-blinded trial of rifampin with either novobiocin or trimethoprim-sulfamethoxazole against methicillin-resistant *Staphylococcus aureus* colonization: prevention of antimicrobial resistance and effect of host factors on outcome. *Antimicrobial agents and Chemotherapy*. 37(6):1334-1342.

- Wang, G.; He, D.; Li, X.; Li, J.; Peng, Z. **2016**. Design, synthesis and biological evaluation of novel coumarin thiazole derivatives as α -glucosidase inhibitors. *Bioorganic Chemistry*. 65: 167-174.
- Wang, S.; Tang, F.; Yue, Y.; Yao, X.; Wei, Q.; Yu, J. **2013**. Simultaneous determination of 12 coumarins in Bamboo leaves by HPLC. *Journal of AOAC International*. 96:942-947.
- Wodak, S.J.; Janin, J. **1978**. Computer Analysis of Protein-Protein Interaction. *Journal of Molecular Biology*. 124: 323-342.
- Wittig, G.; Schöllkopf, U. **1954**. About triphenylphosphine-methylene as olefin-forming reagents (1.mgs.). *European journal of inorganic chemistry*. 87(9):1318-1330.
- Wong, D.T.; Bymaster, F.P.; Engleman, E.A. **1995**. Prozac (Fluoxetine, Lilly 110140), The first selective serotonin uptake inhibitor and an antidepressant drug: Twenty years since its first publication. *Life Sciences*. 57(5):411-441.
- Wood, J.L. **1970**. In: Fishman, W.H. (Ed),. In: Metabolic conjugation and metabolic hydrolysis, vol. II. Academic Press, New York, 61-299.
- Woods, L.L.; Sapp, J. **1962**. A new one-step synthesis of substituted coumarins. *Journal of Organic Chemistry*. 27(10): 3703-3705.
- Wu, G.; Robertson, D. H.; Brooks, C. L. III; Vieth, M. **2003**. Detailed Analysis of Grid-Based Molecular Docking: A Case Study of CDOCKER - A CHARMM-Based MD Docking Algorithm. *Journal of Computational Chemistry*. 24 (13): 1549-1562.
- Xu, W.; Qi, D.; You, J.; Hu, F.; Bian, J.; Yang, C.; Huang, J. **2015**. Coumarin-based 'turn-off' fluorescent chemosensor with high selectivity for Cu^{2+} in aqueous solution. *Journal of Molecular Structure*. 1091: 133-137.
- Yamamoto, K.; Miyake, H.; Kusunoki, M.; Osaki, S. **2010**. Crystal structures of isomaltase from *Saccharomyces cerevisiae* and in complex with its competitive inhibitor maltose. *The FEBS Journal*. 277: 4205-4214.
- Yee, S.W.; Shah, B.; Simons, C. **2005**. Synthesis and antimycobacterial activity of 7-O-substituted-4-methyl-2H-2-chromenone derivatives vs *Mycobacterium tuberculosis*. *Journal of Enzyme Inhibition and Medicinal Chemistry*. 20(2): 109-113.

Yuce, B.; Danis, O.; Ogan, A.; Sener, G.; Bulut, M.; Yarat, A. **2009**. Antioxidative and lipid lowering effects of 7,8-dihydroxy-3-(4-methylphenyl) coumarin in hyperlipidemic rats. *Arzneimittel Forschung - Drug Research*. 59:129-134.

Zani, F.; Vicini, P. **1998**. Antimicrobial activity of some 1,2-Benzisothiazoles having a benzenesulfonamide moiety. *Archiv der Pharmazie*. 331(6): 219-223.

Zawawi, N.K.N.A.; Taha, M.; Ahmal, N.; Ismail, N.H.; Wadood, A.; Rahim, F.; Rehman, A.U. **2015**. Synthesis, in vitro evaluation and molecular docking studies of biscoumarin thiourea as a new inhibitor of α -glucosidases. *Bioorganic Chemistry*. 63: 36-44.

Zayane, M.; Romdhane, A.; Daami-Remadi, M.; Jannet, H.B. **2015**. Access to new antimicrobial 4-methylumbelliferone derivatives. *Journal of Chemical Sciences*. DOI 10.1007/512039-015-0927-6.

Zenteno-Castillo, P.; Muñoz-López, D.B.; Merino-Reyes, B.; Vega-Sánchez, A.; Preciado-Puga, M.; González-Yebra, A.L.; Kornhauser, C. **2015**. Prevalence of diabetic nephropathy in Type 2 diabetes Mellitus in rural communities of Guanajuato, Mexico. Effect after 6 months of Telmisartan treatment. *Journal of clinical and Translational Endocrinology*. 2: 125-128.

Zhang, L.; Meng, T.; Fan, R.; Wu, J. **2007**. General and efficient route for the synthesis of 3,4-disubstituted coumarins via Pd-catalyzed site-selective cross-coupling reactions. *Journal of Organic Chemistry*. 72(19):7279-7286.

Zhang, S.Y.; Meng, L.; Gao, W.Y.; Song, N.N.; Jia, W.; Duan, H.Q. **2005**. Advances on biological activities of coumarins. *Zhongguo Zhong Yao Za Zhi*. 30(6):410-414.

Zhao, D.; Zhou, A.; Du, Z.; Zhang, Y.; Zhang, K.; Ma, Y. **2015**. Coumarins with α -glucosidase and α -amylase inhibitory activities from the flower of *Edgeworthia gardneri*. *Fitoterapia*. 107:122-127.